Influence of Material Variation and Corrosion Deterioration on Seismic Vulnerability Assessment of RC Buildings in North Cyprus

Ismail Safkan

Submitted to the
Institute of Graduate Studies and Research
in partial fulfillment of the requirements for the degree of

Doctor of Philosophy
in
Civil Engineering

Eastern Mediterranean University
June 2018
Gazimağusa, North Cyprus

Approval of the Institute of Graduate Studies and Research

Assoc. Prof. Dr. Ali Hakan Ulusoy
Acting Director

I certify that this thesis satisfies all the requirements as a thesis for the degree of Doctor of Philosophy in Civil Engineering.

Assoc. Prof. Dr. Serhan Şensoy
Chair, Department of Civil Engineering

We certify that we have read this thesis and that in our opinion it is fully adequate in scope and quality as a thesis for the degree of Doctor of Philosophy in Civil Engineering.

Assoc. Prof. Dr. Zehra Çağnan
Co-Supervisor

Assoc. Prof. Dr. Serhan Şensoy
Supervisor

Examining Committee

1. Prof. Dr. Kadir Güler
2. Prof. Dr. Ahmet Yakut
3. Assoc. Prof. Dr. Mehmet Cemal Geneş
4. Assoc. Prof. Dr. Giray Özay
5. Assoc. Prof. Dr. Serhan Şensoy

ABSTRACT

During the last few years there have been a growing interest in studies on corrosion related deterioration, parallel to the increase in the expected service life of buildings. The existing literature reveals that corroded reinforced concrete elements results in a brittle global structural behaviour. Due to the late adaptation of proper construction material standards and seismic design provisions in the Mediterranean region, the current building stock faces significant variation in seismic resistance. Likewise the humid environment and the use of chloride contaminated concrete aggregates resulted in a further deficiency, leading to deterioration of the reinforced concrete elements. In this study, the local concrete material as well as naturally corroded local reinforcing steel from North Cyprus was tested. The provided empirical steel material deterioration relationships were then considered in developing fragility curves for the building stock in North Cyprus. Furthermore, the unique character of the local design practice was simulated on scaled columns. The static cyclic tests were performed to assess the ductility degradation phenomena of the lightly reinforced columns with inappropriate stirrup settings.

Based on the local design information, deterministic frame models were generated in the second part of the thesis. The parametrically assessed concrete strength, allows identifying the corrosion related reduction in seismic resistance of the “seismic” and “pre-seismic” reinforced concrete buildings (i.e. the pre-1999 reinforced concrete structures designed according to modern seismic design provisions and those belonging to a previous era, respectively). The presented fragility functions, highlight the significance of considering the combined corrosion effects, such as reinforcement

buckling phenomena, type specific bond and deterioration models, time period specific material strength, and the corresponding effects in seismic resistance. The corresponding dependence of modelling parameters on seismic performance of seismic and pre-seismic reinforced concrete buildings are then discussed in detail. The results revealed that, considering the combined effects of corrosion resulted in a further 37% reduction in seismic capacity of the pre-seismic models in comparison to seismic models when subjected to the same corrosion level. Finally, the vulnerability curves are presented based on the effect of concrete strength on both building groups.

Keywords: Corrosion, aging effects, seismic fragility, concrete strength, Cyprus

ÖZ

Betonarme yapılardaki korozyon odaklı yıpranmaya olan ilgi, yapılardan beklenen servis süresinin uzamasıyla birlikte artmaktadır. Literatür, korozyona maruz kalmış betonarme elemanların, bina ölçeğinde gevrek göçmeye neden olabileceğini göstermiştir. Akdeniz bölgesindeki yapılar incelendiğinde, gerek modern deprem yönetmeliklerinin gerekse kaliteli malzeme teminindeki geç adaptasyonun sonucu olarak, deprem performansında ciddi farklılık göstermektedir. Bununla birlikte nemli hava koşullarının yanı sıra, içerisinde tuz barındıran beton agregalarının neden olduğu betonarme elemanlardaki korozyon, büyük ölçüde dayanım kaybına neden olmaktadır. Bu çalışma kapsamında öncelikle, Kuzey Kıbrıs'tan elde edilmiş olan yerel beton ve çelik malzemeleri önce test edilerek oluşturulan istatistiki parametreler, hasar görebilirlik eğrilerinin oluşturulması amacıyla kullanılmıştır. Ayrıca tabii şekilde korozyona uğramış donatı çeliği için ise, testler sonucu korozyon oranına bağlı olarak, süneklik kaybını tanımlayan bağıntılar oluşturulmuştur. Yerel tasarım karakterini yansıtacak ölçekli kolonlar inşa edilip, statik döngüsel yükleme ile test edilmiştir. Boyuna donatı oranının az olduğu bu kolonlarda, uygun olmayan etriye düzeninin ve kanca şeklinin genel sünekliğe ciddi etkisi olduğu gözlemlenmiştir.

Tezin ikinci aşamasında ise, yerel tasarım bilgileri göz önünde bulundurularak, Kuzey Kıbrıs'taki az katlı ve orta yükseklikteki yapıları temsil edecek analitik çerçeveler oluşturulmuştur. Sadece ölü yüklerle tasarlanan (1999 yılı öncesi) ve deprem yönetmeliği kullanılarak tasarlanan (1999 yılı sonrası) yapıları temsilen oluşturulan bu çerçeveler, korozyon ve beton mukavemetinin genel deprem performansına etkisini elde etmek amacıyla analiz edilmiştir. Sunulan hasar görebilirlik fonksiyonları sonucu

olarak, korozyon etkisinin modellenmesinde, göz önünde bulundurulan donatı kenetlenmesi, basınç donatısının burkulması ve malzeme mukavemetinin güç yitirmesi gibi parametrelerin ciddi sonuçlara sebep olduğu gözlemlenmiştir. Modellemede kullanılan parametreler tez içerisinde ayrıca tartışılmıştır. Sonuçlar aynı korozyon seviyesine sahip 1999 yılı öncesi inşa edilen yapıların, 1999 yılı sonrası inşa edilen yapılara kıyasla yeni ve deprem yönetmeliği ile tasarlanan yapılara kıyasla yaklaşık %37 daha fazla etkilendiğini göstermektedir. Sonuç olarak, beton mukavemeti odaklı olarak tüm modeller için hasar görebilirlik fonksiyonları elde edilmiş ve sunulmuştur.

Anahtar Kelimeler: Korozyon, yıpranma etkileri, deprem hasar görebilirlik, beton mukavemeti, Kıbrıs

To My Parents

Azmiye and Bekir

ACKNOWLEDGEMENT

I would like to thank my supervisor Assoc. Prof. Serhan Şensoy for his tremendous guidance and support throughout my study. I want to deliver my gratitude to my co supervisor Assoc. Prof. Zehra Çağnan for her visionary and constructive guidance. I am truly grateful for the opportunity given by the Civil Engineering Department, EMU for the research assistantship position, which taught me a lot and paved the path of my academic career.

I owe my deepest gratitude to my parents for their continuous patience and support. I am also thankful to my parents in law, Huriye and Ayhan for their support and encouragements. I would like to express my gratefulness for my colleague Amir Nataj for his continues support, help and motivation and inspiration throughout this study.

Last but not least I am grateful for my beloved wife Nilay Bilsel for her support in every way. This thesis would not have been possible without her love and support.

TABLE OF CONTENTS

ABSTRACT iii

ÖZ v

DEDICATION vii

ACKNOWLEDGEMENT viii

LIST OF TABLES..... xii

LIST OF FIGURES xiv

LIST OF SYMBOLS AND ABBREVIATIONS……..……..….xix

1 INTRODUCTION 1

1.1 Objectives and Limitations.....5

1.2 Thesis Outline 6

2 LITERATURE REVIEW.....10

2.1 Introduction 10

2.2 Seismic Assessment of Buildings. 10

2.2.1 Intensity Measure Properties 10

2.2.2 Damage Indicators.....13

2.2.3 Seismic Fragility Functions 14

2.4 Cost of Repair 18

2.5 Seismic Performance Parameters of Reinforced Concrete Buildings and Corrosion Deterioration 20

2.5.1 Material Properties 21

2.5.2 Confinement.....21

2.5.3 Bond strength (τ_b).....23

2.5.4 Reinforcement Buckling Under Compression 25

2.6 Seismic Hazard History of Cyprus 25

2.7 Seismic Design Codes in Cyprus 27

2.8 Building Stock Statistics of North Cyprus 32

2.9 Seismic Assessment Studies for Cyprus 35

3 EXPERIMENTAL PROGRAMME 39

3.1 Concrete Material Statistics 39

3.2 Local Reinforcing Steel Statistics 41

3.3 Corrosion Impact on Reinforcing Steel 41

3.2 Experimental Study on Plain Confinement Steel 45

3.2.1 Experimental Programme 46

3.2.2 Experimental Test Results 52

4 ANALYTICAL ASSESSMENT 61

4.1 Case Study Models 61

4.1.1 Structural Details of the Models 63

4.1.2 Nonlinear Concrete Model 66

4.1.3 Cover Concrete Deterioration 66

4.1.4 Reinforcing Steel 67

4.1.5 Shear 69

4.1.6 Modelling Beam-Column Connection 70

4.2 Plastic Hinge Properties 71

4.2.1 Calibration of Lumped Plasticity 72

4.3 Viscous Damping Model 73

4.4 Damage Index 74

4.5 Seismicity of Cyprus 75

4.6 Ground Motion Selection 78

5 RESULTS AND DISCUSSIONS 81

5.1 Pushover Analysis.....81

5.2 Fragility Curves 84

5.3 Vulnerability Curves 99

6 CONCLUSIONS 107

REFERENCES.....112

LIST OF TABLES

Table 2.1. Interstorey Drift Ratio (ISD) for different damage levels (%) 14

Table 2.2. Comparison of Central Damage Ratios.....19

Table 2.2. Significant earthquakes in Cyprus (Galanopoulos and Delibasis 1965, Ambraseys 1992, Kalogeras et al., 1999) 26

Table 2.3. Comparison of stirrup spacing by codes TS500 and TEC1998.....28

Table 2.4. Design base shear characteristics.....30

Table 2.5. Comparison of response spectrum ordinates of TEC and EC8 31

Table 2.6. Code spectrum parameters (EC8 and TEC 2007).....32

Table 3.1. Concrete strength statistical data, Northern Cyprus.....40

Table 3.2. Reinforcing steel statistical data, Northern Cyprus. 1974-2014.....41

Table 3.3. Empirical relationships of plain and deformed reinforcement ultimate deformation capacity subjected to corrosion, *X corrosion mass loss percentage 44

Table 3.4. Cube test results of concrete material 47

Table 3.5. Tensile test results of reinforcement steel material.....47

Table 3.6. Experimental test samples (Columns with * adopted from Nataj et al., 2018) 48

Table 4.1. Analytical case study models, deterministic material properties.....65

Table 4.2. Cover concrete compressive strength values for uncorroded reinforcement cross sections and 10% mass loss cross sections: a comparison illustrating level of degradation due to corrosion. 67

Table 4.3. Bond models for plain and deformed bars (CEB-FIB and Lee et al., 2002) 69

Table 4.4. Damage classification for assessment (Safkan et al., 2017).....75

Table 4.5. Strong motion database of Cyprus 77

Table 4.6. Ground motion dataset used for the Incremental Dynamic Analysis 80

Table 5.1. Interstory drift limits (%) for the NC damage thresholds (2 storey frame case study).....84

Table 5.2. Interstory drift limits (%) for the NC damage thresholds (5 storey frame case study).....84

Table 5.3. Probabilistic fragility function parameters for 2-storey frame 90

Table 5.4. Probabilistic fragility function parameters for 5-storey frame 94

Table 5.5. Seismic hazard parameters (Cagnan and Tanircan, 2010) 104

LIST OF FIGURES

Figure 1.1. Longitudinal cracks due to corrosion deterioration in a column. 2

Figure 1.2. Study framework of the thesis 9

Figure 2.1. Corrosion deterioration on reinforced concrete elements 20

Figure 2.2. Comparison of stress-strain relationship of confined and unconfined concrete (From Mander et al., 1988) 22

Figure 2.3. Effectively confined core concrete (From Mander et al., 1988) 23

Figure 2.4. Adhesion bearing and friction stresses on deformed bars 24

Figure 2.5. Bond models for corroded bars (Yalciner et al., 2012).....25

Figure 2.6. Seismicity and Active Fault line of Cyprus Island (CGSD 2014).....26

Figure 2.7. Seismic design code hazard maps, Eurocode 8 in South Cyprus (A) and Turkish Earthquake Code 2007 (B).....31

Figure 2.8. Number of buildings built between 1985-2015 in North Cyprus.....33

Figure 2.9. Annual number of building construction per type 34

Figure 2.10. The distribution of building types built between 1985-2016 34

Figure 2.11. Pre and post 2000 number of building construction per type.....35

Figure 2.13. First Vulnerability Assessment for Cyprus. (Schnabel 1987).....36

Figure 2.14. Vulnerability Assessment for South Cyprus. (Kythreoti 2002) 36

Figure 2.15. Non seismically designed buildings vulnerability curve for buildings in South Cyprus (Kyriakides 2007).....37

Figure 2.16. Fragility curve for a North Cyprus case study (Yalçıner et al., 2015)...38

Figure 3.1. Probability density function for the compressive strength of concrete (f_c) 40

Figure 3.2. Naturally corroded test specimen 43

Figure 3.3. Experimental study on corrosion induced Ultimate strain reduction of reinforcing steel materials 43

Figure 3.4. Stirrup Detailing of the specimens, 135° hook (#5 Left) and 90° hook (#4 Right) 49

Figure 3.5. Specimen with plain stirrup steel (left) and specimen with deformed stirrup steel (right) 49

Figure 3.6. Loading Protocol Adopted from FEMA461. 50

Figure 3.7. Test setup.....51

Figure 3.8. Capture from the test.....51

Figure 3.9. Failure of the specimen # 1 52

Figure 3.11. Hysteretic force-drift data of the specimen # 1 53

Figure 3.12. Hysteretic force-drift data of the specimen # 2 53

Figure 3.13. Hysteretic force-drift data of the specimen # 3 54

Figure 3.14. Hysteretic force-drift data of the specimen # 4 54

Figure 3.15. Hysteretic force-drift data of the specimen # 5 55

Figure 3.16. Hysteretic force-drift backbones of closely tied specimens.....55

Figure 3.17. Comparison of secant stiffness of closely tied specimens 57

Figure 3.18. Energy based assessment of closely tied specimens.....57

Figure 3.19. Cumulative energy based assessment of closely tied specimens.....58

Figure 3.20. Energy based assessment of loosely tied specimens.....59

Figure 3.21. Cumulative energy based assessment of loosely tied specimens 59

Figure 4.1. Analytical model geometries, 5 storey frame (left) and 2 storey frame (right) 62

Figure 4.2. Section properties of the case study models.....64

Figure 4.3. Case study groups explained 65

Figure 4.4. Plain reinforcing steel compression stress – strain envelope, constitutive model by Kashani et al., (2015) 68

Figure 4.5. Trilinear backbone curve (Sivaselvan and Reinhorn 1999) 72

Figure 4.6. Calibration of analytical model with the experimental data (Column #1) 73

Figure 4.7. Difference between initial and tangent stiffness.....74

Figure 4.8. Soft soil amplification based on observed data 76

Figure 4.9. Selected ground motion set by using Conditional Mean Spectra (After Jayaram et al., 2001).....79

Figure 5.1. Incremental dynamic analysis results of 5 storey frame: comparison of pre-seismic(A) design period behaviour respect to corrosion deterioration (B) 85

Figure 5.2. Seismic fragility curves for 2 storey PN1 model.....86

Figure 5.3. Seismic fragility curves for 2 storey PC1 model.....86

Figure 5.4. Seismic fragility curves for 2 storey PN2 model.....87

Figure 5.5. Seismic fragility curves for 2 storey PC2 model.....87

Figure 5.6. Seismic fragility curves for 2 storey PN3 model.....87

Figure 5.7. Seismic fragility curves for 2 storey PC3 model.....88

Figure 5.8. Seismic fragility curves for 2 storey SN1 model.....88

Figure 5.9. Seismic fragility curves for 2 storey SC1 model.....88

Figure 5.10. Seismic fragility curves for 2 storey SN2 model.....89

Figure 5.11. Seismic fragility curves for 2 storey SC2 model.....89

Figure 5.12. Seismic fragility curves for 2 storey SN3 model.....89

Figure 5.13. Seismic fragility curves for 2 storey SC3 model.....90

Figure 5.14. Seismic fragility curves for 5 storey PN1 model.....90

Figure 5.15. Seismic fragility curves for 5 storey PC1 model.....91

Figure 5.16. Seismic fragility curves for 5 storey PN2 model.....91

Figure 5.17. Seismic fragility curves for 5 storey PC2 model.....91

Figure 5.18. Seismic fragility curves for 5 storey PN3 model.....92

Figure 5.19. Seismic fragility curves for 5 storey PC3 model.....92

Figure 5.20. Seismic fragility curves for 5 storey SN1 model.....92

Figure 5.21. Seismic fragility curves for 5 storey SC1 model.....93

Figure 5.22. Seismic fragility curves for 5 storey SN2 model.....93

Figure 5.23. Seismic fragility curves for 5 storey SC2 model.....93

Figure 5.24. Seismic fragility curves for 5 storey SN3 model.....94

Figure 5.25. Seismic fragility curves for 5 storey SC3 model.....94

Figure 5.26. Short rise pre-seismic frames Near Collapse fragility plots 10% mass loss vs. sound condition. 96

Figure 5.27. Short rise seismic frames Near Collapse fragility plots 10% mass loss vs. sound condition. 97

Figure 5.28. Mid rise seismic frames Near Collapse fragility plots 10% mass loss vs. sound condition. 97

Figure 5.29. Mid rise seismic frames Near Collapse fragility plots 10% mass loss vs. sound condition. 98

Figure 5.30. Short rise pre-seismic models comparison with European building stock 99

Figure 5.31. Vulnerability curves for short rise pre-seismic models.....100

Figure 5.32. Vulnerability curves for short rise seismic models.....101

Figure 5.33. Vulnerability curves for mid rise pre-seismic models 101

Figure 5.34. Vulnerability curves for mid rise pre-seismic models 102

Figure 5.35. Effect of corrosion deterioration on seismic period frames at complete damage ratio and relative reduction of corresponding intensity level.....103
Figure 5.36. Effect of corrosion deterioration on seismic period frames at complete damage ratio and relative reduction of corresponding intensity level.....103
Figure 5.37. Expected damage loss in terms of mean damage ratio for the low rise buildings, A) 475 Years return period B) 2475 years return period hazard estimates 105
Figure 5.38. Expected damage loss in terms of mean damage ratio for the mid-rise buildings, A) 475 Years return period B) 2475 years return period hazard estimates 106

LIST OF SYMBOLS AND ABBREVIATIONS

A_g	Peak Ground Acceleration
b_w	Minimum section width
CDR	Central Damage Ratio
D	Longitudinal bar diameter
DI	Damage Indicator
IDA	Incremental Dynamic Analysis
IM	Intensity Measure
ISD	Interstorey Drift Ratio
L	Longitudinal bar length in between 2 adjacent stirrups
MDR	Mean Damage Ratio
MMI	Modified Mercalli Intensity Measure
MRF	Moment Resisting Frame
M_w	Moment Magnitude
PGA	Peak Ground Acceleration
S_a, T_1	Spectral acceleration at fundamental period
T_1	Fundamental Vibration Period
V_b	Base shear
W	Seismic weight of building
β	Dispersion- Standard Deviation
ε_{su}	Ultimate strain capacity of steel
ε_{su}^c	Ultimate strain capacity of corroded steel
Θ	Median Value
τ_b	Bond strength

Φ ()	Standard normal cumulative distribution function
ϕ_L	Longitudinal bar diameter
Δ_w	Mass loss in percentage

Chapter 1

INTRODUCTION

Located at the junction of European, Asian and Arabian plates, Cyprus has an active and heterogeneous tectonic history (Harrison et al., 2004). The island has suffered from many destructive earthquakes in the past, most of which occurred in the southern part (Cagnan and Tanircan, 2010). The last destructive earthquake hit (40 fatalities) in 1953 (Civil Defence Organisation, 2010) and in 1996 (Pilidou et al., 2004). Several attempts were made on seismic design provisions since then. However, the modern seismic design provisions date back to late 1990's, resulting a vulnerable building stock in North Cyprus. Although there is a growth in seismic hazard knowledge of the island with the recent studies, the existing seismic fragility assessment cannot be considered sufficient.

To determine the seismic risk before an earthquake occurs, vulnerability assessment is required to determine the common deficiencies of the seismic resistance of the building stock, required for better and sustainable development of urban planning. Moreover, it inflicts public awareness on the need of earthquake resistant construction. Prediction of the extent of the seismic damage to buildings is important to plan strengthening and upgrading methods. The degree of damage is due to ground motion as well as the response of the buildings, yet there are many uncertainties involved, thus requiring a probabilistic assessment which depends on the seismic hazard as well as the building vulnerability. Fragility curves characterize the vulnerability in relation to the intensity

of the ground motion, which in turn characterized by the intensity measure. Mathematically describing, fragility represents the probability of reaching to a damage level with respect to the intensity of ground motion (Colangelo, 2008).

The corrosion attack on reinforced concrete structural elements are widely investigated by engineers and attempts were made on prediction of behaviour of reinforced concrete elements with corrosion deterioration (Alonso et al., 1998; Coronelli and Gambarova, 2004; Berto et al., 2009; Khan et al., 2014; Pedroasa and Andrade, 2017; Vidal et al., 2004, Yalciner et al., 2015). The marine environment of Cyprus, resulting both humid environment and chloride contaminated concrete aggregates, lead to deterioration of improperly built reinforced concrete building elements at short period of time. The corrosion deterioration is observed on existing buildings where the longitudinal cracks were evident.

Figure 1.1. Longitudinal cracks due to corrosion deterioration in a column.

Brittle behaviour is usually expected as a result of aggressive corrosion attack on reinforced concrete elements. The main aim of engineers has always been the realistic

prediction of corroded reinforced concrete sections. According to the studies on corrosion, attention was drawn to the bond, cover concrete strength, ultimate steel strain reduction. A recent study by Pitilakis et al., (2014) assessed aging effects on European RC buildings by considering reinforcing steel and concrete cover degradation. The study targeted both non-ductile and ductile case studies based on average properties. Although the seismic and pre-seismic detailing rules on European deteriorated buildings were investigated by Berto et al., (2009) and Pitilakis et al., (2014), the corrosion modelling parameters were not utilized in the results where a concrete strength and detailing sensitive judgement could not be possible. One of the latest study on assessment of deteriorated RC buildings by Yalciner et al., (2015) suggests the bond deterioration modelling of deteriorated elements. The study claims a great reduction in seismic performance of an old reinforced concrete frame building. However, the study considers a simplified case study model with singular moderate concrete strength and lacks the combination of deterioration modelling parameters such as buckling of rebars, loss of bond and material specific assessment.

Concrete strength has always been an essential parameter of argument in seismic assessment of buildings. The study by Arslan (2010) suggests negligible structural performance reduction due to the concrete strength. However, the study by Stefano et al., (2013) and Ahmad et al., (2015) considered the brittle failure modes where significant reduction in seismic performance was suggested due to low concrete strength.

Another predominant deficiency of pre-seismic type reinforced concrete structures is the unconfined beam-column joints. As various studies discuss, the brittle behaviour of the unconfined beam-column joints can result in a global failure (Kim et al., 2007,

Calvi et al., 2002, Park and Mosalam 2013, Bayhan et al., 2015). The concrete strength plays an important role on shear mechanism of the unconfined beam-column joints and the study by Ghobarah and Biddah (1999) comments on necessity of beam-column joint modelling for a realistic response estimation of structures.

Buckling phenomenon of the compression reinforcement was widely investigated by engineers. Significant reduction in compression strength of plain reinforcement is observed by Prota et al., (2009), for the plain reinforcement having stirrup spacing length / longitudinal bar diameter ratio (L/D) above 6. Another valuable study by Kashani et al., (2015) analysed fifty cases of corroded compression steel specimens subjected to compression stress with various L/D ratios. The model argues the reduction in buckling stress as a function of corrosion and slenderness ratio L/D.

A significant loss in both yield strength and ultimate strain capacity of the reinforcing steel is expected when reinforcing steel is subjected to corrosion. Yu et al., (2015), studied the natural corrosion effects on reinforcing steel. However, the mechanical property differences of the different corroded reinforcement types were not studied.

The aforementioned studies in literature highlighted the effects of individual corrosion modelling parameters on seismic performance of buildings. However, the combined effect of different concrete strength, beam column joint behaviour, compression reinforcement buckling phenomena, relative reduction of cover concrete and corrosion caused reinforcing steel degradation as well as the corresponding interdependence have not been considered in modelling. The uniqueness of this study is in the use of local experimental data and corrosion modelling methodology. Unlike the previous studies which did not cover the corrosion deterioration with respect to applied seismic

provisions, this study aims to propose a methodology which integrate all these components and assess the seismic deficiency of buildings regarding corrosion deterioration and material properties.

1.1 Objectives and Limitations

The main aim of this thesis is to evaluate the seismic fragility potential of reinforced concrete buildings in North Cyprus. Due to the different construction practice and inadequate material supply, a unique consideration is needed for the assessment of the buildings' seismic capacity in North Cyprus. The nature of the study poses various limitations as follows:

- Firstly, the study is limited in geographic and territorial division of the island. Although there are some noteworthy and in-depth studies on the vulnerability assessment in Southern part of Cyprus, the study covers only the buildings, which are located in the North part of the island. The rationale behind this selection is due to the remarkable variance in the use of building materials and design standards between the two parts of the island. The results of this study, however, would not be applicable only to North Cyprus, but, with the gained insight would also contribute to future studies to be conducted in the Mediterranean region.

- Although the built environment is not entirely limited to reinforced concrete structures, the study is limited only to the reinforced concrete buildings. The pre-1930s constructions in Cyprus were typically relied on masonry and adobe. By the advent of reinforced concrete the number of masonry and adobe buildings declined blatantly. According to the statistics (CTSPO, 2017) the vast majority of the existing building stock is reinforced concrete structures.

- Another limitation is the building type and the number of storeys. The study covers the reinforced concrete buildings, which varies from low to mid-rise building type structures with not more than 5 storeys. The underlying reason for this selection relies on the abundant numbers of such buildings on the North of the island.

- Experimental study on local engineering practice and material distribution is aimed. Time period specific steel and concrete material properties were analysed and statistical distribution was generated. Also the use of plain reinforcement as confinement steel is assessed on scaled columns and the behaviour was adopted on modelling of the analytical study.

- Lastly, the study also aims to target the specific material strength and corrosion level. The concrete strength considered, vary from low to moderate strength and corrosion level is limited to the certain amount where the partial ductility rules could be performed. For this study the modelling of most aggressive corrosion level is excluded due to lack of experimental data. Also the contribution of in-plane in-fill wall are not considered within this study.

1.2 Thesis Outline

Following the introduction given in Chapter 1, a background information and a critical review of existing related studies is given in Chapter 2. Specifically, the seismic fragility assessment studies in Cyprus are summarized and a brief information is given on corrosion modelling studies. The study framework is given in Figure 1.1.

The experimental study is summarized in Chapter 3. In the first part, the concrete strength with respect to time period is investigated statistically in North Cyprus. Two major groups were then generated for grouping the study area. 1999 was chosen to be

the year of transition where the established regulations banned the supply of coastal concrete aggregates. On the other hand, at the same period of time, the import and use of the deformed reinforcement was began. The experimental study was conducted on both sound and naturally corroded plain and deformed reinforcement bars found on the island. The statistically investigated and chosen deterministic limit material property values then used for modelling the case study models. Finally, the hysteretic behaviour of these material and detailing features were tested on scaled columns at laboratory environment. The effect of plain and deformed stirrups on seismic capacity were highlighted.

In Chapter 4 the analytical modelling methodology is presented and adopted to models. Brief information on island's seismicity is given and methodology of ground motion selection is explained. The available damage assessment models in literature were also critically examined and appropriate method is adopted herein. The two-dimensional frame models were created for the purpose of static and dynamic analyses. Advanced modelling for deteriorated reinforced concrete sections were cited in literature and applied by using lumped plasticity approach. Specific moment-curvature relationships were generated for each case study model. Several conditions were then considered for grouping the case study models. Initially the groups were formed under two major time periods. An assumption was made that buildings built before 1999 belong to the "Pre-seismic" period and those buildings built afterwards belong to the "Seismic" period. Each major group then accommodated the sub groups such as low and mid-rise buildings as well as the upper and lower concrete strength of the corresponding time periods.

The Incremental Dynamic Analysis (IDA) was performed on models for the purpose of seismic fragility assessment in Chapter 5 and the effect of corrosion - material dispersion was highlighted. The study also made the material strength based engineering judgement possible on deteriorated buildings. In addition some design suggestions are also drawn in this chapter. Finally, a general conclusion was made on seismic fragility assessment and suggestions were derived on the assessment methods adopted.

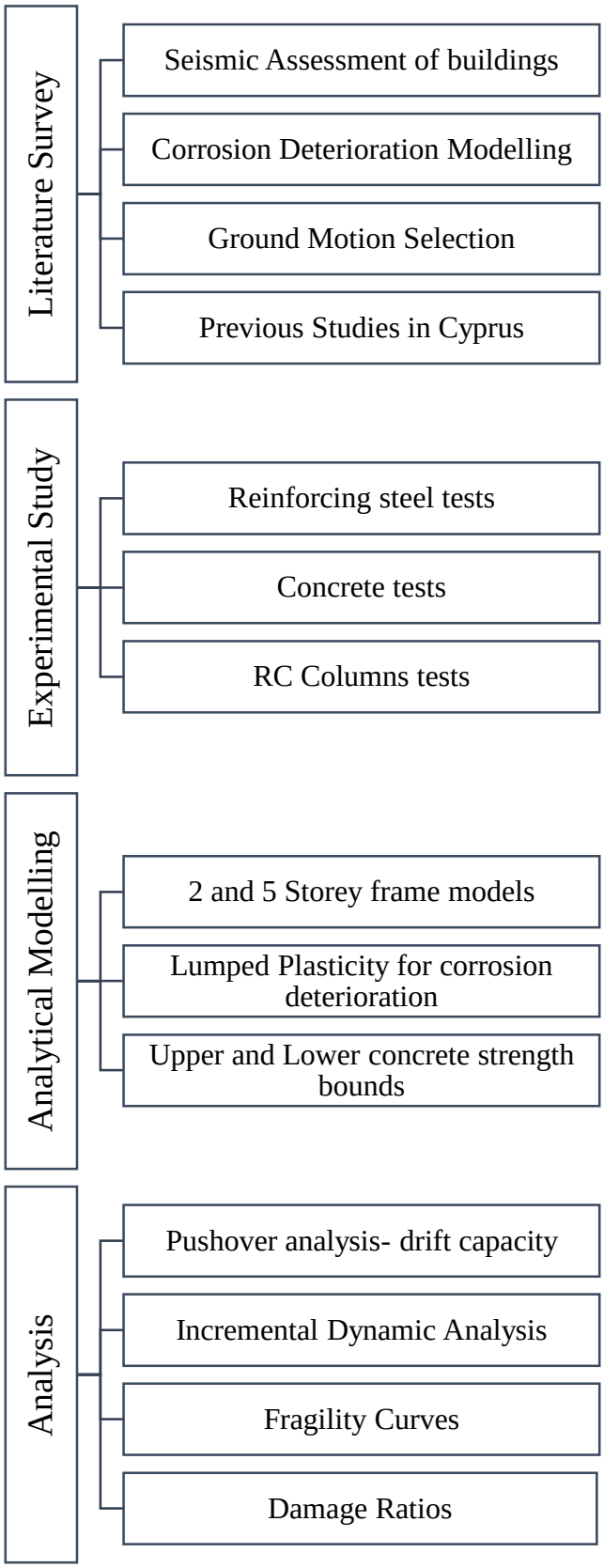

Figure 1.2. Study framework of the thesis

Chapter 2

LITERATURE REVIEW

2.1 Introduction

With the recent devastating earthquakes from 1980's onwards, an increasing demand on seismic assessment of the buildings lead to the development of assessment tools. In this chapter a background on seismic fragility assessment is given and the previous studies in the region are briefly reviewed. The analytical methods for evaluating the existing reinforced concrete building stock are explained in depth. A brief literature review is also presented on previous studies in the region. Also the damage thresholds and ground motion selection methodologies are explained herein.

2.2 Seismic Assessment of Buildings

Estimating the structural reliability against earthquakes has always been an essential requirement in engineering practice. For several decades engineers searched for appropriate assessment methodologies to increase the accuracy of vulnerability estimations. Furthermore, it is essential to know the seismic hazard prior to fragility assessment.

2.2.1 Intensity Measure Properties

Intensity is often used by engineers to describe the strength of the seismic event on surface level in terms of human and building scale. There are several intensity measure scales used for defining the severity of earthquakes. Some of these scales are listed below.

Mercalli Scale and Modified Mercalli Scale: The intensity is mostly defined based on the severity of felt earthquakes and damage to the building result of the earthquakes. Categorisation of earthquakes with respect to intensity is useful in studying and comparing the effects of earthquakes. Although the first intensity scale was introduced by Egen in 1828, the first widely adopted scale was the Rossi-Forel scale, which was developed in the second half of 19th century by merging the works of Rossi and Forel of 1874 and 1881 respectively (Musson et al.,, 2010). Initially 10 intensity levels were introduced mainly based on the severity of building damage. Later in , 1902 the Rossi-Forel scale was developed by Giuseppe Mercalli. Mercalli has retained the original 10-degree scale but considerably improved the description of each grade. This followed by the 12-degree scale of Sieberg in 1912. Sieberg's 1923 version of the scale was translated into English (with minor changes) by Wood and Neumann in 1931. Wood and Neumann's translation became the basis of all 12-degree scales. The arising problems of terminology was resolved by Richter, who also introduced a series of building categories. The phrase "Richter scale", however, became a source of confusion in journalistic usage for local magnitude (ML). This prompted Richter in 1956 to propose the scale to be called the "Modified Mercalli" intensity scale (MMI). Unfortunately, this was proved to be a wrong choice for two reasons: First, data sets were provided with intensity indicated as MMI, without mentioning which scale meant. Second, authors developing various scales began to name their scales as "Modified Mercalli", hence creating further confusion of not knowing "exactly what is meant when MMI appears" (Musson et al.,, 2010).

Magnitude of an earthquake measure the released energy but do not measure how the close distance surface shake severity. The ground motion data (Acceleration-time

data), is used for defining the engineering properties of earthquakes where the several engineering properties are randomly effected due to nature of ground motion. It is often suggested to group these intensity measures in terms of dependence on structural information (Celik, 2007). Some of these important parameters are explained as follows.

Peak Ground Acceleration (PGA) is the maximum ground acceleration (in units of g) recorded in accelerogram data. Accelerograms are recorded in two perpendicular horizontal axes and one vertical axis. PGA is an important intensity parameter and used for design purpose where the earthquake hazard maps are often built based on PGA. However considering the dynamic properties of the earthquakes, PGA is structure independent property and only reflects the short period range behaviour. However, the most engineering structures fall on relatively longer period range, where the PGA as an intensity measure may not be sufficient (Chopra, 2001).

Earthquake intensity is often concerned to play an important role on structural response. The spectral acceleration (S_a,T_1) is the specific elastic acceleration value at specific vibration period. Basically the spectral acceleration is structure dependent intensity measure where the target is the elastic fundamental period resonance range. Due to the different dynamic vibration characteristics of the buildings, the spectral acceleration is an essential parameter for earthquake engineering community with its closer approximation of structure specific target acceleration value. A series of spectral acceleration from an earthquake record, at different period ranges forms the Acceleration Spectrum. The acceleration spectrum is widely suggested by design codes and used by engineers to design new buildings due to its simplicity of selection of corresponding $S_a(T_1)$ at specific structural period. However the accuracy of

estimation may reduce due to the period elongation at post-elastic range (Haselton et al., 2011).

2.2.2 Damage Indicators

Seismic damage to the buildings are usually estimated through displacement parameters. Experimental results, analytical studies and major earthquakes, resulted in precise estimation of displacement measures for the nonlinear response estimation of the buildings. Some of the displacement based damage indicators are listed below.

Ductility Ratio: The ratio of ultimate displacement to yielding displacement is explained by the Ductility Ratio (often called μ). A useful parameter mainly for the monotonically increasing loading. Ductility is often considered to set a limit to global structural plasticity. However difficulty arises for the cyclic loading case where the cumulative effect is being ignored.

Maximum interstorey drift (ISD): The relative displacement between two adjacent storey levels often considered to give information on damage at storey specific level. Some of the existing studies on maximum interstorey drift levels are summarized below. Note that the damage levels are grouped under five damage levels where the homogenisation took place. The first attempt on interstorey drift was made by USNDC (1975) where yield and collapse levels were investigated. Especially with the increase in observational data with the recent earthquakes, resulted in empirical models (Rossetto and Elnashai, 2003), where more conservative limits are highlighted.

Table 2.1 shows the significant variation between the ISD levels investigated by different researchers. Generally the old-type (Pre-seismic) buildings are expected to behave more brittle due lack of deformation capacity. It is essential to evaluate each

type of structure individually where the deformation capacity can vary. The building specific ISD levels are also investigated later in this thesis in Chapter 5.

Table 2.1. Interstorey Drift Ratio (ISD) for different damage levels (%)

		Limited to Non-Structural Components	Light Damage	Moderate Damage	Severe	Collapse
USNDC(1975)	-	0.01	-	-	-	0.04
Ghobarah et al., 1999	Brittle	0.75	-	1.1	1.1-2.5	2.5<
	Ductile	0.75	-	1.3	1.3-4.9	4.9<
FEMA273, 1997	-	-	<1	2-4	4<	-
Elenas (2001)	-	-	0.5	0.5-1.7	1.7<	-
Rossetto and Elnashai, 2003	Non-Ductile MRF	<0.4	0.4-1.0	1-2.4	2.4-4.3	4.3<

2.2.3 Seismic Fragility Functions

Probabilistic approach is often considered in earthquake engineering where one or more uncertainties are usually concerned on decision making at simultaneous order. Probabilistic Fragility Functions show the probability of a structure that will undergo a specified level of damage for the specified intensity measure of seismic event. The

usual type of the fragility function, employs the log-normal cumulative distribution function due to its "non-zero and good fit" characteristics as suggested by Porter et al., (2007). This conditional probability function is given in Eq. 2.1 where DI is the damage level.

$$P\ (DI \mid IM) = \Phi\ (\frac{\ln(x/\theta)}{\beta}) \qquad 2.1$$

Where Φ (): Standard normal cumulative distribution function, θ: Median Value

β: Dispersion- Standard Deviation

"Empirical Assessment" is based on the statistics available upon post-earthquake observation data, probability of damage respect to Intensity Measure (IM) could be established. Initially the empirical functions employed the damage probability matrices, where only the specific IM is concern. The study by Whitman et al., (1974) is often identified as one of the first studies on this era. The study considered the intensity measure of Modified Mercalli Intensity (MMI) and the damage data of large building stock. The limited information on IM at early decades and recently used ground motion prediction equations (GMPE) usually yield to great error when developing vulnerability indexes. Recent development in empirical studies lead to use of fragility functions given a range of IM. Fragility functions consider the probability of a damage level expected to occur at specified intensity measure range. One of the latest empirical study (Rossetto and Elnashai, 2003), considers the Spectral Acceleration at fundamental period (S_a,T_1) and targets the buildings in the Mediterranean region.

The empirical fragility functions lack the uniform distribution of hazard data due to the limited major events in the recent past. Furthermore, the different building

typologies are not often classified since the complexity of on-site information gathering. Last but not least, although the recent development in local instrumentation and the improved knowledge on IMs, the structural behaviour estimation respect to its failure typology, remains the major uncertainty when the empirical functions are concerned.

The difficulty (challenge) in predicting the potential of seismic damage arises mainly from scarcity of damage data, which can be overcome by using analytical methods developed in recent years for the determination of fragility curves. These methods show differences with respect to each other due to the degree of complexity in modelling the structures. There are simple methods as well solely based on unsophisticated equations, such as the ones proposed by Calvi (1999), Pinho et al., (2002) and Crowley et al., (2004), which are designed with the purpose of analysing the fragility of large amount of buildings in a short time period using a structural model just based on simple data such as construction period, construction materials and number of storeys. However, when more comprehensive information is essential mainly for important buildings, especially when there are no empirical data, then detailed analytical procedures are preferred which provide fragility curves. The accuracy of fragility analysis depends on the availability of data as well as the technology. The factors which control fragility analysis include the ground motion parameters, response parameters, modelling assumptions in addition to the analysis techniques used.

Analytical assessment methods for the seismic performance estimation of structures became popular with the development of computational power especially in late 90's. The method requires the modelling of the structural system for the capacities in

flexure, shear etc. at computer environment and applying earthquake forces analytically. Several methods exist, depending on the complexity of analytical model and type of the loading scheme applied. Initially considered equivalent single degree of freedom models, allowing only a rough understanding of damage distribution on structural system, not often preferred by today's engineering community. Even the complex Three-Dimensional models could be solved with ease. Although the elastic procedures are still applied in the era, the nonlinear tools such as Capacity Spectrum Method (ATC-40) and Coefficient Method (initially FEMA 273 and later FEMA 356) are available since late 90's.

The analytical assessment methods for developing the fragility functions could be grouped under two main routes. These are static and dynamic loading schemes. The static loading scheme, considers the application of incremental horizontal loading (so called "pushover analysis") where the analytical model is being pushed to nonlinear stage until the targeted displacement (Chopra, 2001). The static evaluation methods defined in ATC and FEMA procedures, often assumed to consist approximations for the application of loading as well as displacement capacities. However, these methods are often used due to the relatively less computational demand when compared with other dynamic loading methods.

The dynamic nonlinear time history analysis (also known as nonlinear response history analysis) often considered to be a more realistic approach. The method requires the application of ground motion time series with the acceleration values (usually site specific ground motion characteristics are preferred) and assessing the structural response due to the applied dynamic loading. Especially after the proposal of Incremental Dynamic Analysis (IDA) by Vamvatsikos and Cornell (2002) and the

development of the computational power, a special interest on nonlinear dynamic analysis was developed on IDA. The method suggests (which also known as “dynamic pushover”) the application of ground motion with systematically increased intensity measure. This is done by scaling the ground motion intensity parameters (PGA, $S_a(T_1)$, etc.) and running the analysis again. The accuracy of the method in terms of damage distribution is relatively better when compared with the nonlinear static procedures. Two alternatives exist for the damage assessment of the collapse level. One, is the intensity measure (IM) based assessment where the collapse damage identification is specified at the level of intensity parameter that the tangent of IDA is dropped to 20% of its initial value. Above the specified IM the structure is assumed to reach Collapse level. On the other hand, the displacement based (DM) assessment where the specific displacement level is being set as the collapse limit. DM based method is often considered for large number of models where a single collapse drift value is preferred.

2.4 Cost of Repair

The main aim of engineers is to predict the damage respect to seismic intensity. Seismic fragility curves clearly show the probability of each damage state (DS) being exceeded for the given intensity measure. However in terms of loss estimation, the initially given damage states may not be enough. In that case, estimation of loss in terms of the initial cost of building give a better understanding to the decision makers. The decision-makers then can take action on mitigation route. On the other hand it is also important to allow simple and publically available procedure for decision makers for the better understanding of vulnerability. Due to that reason it is often considered to use common intensity measures such as PGA, $S_{a,}(T_1)$ and MMI.

It is often considered to use the "Mean Damage Ratio (MDR)" as single indicator of expected damage in terms of initial value of the building. As suggested by Hwang et al., (1994), the MDR can be calculated by using the central damage ratio (CDR) and probability of damage state at corresponding ground motion intensity. The formulae is given below.

$$MDR_j = \Sigma PDS_{ij} * CDR_i \qquad 2.2$$

Where j: intensity level and i: Damage state and PDS: probability of damage at given intensity level.

CDR is an essential parameter where the estimation is concerned on repair or replacement cost percentage respect to initial cost at specific damage level. Depending on the damage state, several suggestions were made by researchers for estimating the CDR value respect to damage state. The table 2.2 summarises the CDR values suggested by several authors.

Table 2.2. Comparison of Central Damage Ratios

	Hwang et al., 1994	Pasquale et al., 2005	RISK-UE, 2004	Durukal et al.,
Slight Structural Damage	3.5%	2%	3%	20%
Moderate	10%	10%	15%	40%
Severe	65%	40%	50%	90%
Collapse	95%	100%	100%	100%

2.5 Seismic Performance Parameters of Reinforced Concrete Buildings and Corrosion Deterioration

Researchers put huge amount of effort through decades, on evaluation of reinforced concrete buildings in terms of seismic performance. Due to lack of seismic design provisions at early periods, two major groups (Pre-seismic: Buildings with gravity load design and Seismic: Buildings designed with the seismic provisions) are often considered to classify the buildings in terms of seismic characteristics. It should be noted that, main design concern of the most modern building frames, is to avoid collapse at given seismic hazard. Both groups should be evaluated individually while considering the specific modelling parameters for each major groups such as bond strength, confinement, material properties etc. Brittle behaviour is usually expected as a result of aggressive corrosion attack on reinforced concrete elements. According to the studies on corrosion (Berto et al., 2009, Pitilakis et al., 2014, Yalciner et al., 2015), attention was drawn to the bond, cover concrete strength and ultimate steel strain capacity reduction.

Figure 2.1. Corrosion deterioration on reinforced concrete elements

2.5.1 Material Properties

Concrete strength plays significant role in behaviour of reinforced concrete sections. Recent studies show, variation of response occur with different concrete strength levels when bond and shear failure modes are considered (Stefano et al.,, 2013, Ahmad et al., 2015, Verderame et al., 2008, Fabbrocino et al., 2004, Harajli and Dagher, 2008).

Low concrete strength dominated until the seismic design codes set a lower limit of 20 MPa characteristic cylinder compressive strength (TEC 1998) in North Cyprus in 1999. Also at the same time period, the local administrative bodies forbid the use of sea side supplied aggregates. The chloride contaminated sea side supplied aggregates result both corrosion of reinforcement bars and decrease in concrete strength in long term. Detailed statistics through the time periods were given in Chapter 3.

Corrosion results in both steel and covering concrete deterioration. The chemical reaction causes the loss of cross sectional area of steel bar, deterioration of mechanical properties and increase of the volumetric occupation area by corrosion product which deteriorates the cover concrete. An important loss in both yield strength and ultimate strain capacity of the reinforcing steel is expected when subjected to corrosion. The naturally corroded different types of reinforcement bars were evaluated in Chapter 3.

2.5.2 Confinement

The confinement effect is often recognized as being the major influence on concrete material. Several experimental studies (Eg. Mander et al., 1988) were performed late in 1980’s where the confinement effect of stirrups were highlighted.

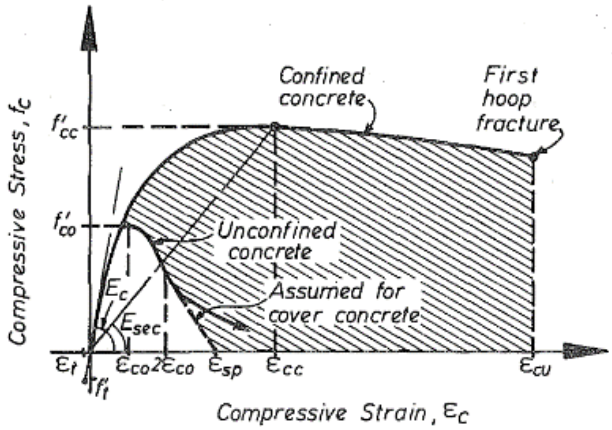

Figure 2.2. Comparison of Stress-Strain relationship of Confined and Unconfined concrete (From Mander et al., 1988)

According to the theoretical confinement model by Mander et al., (1988), both strength and ductility of concrete material is expected to increase if the RC section is well confined. Outer layer of cover concrete is usually assumed to be unconfined. But depending on the longitudinal and lateral reinforcement setting, the inner zone of section (often called “core”), can perform very ductile compared to unconfined concrete. However, in case where the longitudinal reinforcement of the columns are not placed with a close distance, then the area of the confined core reduces as shown in the figure 2.3.

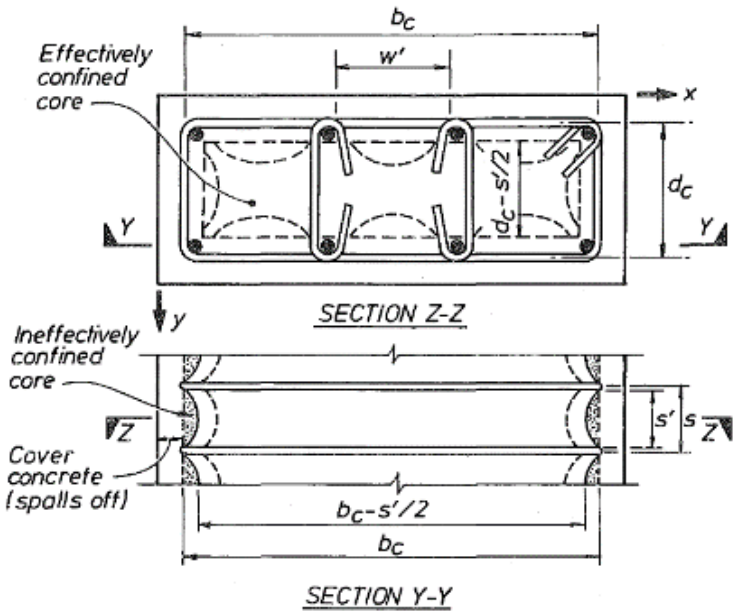

Figure 2.3. Effectively confined core concrete (From Mander et al., 1988)

Stirrups often considered to be fully restrained and the hooks are fully fixed. However due to construction practice, or based on the regulation weaknesses, the smooth surface bars with 90 degrees hooks may result an non-conservative assumption which was widely witnessed at recent earthquakes (Sezen et al., 2003). The performance of stirrups with 90 degree hooks are investigated in chapter 3.

2.5.3 Bond Strength (τ_b)

Longitudinal reinforcement embedded in concrete section faces huge strain cycles in case of the earthquake excitation. It is often studied by researchers (Otani and Sozen, 1972, Alsiwat and Saatcioglu, 1992, Lehman and Moehle, 2000, Sezen and Setzler, 2008) that, the reinforcement bar partially loses its bonding and causes slippage. The slippage can cause significant displacement of section, and should be evaluated carefully. Although different strength and ductility levels often considered in classification of reinforcement, the “smooth” and “deformed” surface types, (namely “Pre-seismic” and “seismic” respectively) believed to dominate the seismic response. Due to the weak bond characteristics, the smooth surface bars were banned soon after

the destructive earthquake hit Turkey in 1999 and major revision on seismic provisions took place in Cyprus. The bond behaviour of smooth surface bars depends only on friction between bar and concrete. The friction strength is only influenced by the tensile strength of surrounding concrete. However, the deformed reinforcement bars, create both radial and friction stresses (τ_{bf}) on covering concrete where better bond is developed compared to smooth surface bars. The figure below shows the components of bonding stresses on deformed bars.

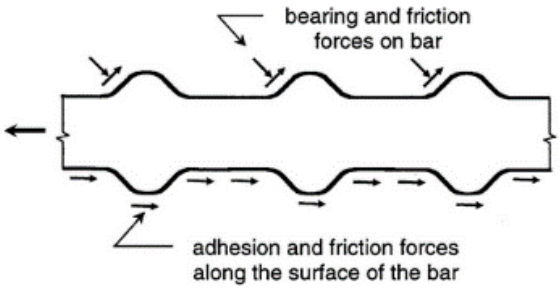

Figure 2.4. Adhesion bearing and friction stresses on deformed bars (MSD, 2018)

A significant amount of bond strength reduction occurs with corrosion. The corroded bar tends to slip at earlier stress due to surrounding weak corrosion product. An assumption of perfect bond between reinforcement and surrounding concrete in modelling may cause an un-conservative results as suggested by Kwak and Kim (2006).

The study by Yalciner et al., (2012), studies the bond strength of deformed bars due to accelerated corrosion. The study suggests preliminary increase in bond strength due to first initiation of corrosion up to 4% mass loss (Figure 2.5). Then the bond strength drops drastically with increasing mass loss. When 10% critical mass loss is tested then the residual bond strength is suggested to be less than 20% of its initial value.

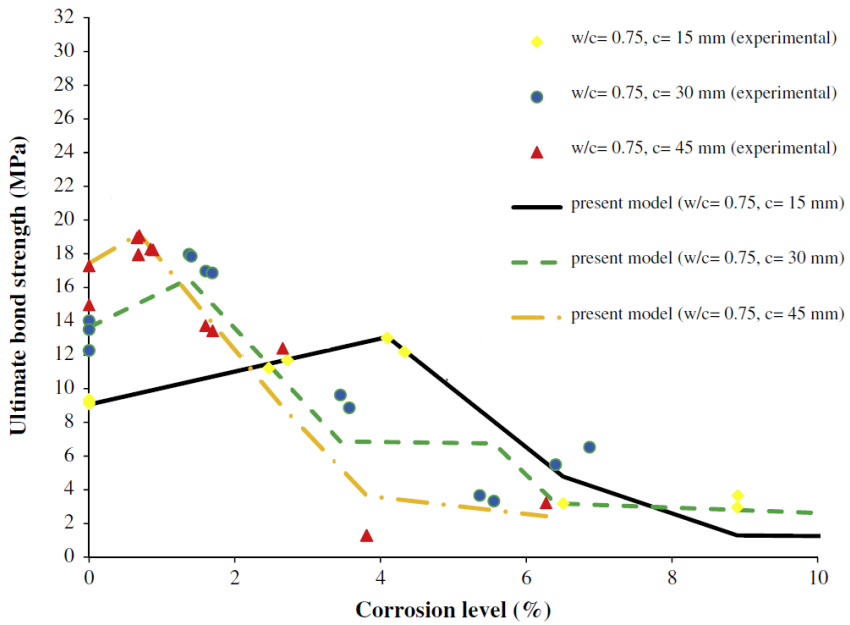

Figure 2.5. Bond models for corroded bars (Yalciner et al., 2012)

2.5.4 Reinforcement Buckling Under Compression

Reinforcement steel is often assumed to show tension like behaviour for the compression side as well. However, the recent studies (Dhakal and Maekawa, 2002, Kashani et al., 2015) show that, when the clear distance of unrestrained bars is large, the bar buckles with the moment applied. Often "L" the unrestrained length of longitudinal bar and "D" the diameter of longitudinal bar is considered for buckling-critical limits L/D. The model provides the reduction in buckling stress as a function of corrosion and slenderness ratio L/D. Detailed model is given later in Chapter 4.

2.6 Seismic Hazard History of Cyprus

Cyprus experienced many destructive earthquakes through its history. So called Cyprian Arc which separates the Eurasian and African tectonic plates, passes through the southern coastline of Cyprus (Cagnan and Tanircan, 2010). The figure 2.6 shows the seismicity that is widely distributed on mainly southern region of the island. In addition, it can be observed that although the densities of the events are higher along

the southern coastline of the island, significant on shore events also hit the island in past.

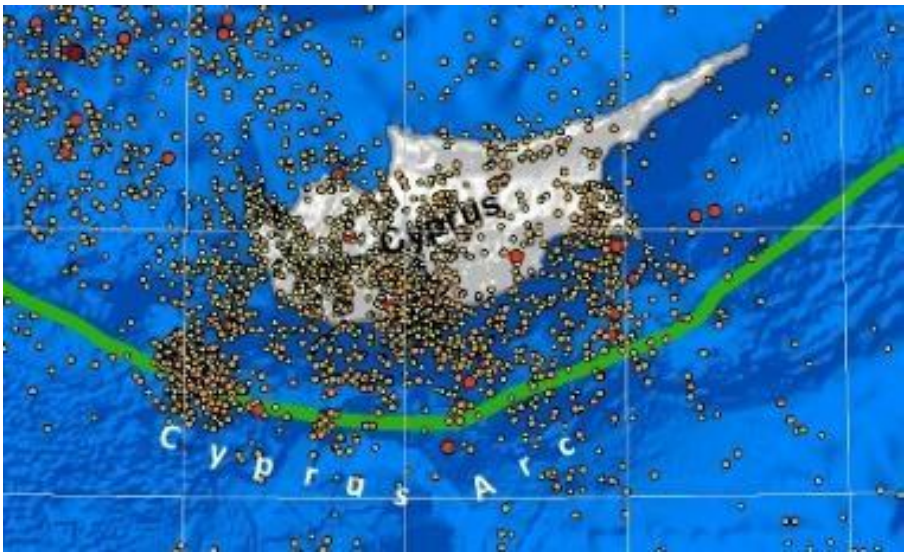

Figure 2.6. Seismicity and Active Fault line of Cyprus Island (CGSD 2014)

The widely populated cities in Cyprus have experienced destructive earthquakes where the catastrophe remembered through centuries (see Table 2.2). The intensity of historical earthquakes, was estimated after centuries by the help of historical records on damage to structures. Although the historical information was utilised, the ground shake estimation by using those events remain unclear.

Table 2.2. Significant earthquakes in Cyprus (Galanopoulos and Delibasis 1965, Ambraseys 1992, Kalogeras et al., 1999)

Year	342	1222	1577	1785	1940	1996
M_w	7.4	1222	1577	1785	1940	6.7

With the help of recent instrumental data as well as developed knowledge on seismicity of Cyprus, several attempts were made on developing the seismic hazard map. The first study on seismic hazard maps of Cyprus was conducted by Ergunay and

Yurdatapan in 1973 (Cagnan and Tanircan, 2010) where in total 4 seismic zones were defined. Similarly in 1992, Republic of Cyprus, Geological Survey Department published the hazard map to be used along with the seismic design code in South Cyprus. The Turkish Earthquake Code 1998 was announced in North Cyprus in 1999. Although several studies were conducted in 1997 (Erdik et al., 1997 and Can 1997), the studies were ignored and Turkish Seismic Zones of 2 and 3 (A_g: 0.3g and 0.2g respectively) were utilised since 1999 in North Cyprus.

According to the recent study by Cagnan and Tanircan (2010), the current practice in North Cyprus underestimates the seismic hazard. The authors also suggest the use of Eurocode 8 in North Cyprus where the hazard estimation coincides with the recent studies.

2.7 Seismic Design Codes in Cyprus

Recent earthquakes in the region proven the fact that the Mediterranean RC building stock built until late 1990's face significant seismic resistance deficiencies (Sezen et al., 2003). British Standards (initially CP110 and later BS8110) were involved in design process of reinforced concrete sections where in the beginning of 1980's, Turkish Standards 500 begun to be used in North Cyprus. Design process initially considered gravity load design only. The first seismic design provision in North Cyprus was accepted in 1992 (CTCCE, 1992) and later in 1999 the Turkish Earthquake Code 1998 (TEC, 1998) was adopted. The buildings constructed before the major seismic design code face significant seismic resistance deficiencies as these buildings designed against gravity load only. Table 2.3 compares the reinforcement detailing rules of pre-seismic and seismic period codes.

Table 2.3. Comparison of Stirrup Spacing by codes TS500 and TEC1998.

	Gravity Load Design (TS 500, 2000)	Seismic Design (Turkish Earthquake Code 1998)
Maximum Stirrup Spacing	$\leq$ 250mm $\leq b_w$ $\leq 12\ \phi_L$	$\leq$ 100 mm (at confined region) $\leq b_w / 3$
Rebar Type	Mild - Plain	High Yield - Deformed

Where b_w is minimum section dimension and ϕ_L is Diameter of Longitudinal bars.

Several studies were conducted on seismic resistance of the gravity load designed buildings after major earthquake hit Turkey in 1999. Regardless of the concrete strength and lateral reinforcement case, on the average the TEC-75 buildings have 30% less displacement capacity, for the “Life Safety” displacement level, when compared to the TEC-98 buildings. (Ozmen and Inel 2012).

Especially after the major earthquake in Turkey in 1999, several attempts were made by researchers to assess the performance of Turkish Seismic Code 1975. Akkar et al., (2005), shows how the base shear capacity differs between codes. Midrise buildings up to 5 storey levels were investigated mostly at short fundamental period range. The study show that the design base shear underestimates the demand when compared with the modern seismic design codes.

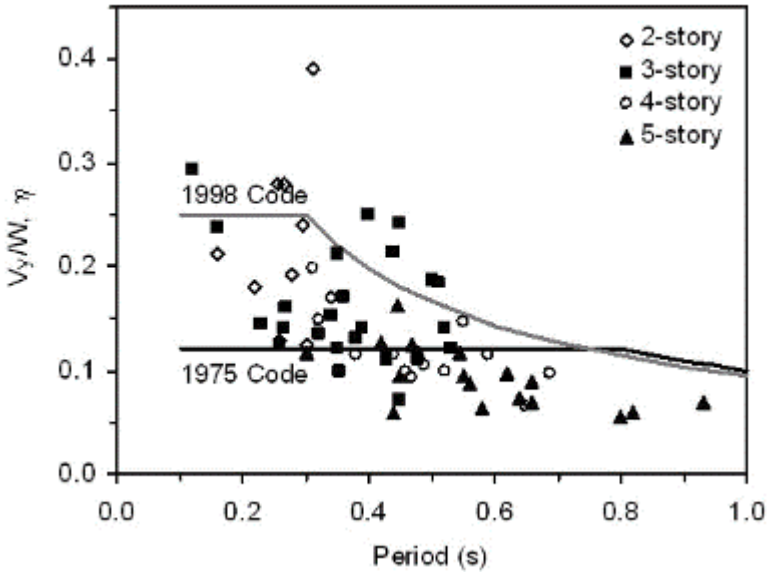

Figure 2.7. Comparison of design spectrums (Akkar et al., 2005)

On the other hand, the seismic design code 1975 supplied significant detailing rules that are similar to the modern codes. The location and length of the confined zone regions, maximum spacing between the stirrups at confined regions, minimum and maximum reinforcement ratios, minimum required development length and last but not least the 135° bent stirrup hooks were all suggested by the 1975 code. However, due to the difficulty in adoption of the code by local bodies, the application of code was found to be limited. With the announcement of the "1992 Practical Earthquake Detailing Rules" by the Turkish Cypriot Chamber of Civil Engineers, an attempt was made to bring the minimum conditions of basic seismic detailing rules to law. The main improvement was the definition of confined region for the columns and minimum longitudinal steel ratio which was brought from 0.005 to 0.008.

Table 2.4. Design Base Shear Characteristics

	South Cyprus	North Cyprus
Pre-seismic Period	*Minimum Requirements for earthquake resistance structures* Since 1985 V_b/W: 0.1g	*Turkish Earthquake Code 1975* Since 1980 (only compulsory for more than 4 storey buildings) V_b/W: 0.1g
Transition Period 1990`s	*Cyprus Seismic Code* Since 1994 V_b/W: $\frac{2.5xAg}{2}$ When $T<T_1$ V_b/W: $\frac{Sx2.5xAg}{2} x \frac{T}{T_1}$ When $T>T_1$	*Practical Seismic Design Detailing Rules (Up to 4 Storey buildings)* Since 1993 No base shear Conceptual detailing
Modern Period (Seismic Period)	*Eurocode 1998* Hazard based spectrum with soil amplification	*Turkish Earthquake Code 1998 (Replaced later in 2007)* Hazard based spectrum without soil amplification

Compared with South, although the similar base shear method was suggested by the 1975 code. But the application of code was optional for the buildings below 4 storeys (also for the 5 storey with car park at the ground floor), until the announcement of decent design code in 1999. When compared with the building stock, unlike to the South the pre-seismic period buildings in North were designed only by gravity loads. Without decent base shear, no limitation on spacing of longitudinal steel and still having plain reinforcement as the major source of steel, the basic practical seismic design regulation is assumed to belong “Pre-seismic” period.

Table 2.5. Comparison of response spectrum ordinates of TEC and EC8

	$T \leq T_B$	$T_B \leq T \leq T_C$	$T \geq T_C$
TEC	$S_e = a_{gR}[1 + 1.5\frac{T}{T_B}]$ $S_d = \frac{a_g}{R_a}[1 + 1.5\frac{T}{T_B}]$	$S_e = 2.5 \cdot a_{gR}$ $S_d = \frac{2.5 \cdot a_g}{R_a}$	$S_e = 2.5 \cdot a_{gR}[\frac{T_C}{T}]^{0.8}$ $S_d = \frac{2.5 a_g}{R_a}[\frac{T_C}{T}]^{0.8}$
EC8	$S_e = a_g \cdot S[1 + \frac{T}{T_B}(\eta 2.5 - 1)]$ $S_d = a_g S[\frac{2}{3} + \frac{T}{T_B}(\frac{2.5}{q} - \frac{2}{3})]$	$S_e = 2.5 \cdot a_g \cdot S \cdot \eta$ $S_d = \frac{2.5}{q} \cdot a_g \cdot S$	$T_C \leq T \leq T_D \rightarrow S_e = 2.5 a_g \cdot S \cdot \eta \cdot [\frac{T_C}{T}]$ $T_C \leq T \leq T_D \rightarrow S_d \begin{cases} = \frac{2.5}{q} a_g \cdot S \cdot [\frac{T_C}{T}] \\ \geq \beta \cdot a_g \end{cases}$ $T_D \leq T \leq 4s \rightarrow S_e = 2.5 a_g \cdot S \cdot \eta \cdot [\frac{T_C T_D}{T^2}]$ $T \geq T_D \rightarrow S_d = \frac{2.5}{q} a_g \cdot S \cdot [\frac{T_C T_D}{T^2}] \geq \beta \cdot a_g$

(A)

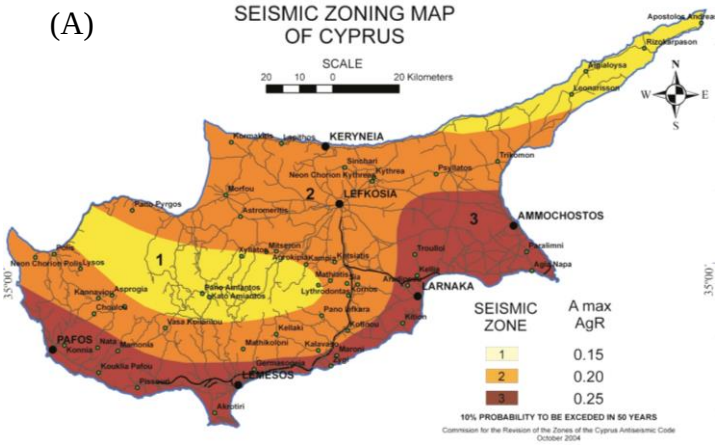

(B)

Figure 2.8. Seismic design code hazard maps, Eurocode 8 in South Cyprus (A) and Turkish Earthquake Code 2007 (B)

Table 2.6. Code Spectrum Parameters (EC8 and TEC 2007)

	Soil Factor		Beginning of Peak range (seconds)		End of Peak range (seconds)	
Soil Type	EC8 (S)	TEC 2007	EC8 (T_B)	TEC 2007 (T_A)	EC8 (T_C)	TEC 2007 (T_B)
Type A or Z1	1	1	0.15s	0.10s	0.40s	0.30s
Type B or Z2	1.2	1	0.15s	0.15s	0.50s	0.40s
Type C or Z3	1.15	1	0.20s	0.15s	0.60s	0.60s
Type D or Z4	1.35	1	0.20s	0.20s	0.80s	0.90s
Type E or Z4	1.4		0.15s		0.50s	
S1 and S2	EC8 requires special studies to provide the corresponding values of *T*B, *T*C and *T*D.					

The modern period design code suggested base shear values were analysed by the author in another study (Safkan, 2012), and up to 30% difference was obtained when EC8 and TEC2007 were compared for the residential buildings Cyprus. Although similar PGA values were suggested by both codes on hazard maps, due to the soft soil amplification criteria and relatively less maximum base shear reduction factor (q) of EC8, a more conservative base shear values are expected for the modern era buildings in South Cyprus.

2.8 Building Stock Statistics of North Cyprus

Separation of communities in 1974 lead to confusion in settling and yet construction industry remained almost passive. In early 1980's, the post-war construction industry started to be formed in North Cyprus with the increasing housing demand. The demand increased linearly from 1985 to 2003. With the political uncertainty in 2003 and onwards there was a great increase in number of buildings built. Total of 2500 buildings were built in 2003 where the construction industry faced 385% increase in

demand. The major seismic revision, Turkish Earthquake code 1998 was in charge in that period where the mass construction increase hit the North Cyprus.

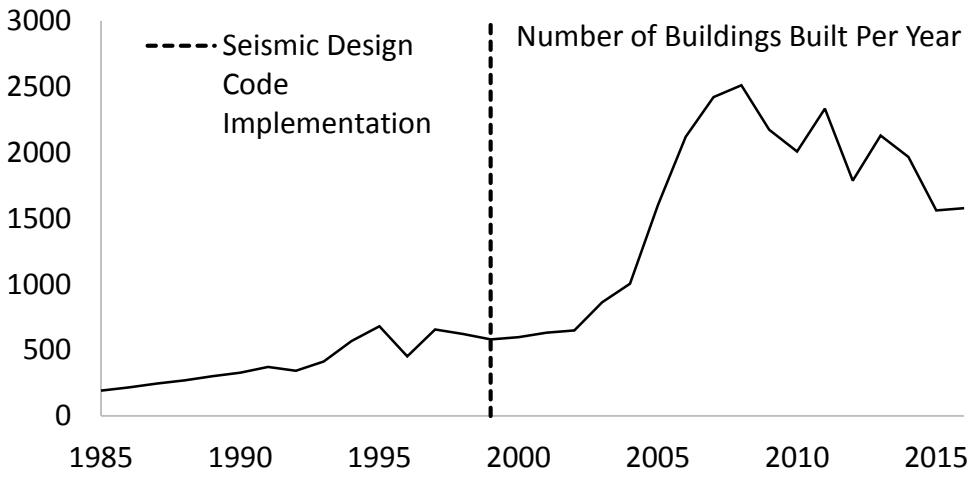

Figure 2.9. Number of buildings built between 1985-2015 in North Cyprus

The buildings built in between 1985-1993, follow a uniform trend where an average of 300 buildings built every year. There is a gradual increase in both low and mid rise building construction where the average amount of construction rose by 100% in years 1993-2003. However from 2003 onwards, the number of low rise building construction gone up by almost 5 times where the midrise buildings were not influenced in that intensity. The peak number (in total 2240) of low rise buildings were built in 2008. Since 2008 the demand on low rise buildings faced a decrease in popularity. Unlike to the low rise buildings, the intensity of the mid-rise building construction became more popular in 2006 and onwards.

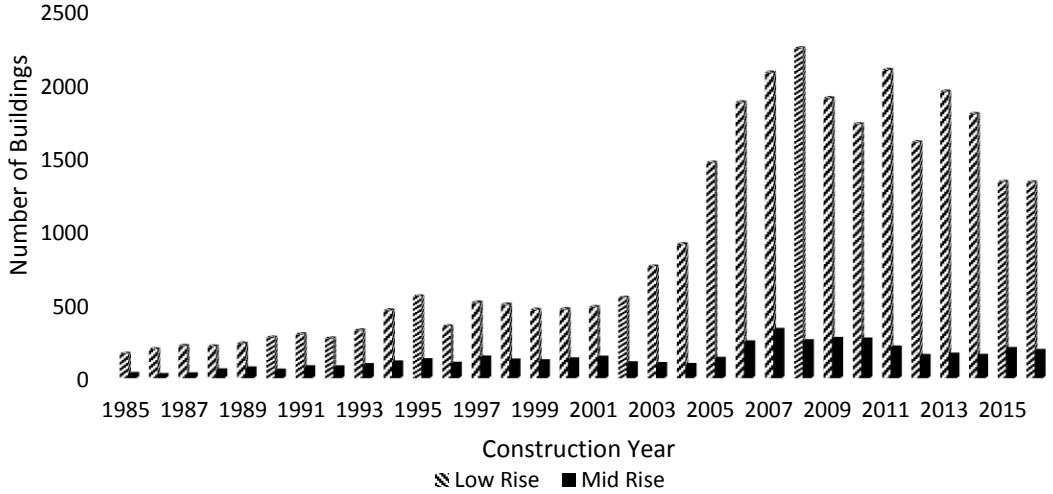

Figure 2.10. Annual number of building construction per type

The grouping of the building types were considered for the evaluation purpose. When compared, only 0.8% of the buildings that are built in last 30 years have more than 5 storeys. Due to that reason those high rise buildings are not considered within this study. The mid rise buildings (3-5 storeys) form only the 13% of the buildings that are built in last 30 years. The rest of the buildings are limited to 2 storeys (Figure 2.12).

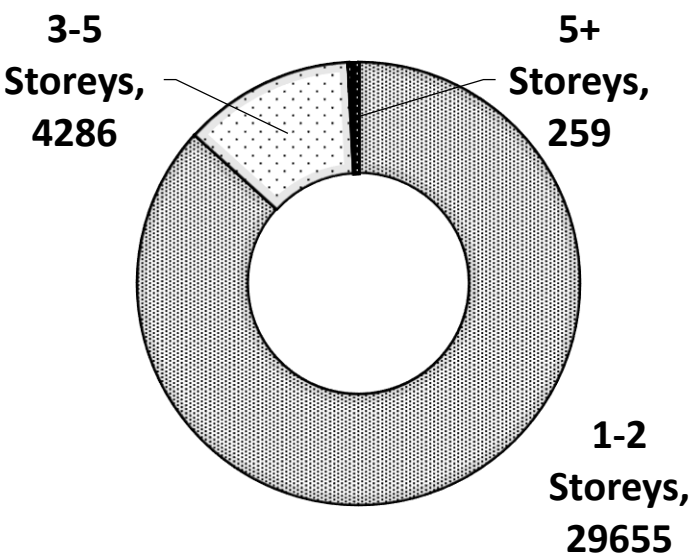

Figure 2.11. The distribution of building types built between 1985-2016

The years where the ready mix concrete facilities first started and the major seismic design provision (Turkish Earthquake Code 1998), was chosen to be the year of transition in construction industry. The result of assumption also shows the seismic code was employed in period where the vast majority of buildings were built (Figure 2.13).

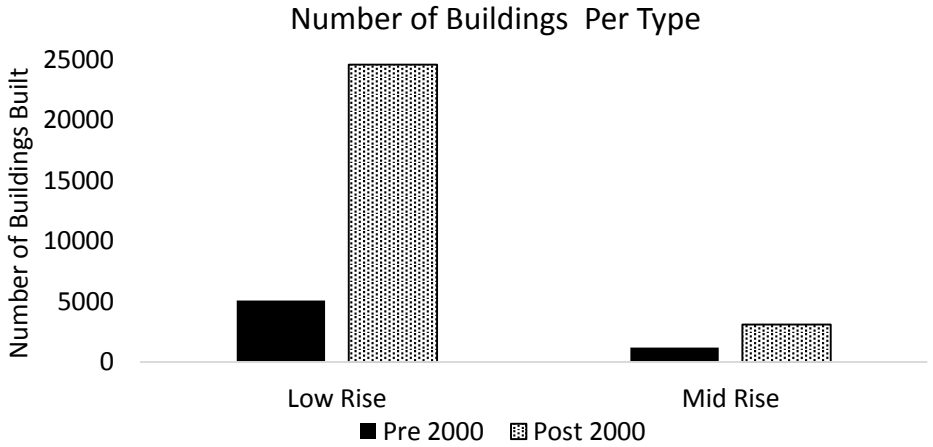

Figure 2.12. Pre and post 2000 number of building construction per type

2.9 Seismic Assessment Studies for Cyprus

The first attempt to derive vulnerability index for southern Cyprus was made by Schnabel (1987). The study considered the data of countries having similar construction type. The intensity measure was MMI scale. Later, Kytherito (2002) studied the seismicity of the island in depth, developed the vulnerability function based on empirical data available from the recent earthquakes. Finally an improvement was made on Schnabel's vulnerability index by Kytherito, but due to the limited number of events, the reliability of the index is still unclear. Figure 2.14 and 2.15 compares the original Schnabel and Kytherito indexes.

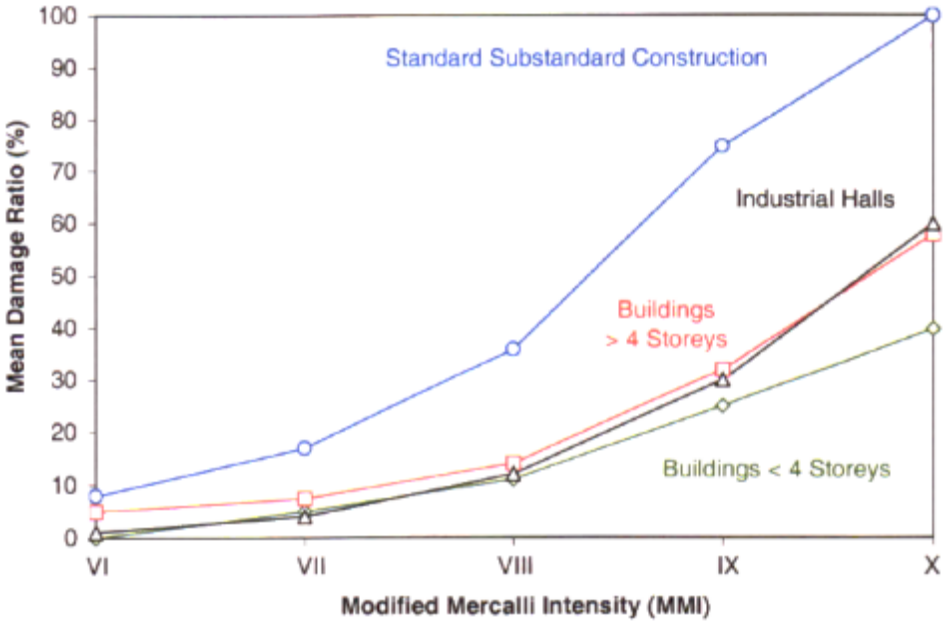

Figure 2.13. First Vulnerability Assessment for Cyprus. (Schnabel 1987)

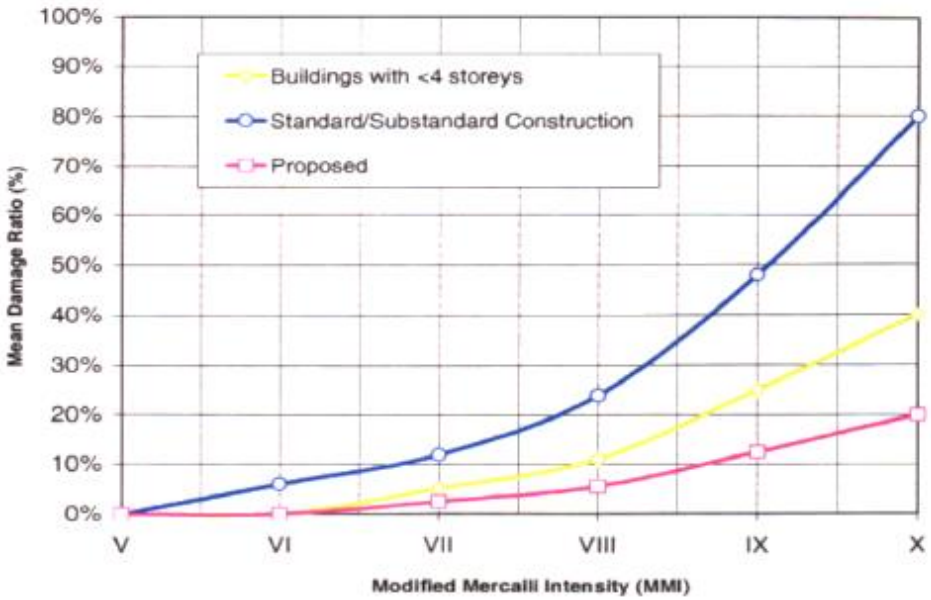

Figure 2.14. Vulnerability Assessment for South Cyprus. (Kythreoti 2002)

Due to lack of recent data, the empirical vulnerability functions are questioned for the validity in Cyprus. Analytical approach is often considered as a better option where a complete loss data do not exist. One of the latest study by Kyriakides in south Cyprus, analytically assessed the building stock against seismic vulnerability potential. An

attempt was made on modelling methodology to consider the brittle failure modes which was ignored in previous studies (Kyriakides, 2007). For the evaluation of structural response, he elaborated a revised capacity-spectrum method. In addition, Kyriakides considered damage index indicator based on fundamental period shift and then the damage limits were assigned. Both old and new construction types were considered within the study. However low concrete strength due to bad practice and corrosion effects were not considered. Figure 2.16 shows the vulnerability curve by Kyriakides (2007) where the intensity measure is the PGA.

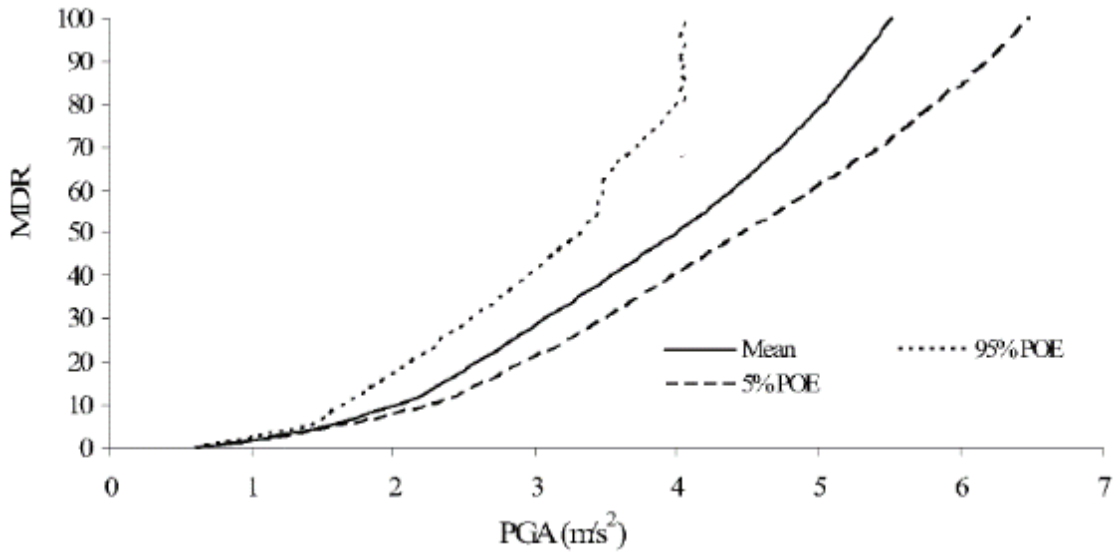

Figure 2.15. Non Seismically Designed Buildings Vulnerability Curve for buildings in South Cyprus (Kyriakides, 2007)

A valuable study by Yalçıner et al., (2015) assessed a North Cyprus case study building by considering the corrosion deterioration. Several brittle failure mechanisms such as bond and cover concrete deterioration were considered within the study and fragility curves were generated for different ages based on linear degradation assumption. Nonlinear dynamic analysis was considered and PGA was utilized as the intensity measure. A great reduction in seismic performance of case study building was

presented due to corrosion deterioration. However the information on seismically designed deteriorated structures in Cyprus remain unstudied.

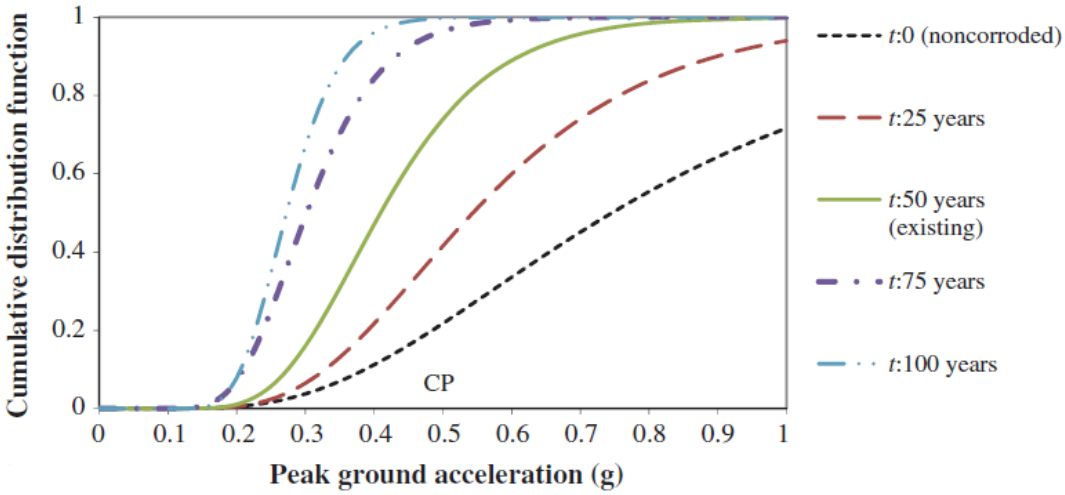

Figure 2.16. Fragility Curve for a North Cyprus case study (Yalçıner et al., 2015)

All studies so far considers the PGA as the intensity measure which allow no such soil specific loss estimation. A brief information on site condition in Cyprus is given in chapter 4. Although some fragility studies exist in the era, the available fragility functions lack the local material variability and the effect of corrosion deterioration on old and new type reinforced concrete buildings. This study attempts to fill the gap in this particular research area.

Chapter 3

EXPERIMENTAL PROGRAMME

In the first phase of the experimental study, the local material characteristics including the compressive strength of concrete and yield strength of steel variation with respect to construction period were investigated. Naturally corroded reinforcement bars were subjected to tensile test and correlation between the corrosion level and mechanical properties were studied. In the second phase, an experimental testing program on scaled columns was conducted to investigate the plain stirrup effects and the calibration of the analytical study.

3.1 Concrete Material Statistics

The low strength concrete is often expected to result in a brittle behaviour. According to the study by Stefano et al., (2013), concrete strength variation has a severe effect on structural response. Likewise, Kim and Lafave (2007) studied the parameter affecting the shear behaviour of the unconfined beam – column connections and the concrete strength found to be one of the most governing parameter. Ahmad et al., (2015) investigated the reduction in seismic performance due to the variation in concrete strength. A great difference was observed when lower and upper boundaries were compared.

Based on the experimental data provided by Eastern Mediterranean University, Civil Engineering Department, Materials Laboratory, 880 test specimen from North Cyprus were utilised and significant variation in results were obtained. Due to large variation

in compressive strength of concrete, upper and lower boundaries corresponding to each construction period were investigated. The pre-seismic design period ends in 1999 where the major obligatory seismic design rules are published. The statistical distribution of the concrete compressive strength were generated for both time periods and are given in Figure 3.1.

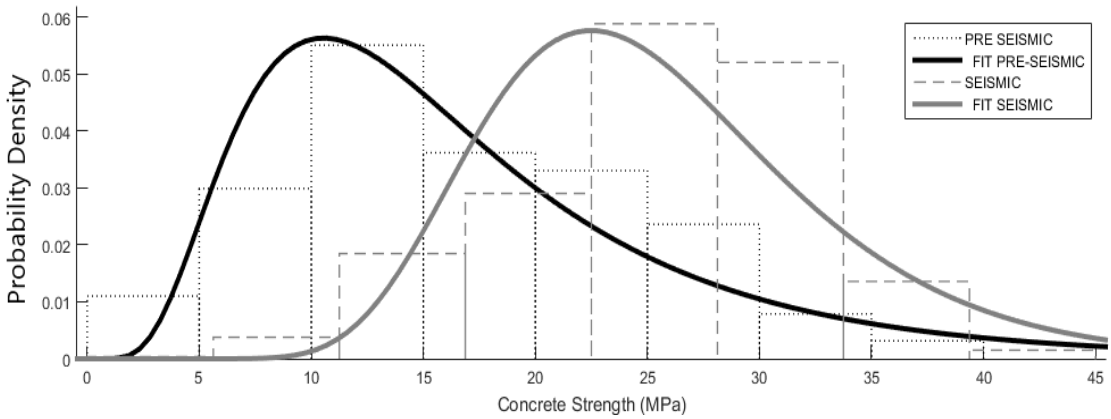

Figure 3.1. Probability density function for the compressive strength of concrete (f_c)

Table 3.1. Concrete strength statistical data obtained in between 1974-2014, North Cyprus.

Type	Mean Compressive Strength (MPa), μ	Median Compressive Strength (MPa)	Log Std. Deviation	Distribution
Pre-Seismic Period	17	14	0.59	Log-Normal
Seismic Period	26	25	0.31	Log-Normal

Log normal distribution mainly due to its non-negative characteristics were considered (Figure 3.1). 35% difference in mean compressive strength was also obtained between

the two periods. Mean, median and logarithmic standard deviation of concrete strength for both periods are also presented in Table 3.1.

3.2 Local Reinforcing Steel Statistics

Until the end of 1998, the plain reinforcement steel was in use in the Northern part of island. The reinforcement steel S420 where the specifications are given in DIN 488-1(1986) was adopted by Turkish Earthquake Code (1998) in 1999. The difference between plain and deformed reinforcement is not only geometric shape but the mechanical properties. Experimental data available from Eastern Mediterranean University, Mechanical Engineering Laboratory obtained and statistical distributions were generated. Based on the available data in total 1192 specimen were utilised for both plain and deformed bars. Table 3.2 summarizes the locally obtained mean mechanical properties of both plain and deformed reinforcement.

Table 3.2. Reinforcing Steel Statistical Data, Northern Cyprus. 1974-2014

Type	Mean Yield Strength (MPa)	Mean Ultimate Strength (MPa)	Mean Ultimate Strain	Distribution
Plain	260	390	20%	Normal
Deformed	460	635	17%	Normal

3.3 Corrosion Impact on Reinforcing Steel

Mainly due to the sea-side sourced aggregates, the chloride induced corrosion is often observed in Cyprus. The corrosion effects on reinforcement steel were often studied by researchers pointing the fact that different chemical composition of the deformed

and plain reinforcement results not only on mechanical behaviour difference but also different corrosion vulnerability. The study by Du et al., (2005) tested different types of reinforcements, the plain reinforcement steel is found to be more vulnerable against corrosion. In this study an experimental work was conducted on the naturally corroded reinforcing bars from the existing buildings as a part of assessment programme. Similar experimental studies on corrosion, the mechanical deterioration is analysed as a function of mass loss. The experimental study by Lee and Cho (2009) concluded that pitting (localised corrosion) occurs mainly due to chloride induced corrosion. However the study tested only the corroded deformed bars with an accelerated corrosion method. The experimental studies by Castel et al., (2000) and Yu et al., (2015) investigated the mechanical deterioration effects on naturally corroded reinforcing bars. However, the developed empirical relationships did not specify reinforcement type specific results.

Within the coverage of this study, naturally obtained corroded bars from the existing buildings belonging to the same construction periods were tested for tension (Figure 3.2). The undisturbed steel material was gathered from old type buildings. The test protocol ASTM G1 – 03 Standard Practice for Preparing, Cleaning, and Evaluating Corrosion Test Specimens (2003) was adopted for this study where the mechanical cleaning procedure was applied on specimen in order to not change the mechanical properties. The mass loss was calculated by assuming the initial weight and weighing the corroded specimen.

Experimental study was concluded by generating an empirical relationship between mass loss and mechanical characteristics of the reinforcement (See Figure 3.3). A linear relationship is suggested for the corrosion vs yield strength as suggested by

Apostolopoulos and Papadakis (2008) and Lee and Cho (2009). The assumption suggests for 1% of the mass loss uniform reduction of cross sectional area. In this study an exponential plot was fitted to the corrosion vs ultimate strain reduction results.

Figure 3.2. Naturally corroded test specimen

The Matlab Curve Fitting Toolbox (Mathworks, 2002) was used in this study in order to assign best exponential fit to the ultimate strain relationships. A nonlinear trend was observed where the strain capacity initially faced significant reduction up to 10% mass loss and relatively less for the greater mass loss.

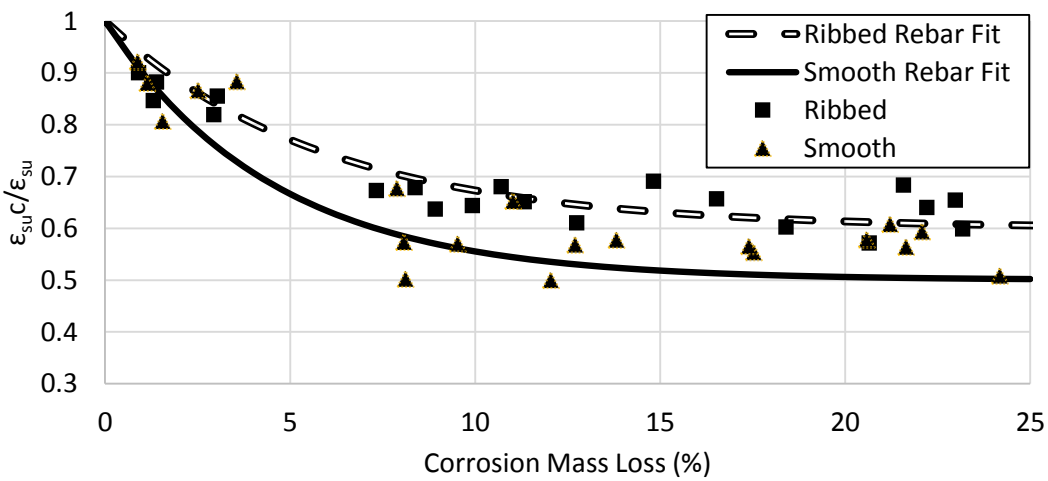

Figure 3.3. Experimental study on corrosion induced Ultimate strain reduction of reinforcing steel materials

Table 3.3. Empirical relationships of plain and deformed reinforcement ultimate deformation capacity subjected to corrosion

	Plain Bars	Deformed Bars
Corroded bar deformation capacity	$\varepsilon_{su}^{c} = (0.5*e^{(-0.223*X)}+0.5)\ \varepsilon_{su}$	$\varepsilon_{su}^{c} = (0.4*e^{(-0.174*X)}+0.6)\ \varepsilon_{su}$
R^2	0.76	0.85

Where X corrosion mass loss percentage, ε_{su} is initial strain capacity of bar, and ε_{su}^{c} is the strain capacity of the corroded bar.

The test was concluded by investigating the corrosion effect on each reinforcement type individually. The smooth reinforcement bars were found to be more fragile when compared with the deformed bars. Although the initial strain capacity (ε_{su}) of smooth bars is greater compared to deformed bars, the corrosion influence caused greater reduction to the corroded strain capacity (ε_{su}^{c}). However if the current assessment practice is considered (TEC 2007), both bar types satisfy the ultimate strain limit of 0.06 even with 25% mass loss condition.

Experimental study on material properties were concluded by generation of distribution parameters. These parameters are used in chapter 4 for modelling purposes where the lower median and upper boundaries were considered. Experiments on corroded bars concluded by showing significant reduction in elongation capacity. The provided relationship also can be used for modelling aggressive corrosion which lies beyond the scope of this thesis.

3.2 Experimental Study on Plain Confinement Steel

Confinement effect of the non-conforming stirrups has always been the concern for investigating the old-type reinforced concrete columns. Recent devastating earthquakes confirm the improper detailing defects on seismic performance of the reinforced concrete buildings. Poorly detailed sections tend to fail under shear if the shear demand is not satisfied. Recent studies (Sezen and Moehle, 2004, Elwood and Moehle, 2005, Galanis and Moehle, 2015) show that sections with initially sufficient shear strength may fail under shear with increasing ductility demand. Another significant shear vulnerability may arise by hook opening of the improperly detailed stirrup. In 1999, Turkey witnessed the failures due to the hook opening of the improperly detailed columns as a consequence of the earthquake (Sezen et al., 2003).

The plain surface reinforcement steel was used in the majority of the seismically prone regions until late 90's. Even the specifications restricting the use of plain reinforcement was added in the seismic codes, the use was continued only as confining reinforcement. The post event investigation teams reported (Bilham et al., 2003 and Kaushik et al., 2016) the inadequate setting of confining reinforcement hooks resulted extensive damage to the buildings in Nepal, Turkey etc.

The study by Lam et al., (2003) and Lyn (2001) investigated the shear behaviour of RC columns with 90° hook stirrups and the longitudinal reinforcement ratio higher than 2% where the shear critical behaviour was highlighted. Although these studies proven the effect of the improper detailing of the stirrups, the effect on the low longitudinal reinforcement ratio and high shear span to depth ratio remains unclear.

The modern seismic design codes require well tied at 135° hooks for confinement steel. However due to improper supervision on site conditions, even the modern seismic design details may suffer inadequate hook application on confinement steel. The recent earthquakes proved the fact that, confinement steel bent at 90 degrees results buckling of compression reinforcement or shear failure (Sezen et al., 2003). On the other hand a great contribution is made by Kashani et al., (2015) on modelling of buckling behaviour of the compression reinforcement respect to confinement properties, however there is no study on comparison of deformed and plain confinement steel closed at 90 degrees.

The time period covering the gravity load design and the initial basic seismic provisions, not much attention was paid on detailing of the reinforced sections. Due to the lack of base shear design, the sections usually were designed for the minimum reinforcement ratio. Thus the majority of the old-type sections become flexural critical rather than the shear critical. This study investigates the effect of plain confining reinforcement on ductility of the reinforced concrete columns. Low strength concrete representing the pre-seismic period were cast with deformed longitudinal steel and both plain and deformed confinement steel comparing non-engineered reinforced concrete practice of the modern period.

3.2.1 Experimental Programme

Scaled columns were tested at Eastern Mediterranean University Structural Engineering Laboratory. The study aimed to investigate the influence of stirrup setting on global behaviour of squared column sections.

The concrete strength representing the pre-seismic period, was used at experiments. The relatively low concrete strength was considered for its bond and shear behaviour. On the other hand two different type of reinforcement was utilized. The deformed and relatively higher strength reinforcement steel was used for the longitudinal bars and smooth surface mild reinforcement steel was used for the stirrups.

Table 3.4 Cube test results of concrete material

Specimen	$f_{cu,28}$:(MPa)
Sample 1	17.3
Sample 2	16.8
Sample 3	17.5

Table 3.5 Tensile test results of reinforcement steel material

	f_y, MPa	f_u, MPa	ϵ_y	ϵ_{su}
Longitudinal (Deformed)	451	508	0.0022	0.17
Stirrup (Deformed)	460	519	0.0023	0.18
Stirrup (Plain)	282	360	0.0014	0.24

Experimental programme aimed to assess the individual effect of stirrup surface and hook properties on initially non-shear critical reinforced concrete columns. First three specimens have same stirrup spacing at 80 mm. However, specimen #1 has deformed bars where #2 and #3 has plain stirrup bars. The hook configuration also differs where #1 and #3 has 135° hooks and #2 has 90° hooks.

Table 3.6 Experimental Test Samples (Columns with * adopted from Nataj et al., 2018)

Specimen	Confining reinforcement	Stirrup Type	Hook Angle	Longitudinal Bars
#1*	Φ8/80mm	Deformed	135	4Φ12
#2	Φ8/80mm	Plain	90	4Φ12
#3	Φ8/80mm	Plain	135	4Φ12
#4	Φ8/200mm	Plain	90	4Φ12
#5*	Φ8/200mm	Deformed	135	4Φ12

Last two specimens has 200mm stirrup spacing, where specimen #4 has plain bars with 90° hooks and specimen #5 has deformed bars with 135° hooks. With no close confinement steel, the design represents pre-seismic period. The total clear height of the columns are 1200mm.

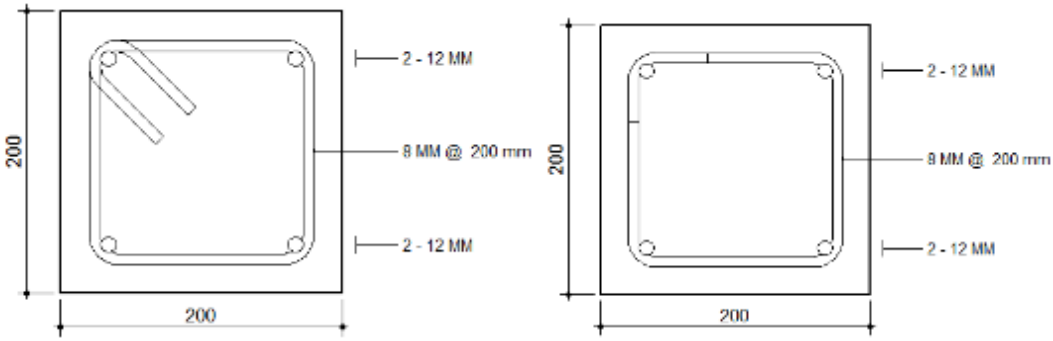

Figure 3.4. Stirrup Detailing of the specimens, 135° hook (#5 Left) and 90° hook (#4 Right)

Figure 3.5. Specimen with plain stirrup steel (left) and specimen with deformed stirrup steel (right)

The loading protocol provided in FEMA461 (2007) was adopted in test protocol. Axial and horizontal forces were applied on scaled cantilever like free end columns. The displacement increments were applied until maximum targeted amplitude was observed. Initial amplitude, was generated by considering the maximum targeted amplitude and the following amplitudes were generated by a function of sequential drifts. The test protocol is given below.

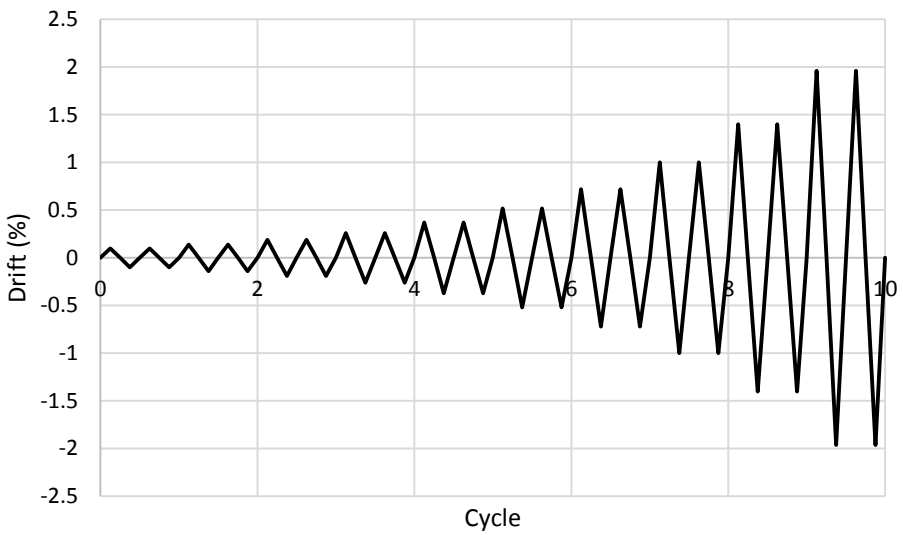

Figure 3.6. Loading Protocol Adopted from FEMA461.

The test was carried out by applying axial force first through a hydraulic jack on top with double hinges. Then the static-cyclic drift increments were applied horizontally by adopting the FEMA461 regulation. The cycles were generated until the strength capacity was dropped to 80% of the initial value. Displacement controlled increments were applied in 10 repetitive steps. The speed of the increments was kept at slow level where the dynamic effects were also avoided. Axial load was kept constant by continuously adjusting the vertical hydraulic jack after each cycle. The total axial load was also kept at 300kN and manually adjusted.

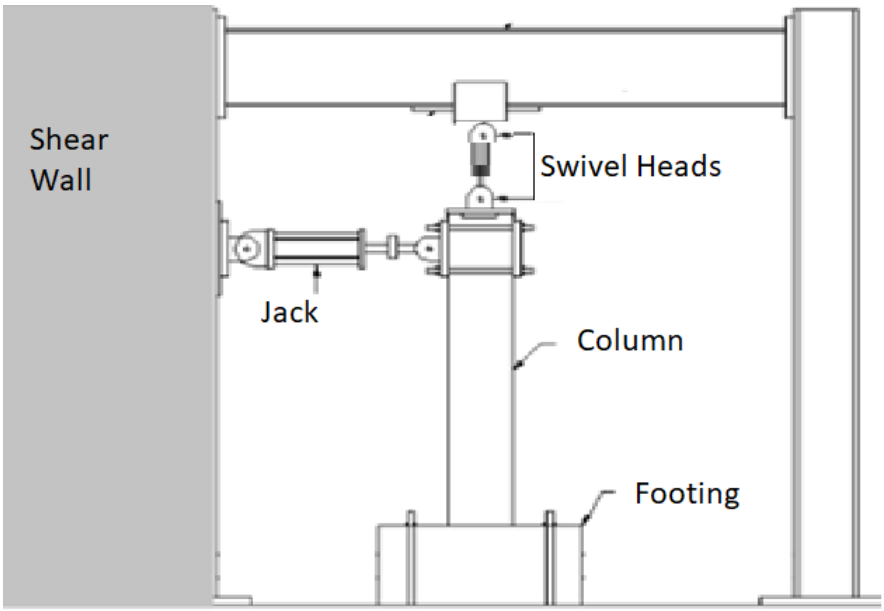

Figure 3.7. Test setup

Figure 3.8. Capture from the test.

3.2.2 Experimental Test Results

The experiment was concluded by observing visual damage and force displacement hysteretic behaviour. The all specimen exhibited flexural failure due to long shear span to depth ratio and low longitudinal reinforcement ratio. Figure 3.9 below shows the failure of specimen # 1.

Figure 3.9. Failure of the specimen # 1

The test was carried out by considering several response parameters. Although the ductility is an essential parameter, the energy concepts were adopted herein by comparing the strength and stiffness. The hysteretic response to cyclic loading of each specimen is given as follows.

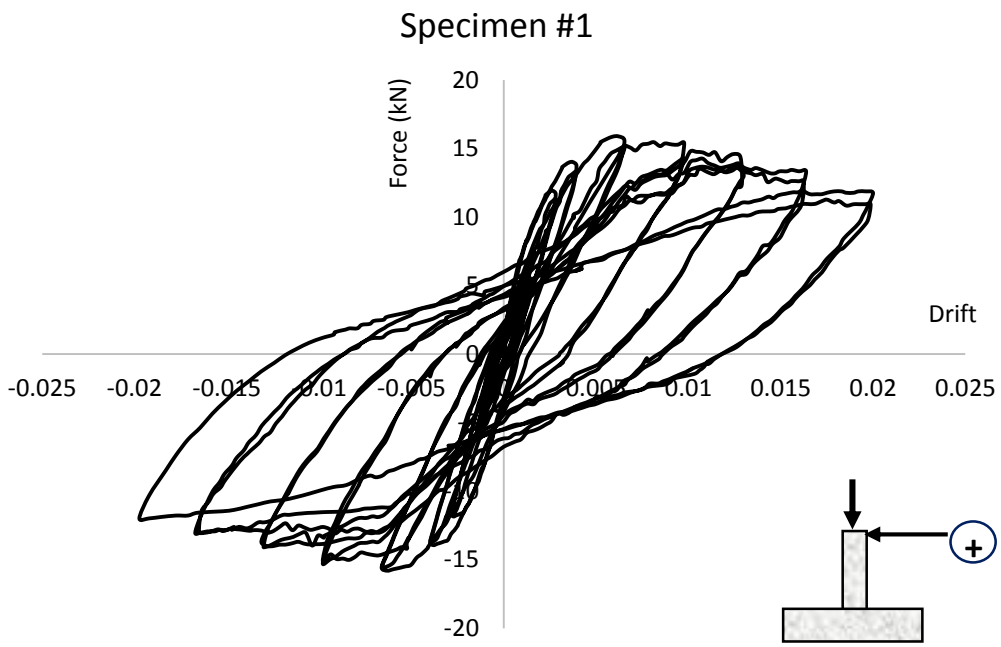

Figure 3.11. Hysteretic Force-Drift data of the specimen # 1

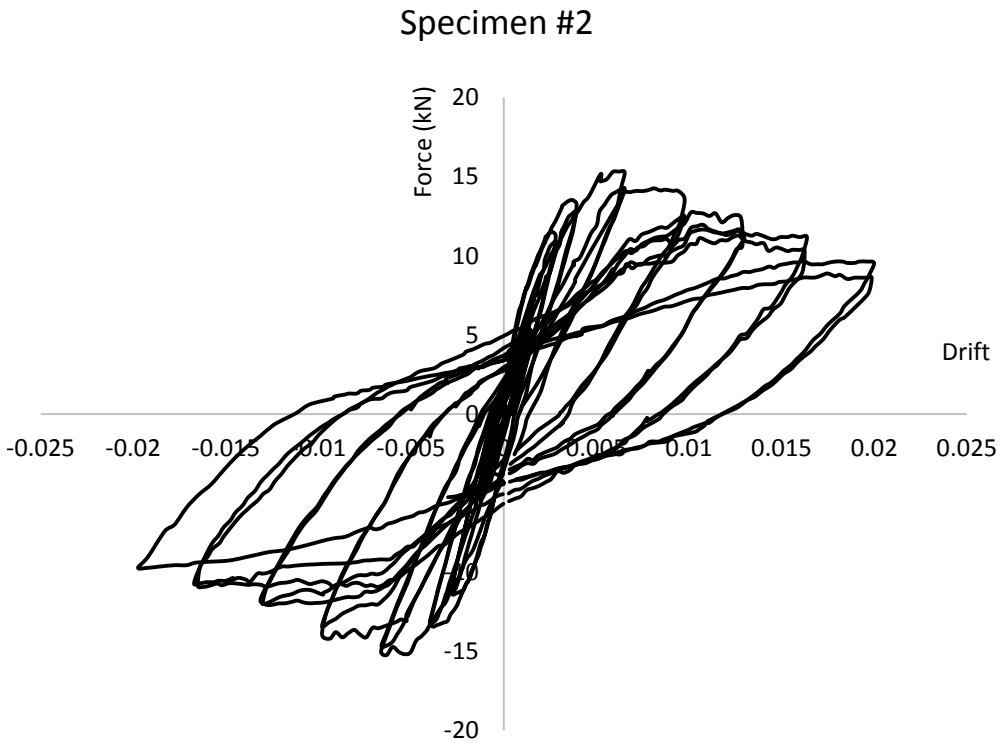

Figure 3.12. Hysteretic Force-Drift data of the specimen # 2

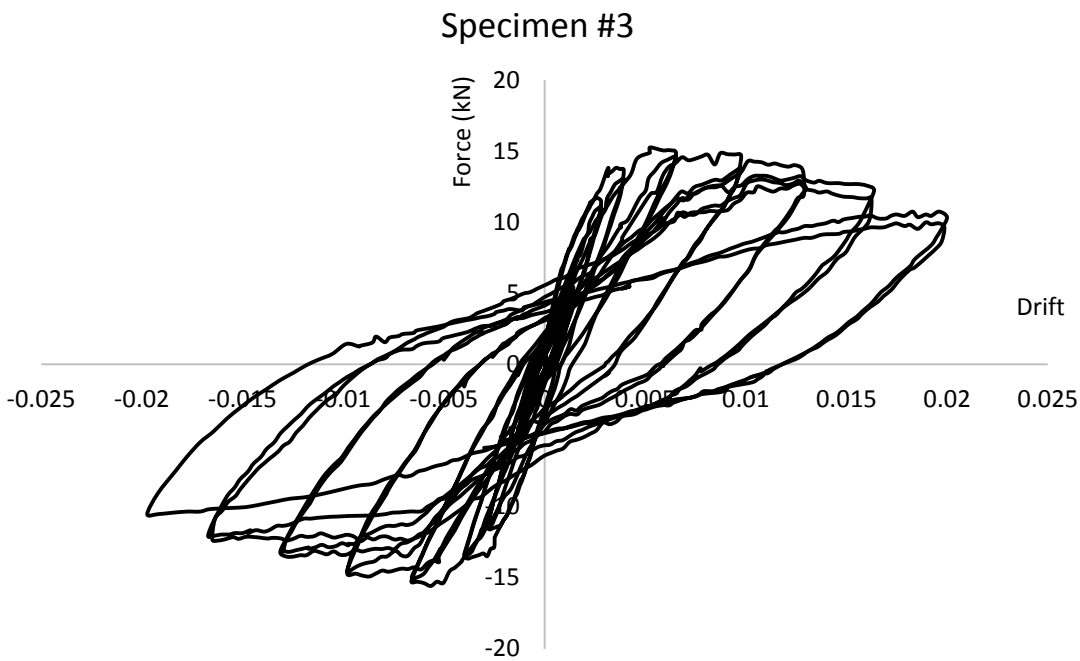

Figure 3.13. Hysteretic Force-Drift data of the specimen # 3

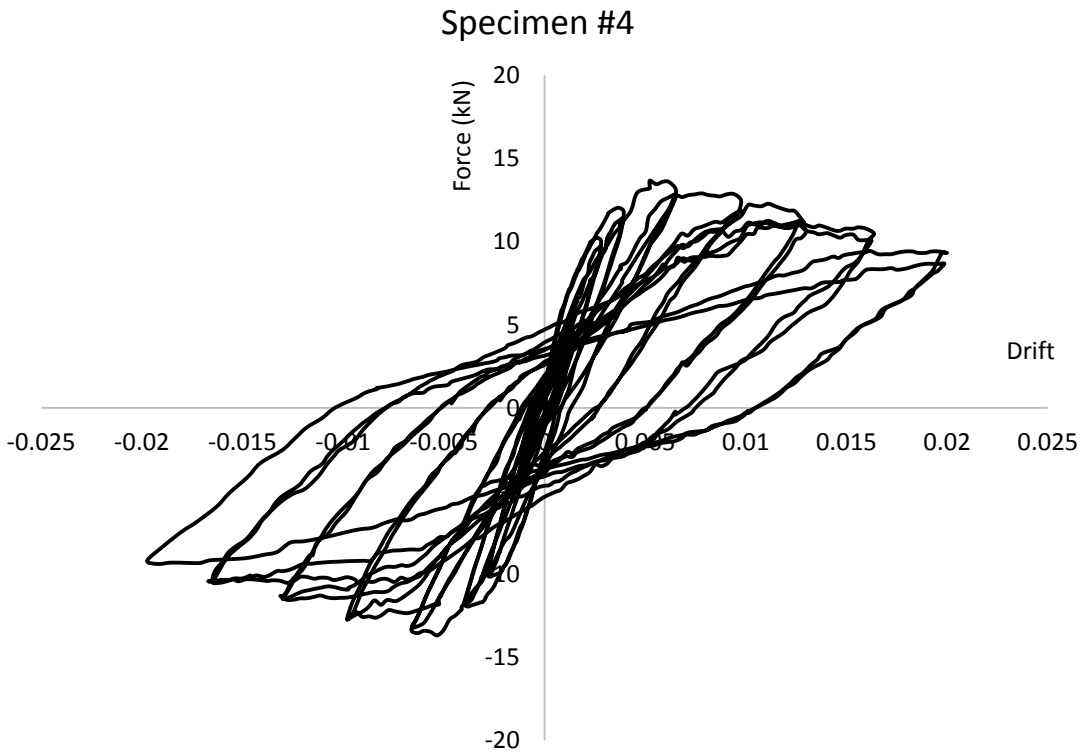

Figure 3.14. Hysteretic Force-Drift data of the specimen # 4

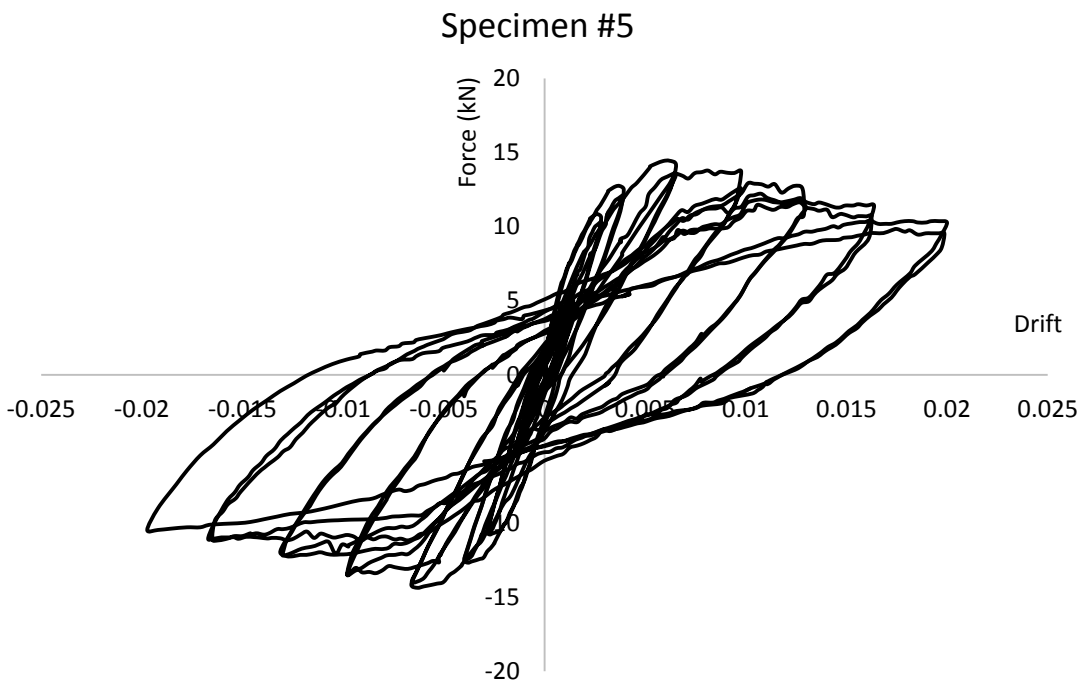

Figure 3.15. Hysteretic Force-Drift data of the specimen # 5

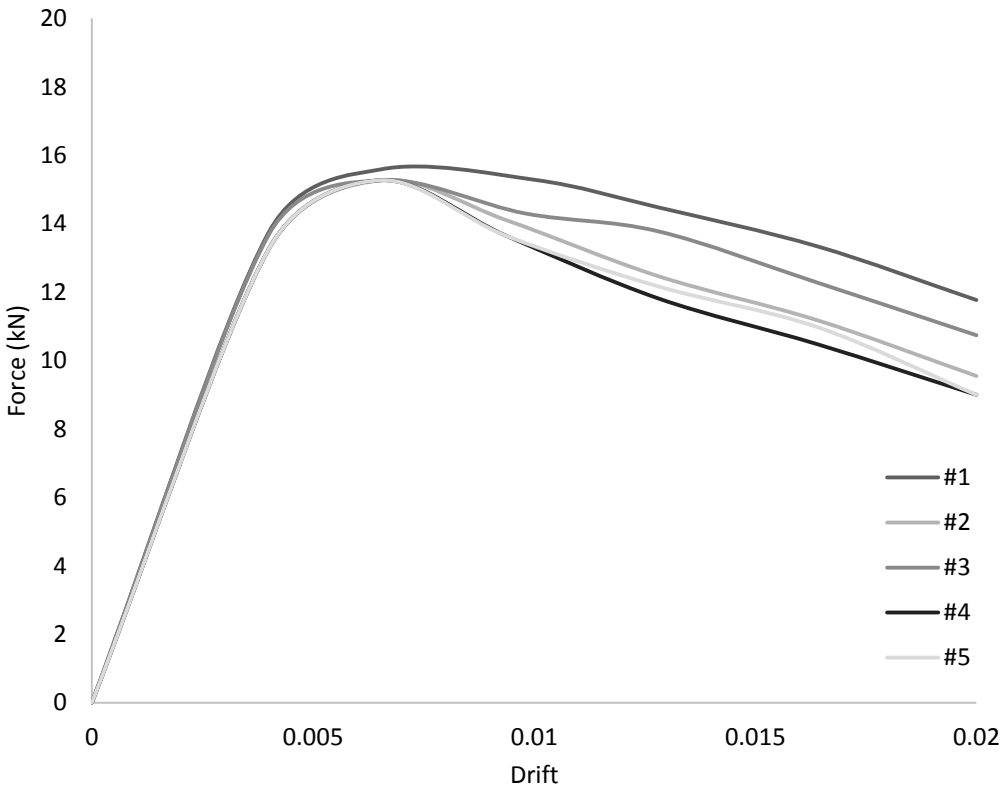

Figure 3.16. Hysteretic Force-Drift backbones of closely tied specimens

No visual difference was observed for the specimens tested. First the flexural cracks were initiated and with the repetitive increments the cover concrete spalled. The 20% strength decay occurred at early stages and no visual observations of hook opening and bar buckling took place.

When the hysteretic behaviour of the specimens were investigated, a moderate behaviour was observed. The pinching effect was evident especially for the specimen #2 which led to the reduction in absorbed energy and discussed later in this thesis. Loading and unloading stiffness as well as maximum strength differed for the specimens #1 and #2. No failure of the stirrup steel was observed at the end of the test due to the flexural failure mode. The difference at the initial yielding stage was observed to be insignificant. However at later stages, with the cumulative cycles the difference became more evident.

Initial stiffness of the specimen at early loading steps, was not influenced when different stirrup setting was tested. Furthermore, no difference in flexural cracks were evident during the initial period of test. The stiffness decay started for the specimen # 1 and #3 at 5th cycle where the cyclic deterioration resulted both the reloading and unloading stiffness reduction. Figure 3.16 shows the force versus lateral drift where initially no strength and stiffness decay was observed. However on later loading stages, especially after the peak amplitude in strength was reached, the difference in behaviour became more evident. Figure 3.17 shows the secant stiffness of last 6 cycle increments. An apparent difference between specimen #1 and #2 occurs at post cracked stage which caused huge difference in energy absorption.

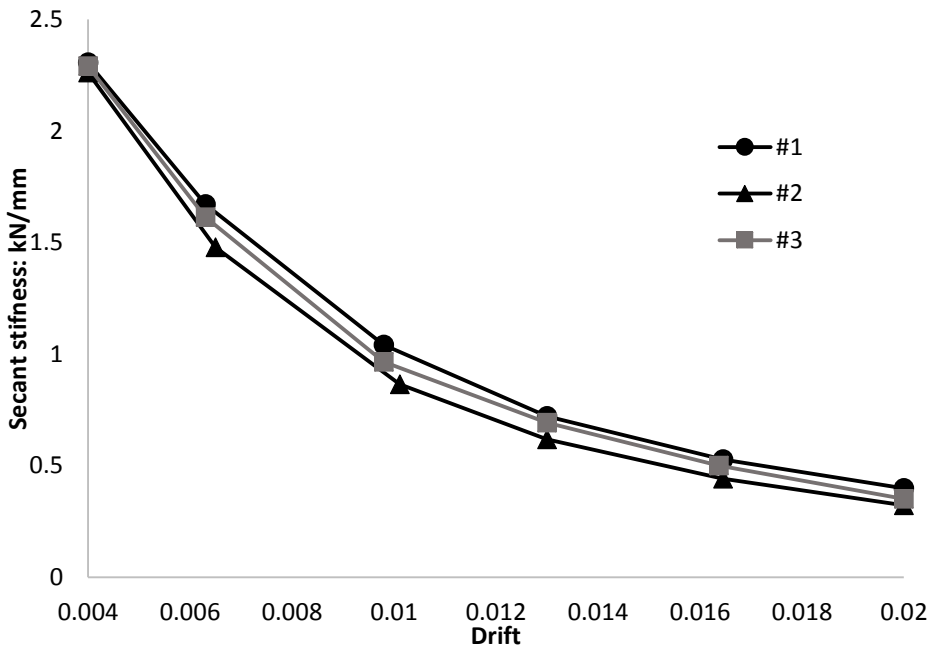

3.17. Comparison of secant stiffness of closely tied specimens

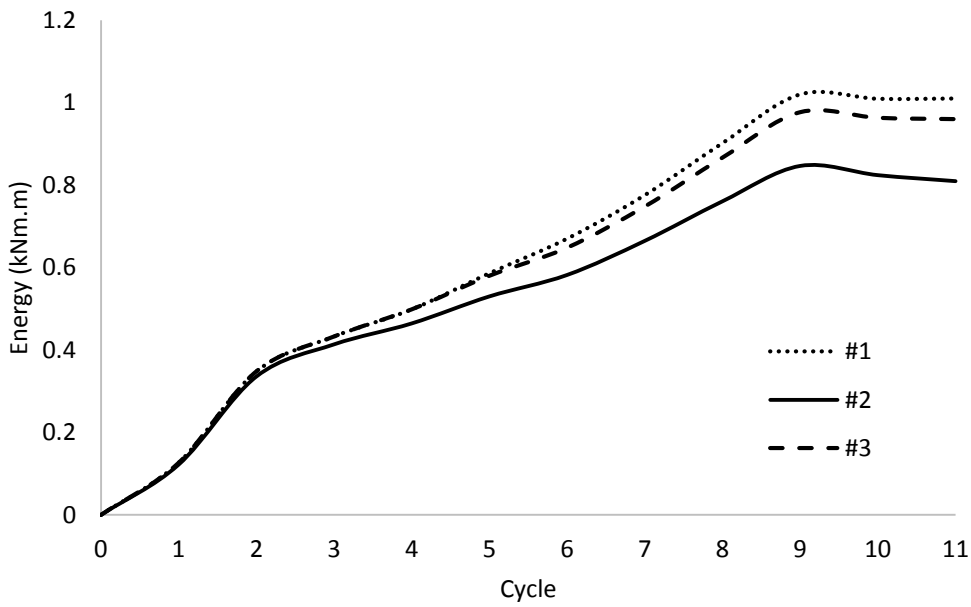

3.18. Energy based assessment of closely tied specimens

Starting with the initial cycles, the specimen #2 faced deterioration in energy. Reduction in absorbed energy was evident, when the 3rd and onward cycles were investigated. The difference in absorbed energy per cycle for specimens #1 and #2 at cycle number 6 is 13% and at cycle 11 is 20%. Unlike to the specimen #2, the relative

energy decay of specimen #3 started at the 5th cycle. A maximum of 5% difference was obtained when #1 and #3 were compared in terms of energy per cycle. Nevertheless, the dissipated cumulative energy do not significantly differ for the specimen #1 and #3. Figure 3.19 shows the cumulative energy absorption after each cycle. An obvious energy reduction was observed for the specimen #2 where a total of 14% less energy was absorbed in the end of the test.

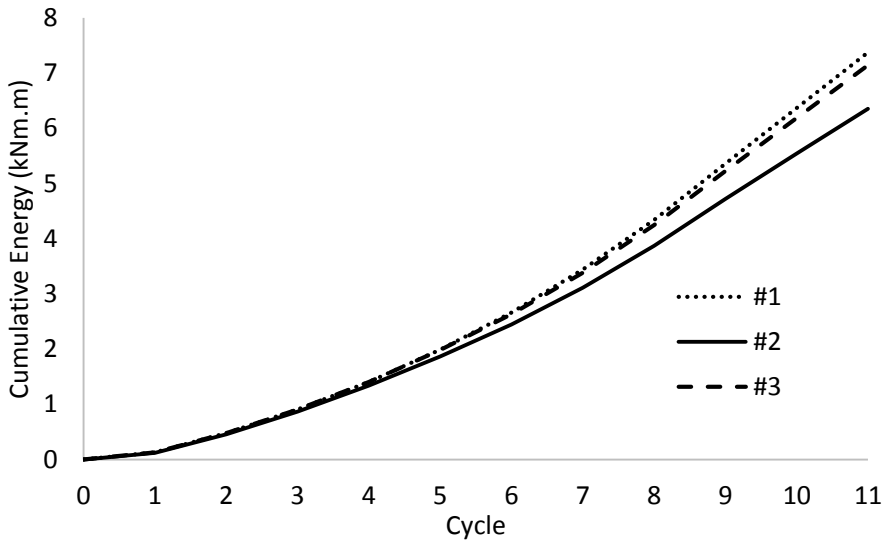

Figure 3.19. Cumulative energy based assessment of closely tied specimens

The rest of the specimens were aimed to test the pre-seismic period detailing conditions where close stirrup setting did not exist. No considerable performance decay until the late stages of the test was evident when #4 and #5 were investigated. When the 11th cycle was investigated, in which the major capacity drop occurred, 10% difference in energy was observed.

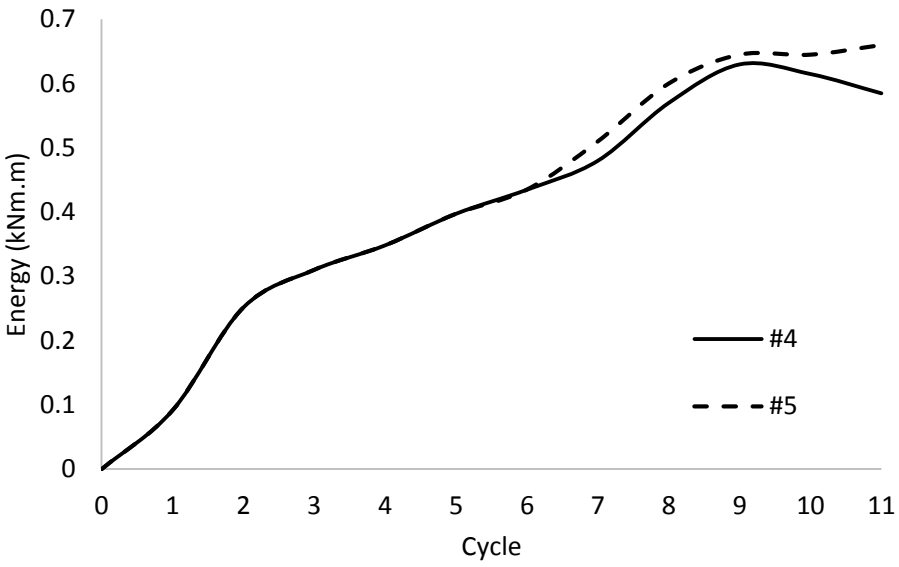

Figure 3.20. Energy based assessment of loosely tied specimens

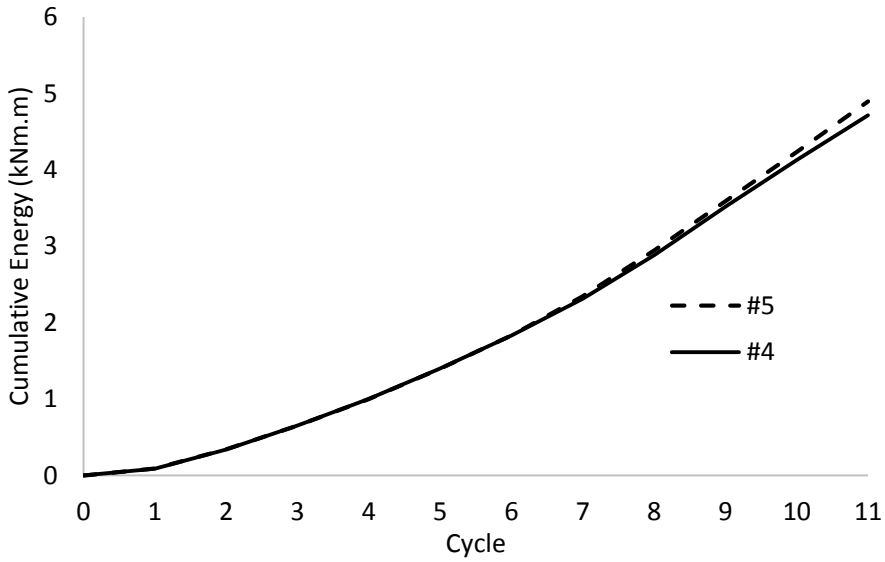

Figure 3.21. Cumulative energy based assessment of loosely tied specimens

Crush of concrete and cover spalling phenomenon was observed in the last cycle for all specimens. But apart from the visual observations, the plain surface 90° stirrups resulted in major energy reduction when closely tied specimens were investigated. The reduced stiffness and ductility were observed at late stages of the loading period. Thus the evaluation of such columns with plain stirrups having 90° hooks require a special

attention in order to consider pinching and stiffness decay. Underestimating such behaviour may result in non-conservative response of improperly detailed columns.

In general the greatest difference was obtained for the columns with close stirrups. When #1 and #2 were compared a 19% reduction in drift capacity was read due to the 90° plain surface stirrups. On the other hand, only 4% reduction was obtained when the 135° plain and deformed stirrups were compared. The drift capacity difference on columns with lightly reinforced columns is rather less. Due to the larger spacing of stirrups of the column #4 and #5, the confinement effect is rather less compared to specimen #1, #2 and #3.

The proposed study evaluated the response of lightly reinforced rectangular RC columns with high shear span to depth ratio. The test specimen were designed by considering the local material of the pre-seismic period. Thus the low concrete strength and plain surface stirrup reinforcement scenario was utilized. Therefore the test results are not applicable to high concrete strength condition.

This study aimed to investigate the seismic performance of the improperly tied plain surface stirrups. Unlike the previous studies, non-shear critical columns with light longitudinal reinforcement ratio were investigated. The test results are utilised later in modelling where definitions are given in Chapter 4. As a recommendation for the future studies, a ductility reduction factor can be created if an axial load sensitive study is to be performed.

Chapter 4

ANALYTICAL ASSESSMENT

Based on the local components of analytical assessment properties, a test structure was formed by considering, experimental material properties, local hazard data, local construction practice (in terms of number of storeys and structural detailing parameters), and advanced corrosion models. The case study models are based on deterministic parameters with the purpose of corrosion and material related performance decay was aimed. In this chapter initially the deterministic parameters are explained and the information on case study models were given. Then the modelling strategy is explained where the lumped plasticity moment-curvature relationships were derived for both corroded and un-corroded conditions. A brief information on historical ground motion database is also given and ground motion selection strategy was explained.

4.1. Case Study Models

Upon investigation of local construction statistics as well as design practice, two deterministic analytical models were tested. 2 and 5 storey frame structures were generated representing the low and mid-rise building stock. The building frames were then utilized to compare the material and seismic detailing rules respect with corrosion deterioration. The modifications were made on material and section details to facilitate advanced corrosion modelling. The corrosion effects were used to model the ground level columns where the degradation is usually expected to form. The numerical case study models are given in figure 4.1.

Seismostruct v2016 (2016) structural analysis tool was utilized within this study. Nonlinear Incremental Dynamic Analysis (IDA) was performed on case study models. The modelling methodology consists of concentrated plasticity at member ends for shear-flexure capacities of members and also at member joints where the beam-column joint shear strength was assigned. Corrosion modelling was considered at the ground floor columns where modification were made on moment curvature relationships in which explained later in this chapter.

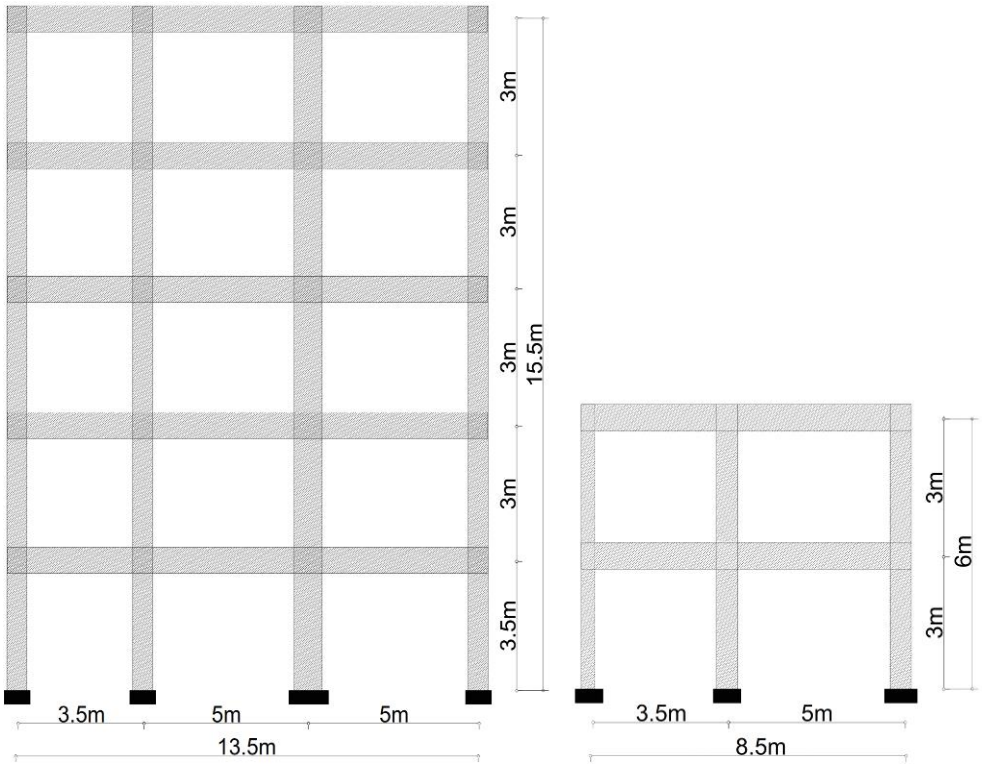

Figure 4.1. Analytical model geometries, 5 storey frame (left) and 2 storey frame (right)

A deterministic approach was considered for the section models with the purpose of highlighting the relative reduction due to both material and corrosion effects. The reinforced concrete sections were modelled by adopting deterioration models such as bond, mechanical and constitutive behaviour of steel and cover degradation. The plastic hinge properties of each column was modified by combining the statistical

material groups and different deterioration levels. The same concrete strength was used for the entire frame and the variation of the concrete strength between structural elements or different stories is not considered within this study.

Corrosion on reinforced concrete members results the expansion of reinforcement where the longitudinal cracks occur. As the crack width increases the effectiveness of the concrete cover decreases and leads to loss of bond. According to the recent studies, such an aggressive corrosion level is expected to occur at 13-15% mass loss of rebar (Nepal and Chen 2015, Zhou et. al 2015). In this study the corrosion is modelled at 10% mass loss for convenience. The case study models consider the 16th, 50th and 84th percentiles as the lower, median and upper concrete strength levels for each time period.

4.1.1 Structural Details of the Models

Pre-seismic models often have 200mm section width where the limit was raised to 250mm later in seismic period. Narrow old-type sections are usually lightly reinforced in both longitudinal and lateral directions. However, the diameter of longitudinal steel bars were greater in pre-seismic period due to mild steel properties. Adaptation of deformed bars allowed the use of higher strength steel material where the longitudinal bar diameter is reduced later in seismic period. The section properties are given in following figure 4.2.

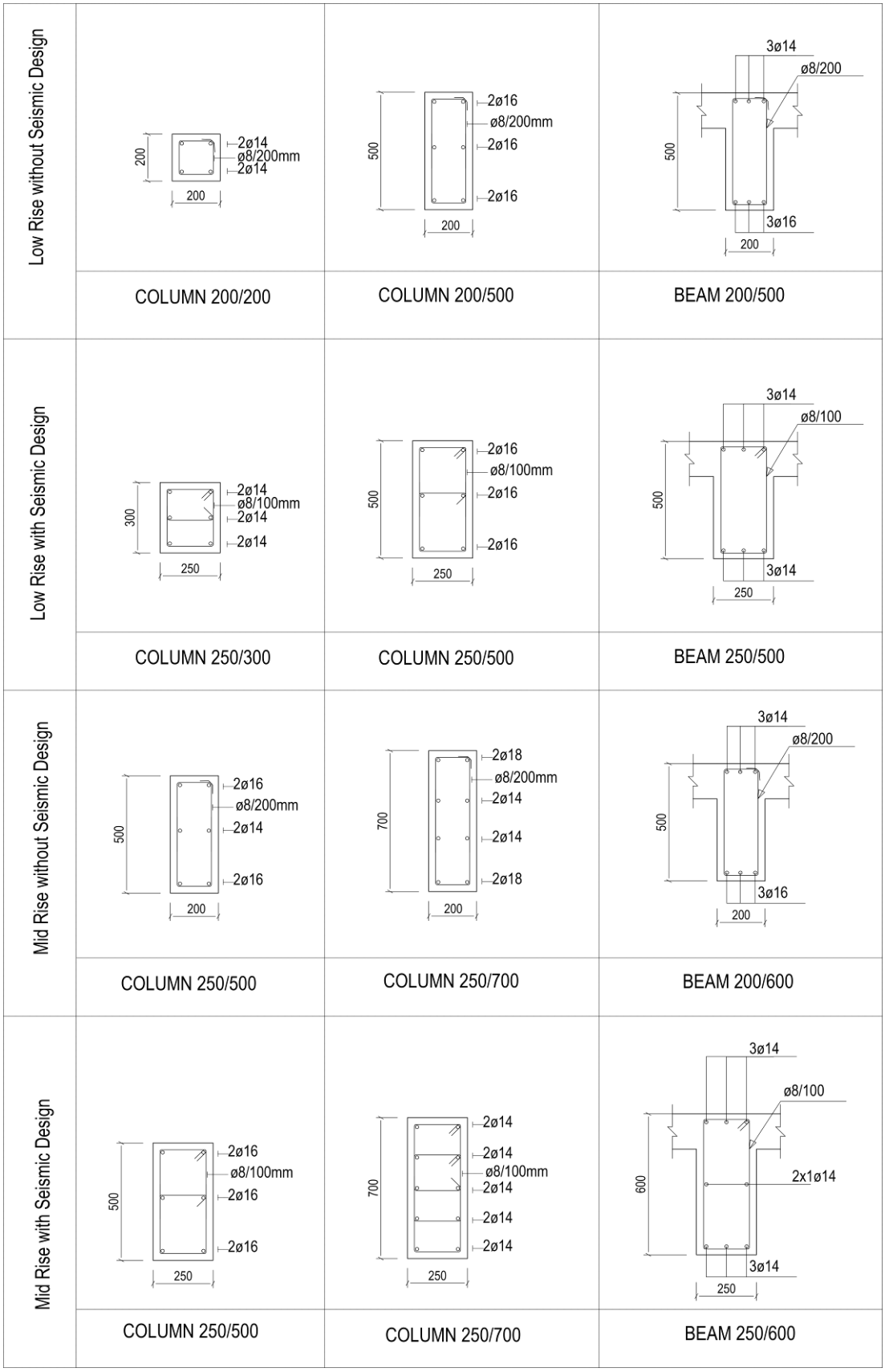

Figure 4.2. Section Properties of the case study models

Table 4.1 Analytical Case Study Models, Deterministic Material Properties

	No Corrosion	10% Corrosion	Concrete Strength	Rebar Type
Pre-Seismic Period <1999	PN1	PC1	8MPa	Plain F_y: 260MPa
	PN2	PC2	17MPa	
	PN3	PC3	26MPa	
Seismic Period >1999	SN1	SC1	18MPa	Deformed F_y: 460MPa
	SN2	SC2	26MPa	
	SN3	SC3	33MPa	

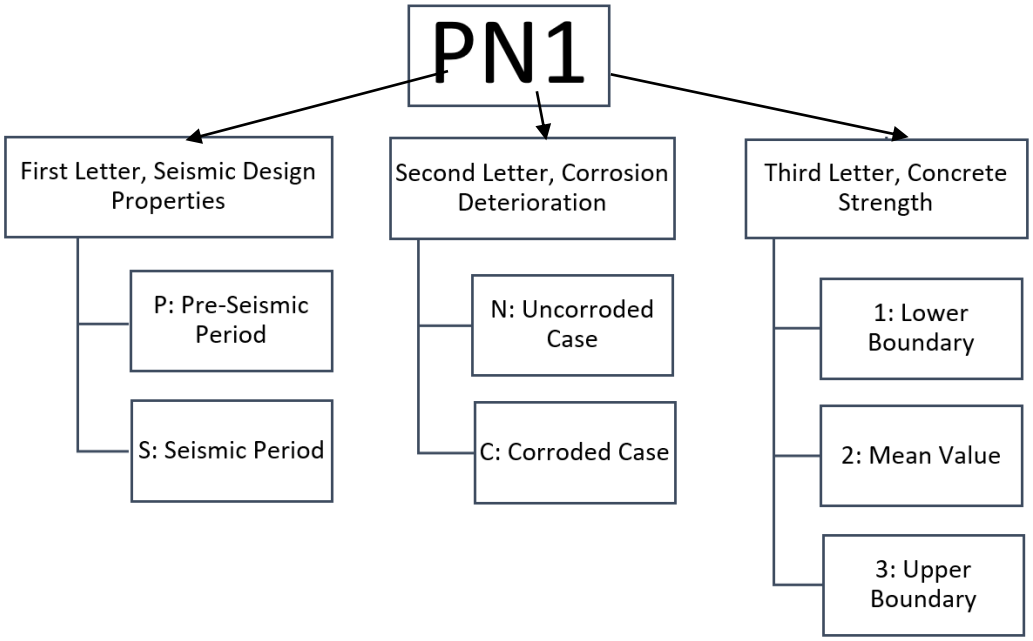

Figure 4.3. Case study groups explained

Deterministic material properties were assigned to analytical case study models. The method of analysis was aimed to investigate the material specific variance in seismic performance. Upper, lower and mean values of the concrete strength have been investigated by considering the local material distribution data. Due to the low

variance in steel material, constant steel properties were assigned to corresponding groups.

4.1.2 Nonlinear Concrete Model

Nonlinear behaviour of concrete is expected to be improved when the section core is well confined (Mander et al., 1988). The study by Mander et al., (1988) show that analytical model represents a good estimation of nonlinear behaviour and also allows the modification of confinement factor. The model provides a function which converts the applied confinement reinforcement type and quantity to the effective lateral confining stress.

4.1.3 Cover Concrete Deterioration

The degradation of the concrete cover respect to corrosion rate is also considered by adopting the methodology suggested by Coronelli and Gambarova (2004). The adopted model uses the crack width as a function of expansion in diameter due to corrosion products. Due to the amount of corrosion product produced, the mass loss for larger bar sizes would cause significantly more damage to the surrounding concrete compared to small bars. The equations from 2 to 5 are adopted for modelling cover strength degradation.

$$f_c^* = f_c / (1 + K (\varepsilon_1 / \varepsilon_{co}) \quad 4.1$$

$$\varepsilon_1 = (b_f - b_o) / b_o \quad 4.2$$

$$b_f - b_o = n_{bars}\, w_{cr} \quad 4.3$$

$$w_{cr} = 2\, \pi\, (v_{rs} - 1)\, X \quad 4.4$$

Where f_c^* is cover concrete strength, f_c initial concrete strength, K is coefficient related to bar diameter and roughness, ε_{co} is strain at peak concrete stress, ε_1 is average tensile strain. The strain ε_1 is estimated by equation 4.2 where b_f is section width in post corroded stage and b_o is initial section width. The b_f can be approximated by using

equation 4 where the number of bars is nominated by n_{bars} and corrosion related crack width w_{cr} which can be estimated by using equation 4.4 (Molina et al., 1993). X is corrosion depth and v_{rs} is expansion ratio.

In this study old-type reinforced concrete columns where the longitudinal bar sizes are larger as the yield stress of plain reinforcement is low. Also the section width is 20% tighter where the longitudinal bars are closer. The cover concrete strength reduction is estimated to be 69% for the old type and 58% for the new type RC columns when subjected to 10% corrosion. In general the cover strength reduction of the new RC columns is estimated to be 26% less when compared with the old type RC columns. This is due to the less corrosion product generation of the smaller diameter deformed bars as well as the greater width of the new type columns. The comparison is given in the Table 4.2.

Table 4.2. Cover concrete compressive strength values for uncorroded reinforcement cross sections and 10% mass loss cross sections: a comparison illustrating level of degradation due to corrosion.

	Uncorroded	10% Mass Loss Midrise	10% Mass Loss Short rise
Old Type RC	1.0 f_c	0.31 f_c	0.37 f_c
Seismic Design RC		0.42 f_c	0.42 f_c

4.1.4 Reinforcing Steel

The reinforcing steel has a significant role on section behaviour when exposed to corrosion. Tension behaviour of the corroded rebar is modelled by the use of empirical relationships as an outcome of the experimental study on material

deterioration. The modelling of the compression reinforcement on the other hand considers the buckling phenomena of the poorly confined bars. The study by Kashani et. al (2015) is adapted for modelling the compression reinforcement behaviour for the bars with confinement span to diameter ratio (L/D) higher than 6. On the other hand for the sections with L/D less than 6 the model suggests the use of tension envelope for the compression steel. The case study models for the seismic design period (SN and SC groups) were assigned the tension envelope for both tension and compression reinforcement. The following model by Kashani et al., (2015) was adopted for modelling the post buckling behaviour of the compression reinforcement for the gravity load designed cases where the L/D ratio is in the range 8-30.

$$\sigma_c : \sigma^* + (\sigma_y - \sigma^*) \exp(- (\rho_1 + \rho_2\sqrt{\varepsilon_p})(\varepsilon_p)) \qquad 4.5$$

Where σ_c is the corroded reinforcement post buckling compressional stress, ρ_1 is the initial tangent of the post-buckling response curve, ρ_2 is the rate of change of the tangent, σ^* is the asymptotic lower stress limit of the post-buckling curve and ε_p is the plastic strain. σ_y is the yield stress at tension condition.

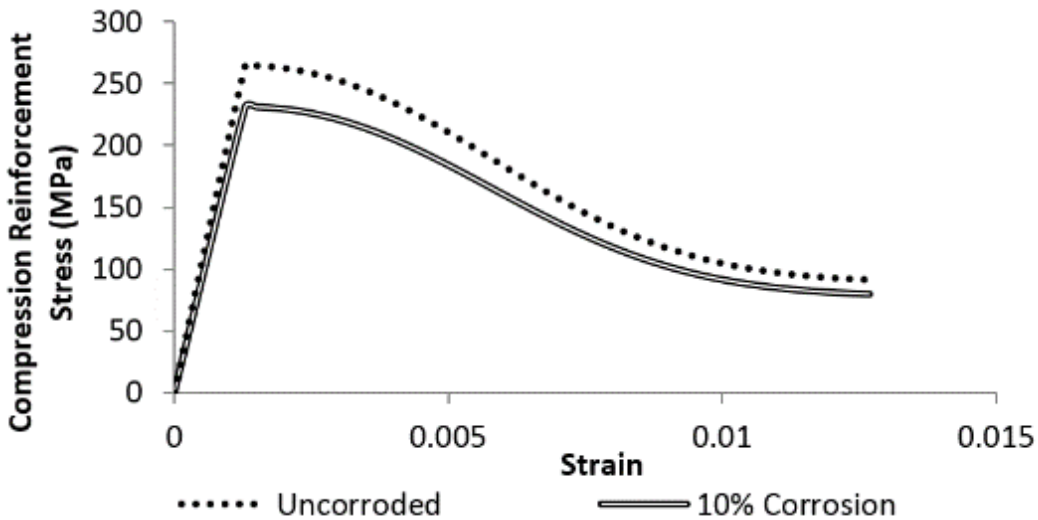

Figure 4.4. Plain Reinforcing Steel Compression Stress – Strain Envelope, Constitutive Model by Kashani et al., (2015)

An assumption of perfect bond between reinforcement and surrounding concrete in modelling may cause un-conservative results as suggested by Kwak and Kim (2006). Bond strength for the plain bars developing as a result of plain friction action is lower whereas the deformed bars tend to exhibit much greater bond characteristics due to the radial component. On the other hand corrosion results in a significant bond deterioration. The bond reduction model by Lee et al., (2002) was adopted and the bond strength for each model was updated with respect to corrosion level. Bond and corrosion models are given in Table 4.3.

Table 4.3 Bond models for Plain and Deformed Bars (CEB-FIB and Lee et al., 2002)

	τ_{max}	$\tau_{max,\ Corroded} / \tau_{max,\ Uncorroded}$
Plain Bars	$\tau_{max} = 0.3\sqrt{f_c}$	$e^{-0.0561\Delta w}$
Deformed Bars	$\tau_{max} = 2.5\sqrt{f_c}$	

Where: τ_{max} = maximum bond strength (MPa) and f_c = the compressive strength of concrete (MPa). Δ_w = mass loss in percentage

4.1.5 Shear

Poorly detailed sections tend to fail if the shear demand is not satisfied. Recent studies (Sezen and Moehle, 2004, Elwood and Moehle, 2005, Galanis and Moehle 2015) show that sections with enough shear strength may fail under shear with increasing ductility demand. Another significant shear vulnerability may arise by hook opening of the improperly detailed stirrup. In 1999, Turkey witnessed the failures due to the hook opening of the improperly detailed columns as a consequence of the Kocaeli

Earthquake (Sezen et al., 2003). An assumption was made on opening of 90 degrees stirrup hooks when modelling the shear strength of old type sections. A similar methodology is suggested by Ersoy et al., (2008) where the steel contribution to the shear strength is assumed to be vanished once the cover concrete spalls.

The two component shear strength model by Sezen and Moehle (2004) was adopted for modelling which is given for the convenience of the reader in Eq 4.6. The model also suggests up to 30% reduction in strength due to increase in flexural ductility. The model uses an empirical reduction coefficient *k* which modifies both of the shear strength components with respect to ductility.

$$V_n = V_{steel} + V_{concrete} = k\left(\frac{A_v}{s} f_y d\right) + k\left(\frac{0.5\sqrt{f_c}}{a/d}\sqrt{1+\frac{P}{0.5\sqrt{f_c}\,A_g}}\right)0.8A_g \qquad 4.6$$

Where k: coefficient related to ductility, a: shear span, d: depth of section, P: axial load, A_g: gross area of the section, s: stirrup spacing, A_v: stirrup area, f_y: stirrup yield strength.

Corrosion level was assumed to be equal for both longitudinal and stirrup reinforcement. Reduction in yield stress as well as ultimate strain was considered for stirrups. However the stirrup bond loss was not utilised in this thesis for convenience. As a final point, a combined hysteretic behaviour is generated for each case by combining the slip, shear and flexural deformations as suggested by Sezen and Chowdhury (2009). The plastic hinge properties are explained later in this thesis.

4.1.6 Modelling Beam-Column Connection

The non-seismically designed (unconfined) beam-column connections usually suffer shear failures when subjected to earthquakes. The lack of confining reinforcement at the beam-column connection, causes high shear stress on concrete. Modelling of a

beam-column joint is possible by assigning the diagonal struts with an equivalent shear strength. As stated by Park and Mosalam (2013), with an increase in beam depth the steeper the diagonal strut is generated where the horizontal shear strength decreases. This is the case especially for the gravity load designed apartment's upper storey beam-column connection, where the columns were designed for less cross sectional area. The joint model by Park and Mosalam (2013) was adopted in this study.

4.2 Plastic Hinge Properties

The plastic behaviour of the frame section properties often modelled by using lumped plasticity at both member ends. The frame models were generated by considering the model specific moment curvature relationships and application through the zero length link elements. The hysteretic behaviour was modelled by adopting the multilinear hysteretic rule (Sivaselvan and Reinhorn 1999) with polygonal detailing capacity. The hysteresis rule was initially developed by Park et al., (1987) and later developed by Sivaselvan and Reinhorn (1999) by allowing the modification of the rule by adjusting branches as function of force displacement relationships. A Tri-Linear backbone curve was adopted for the purpose of best fit to the experimental results.

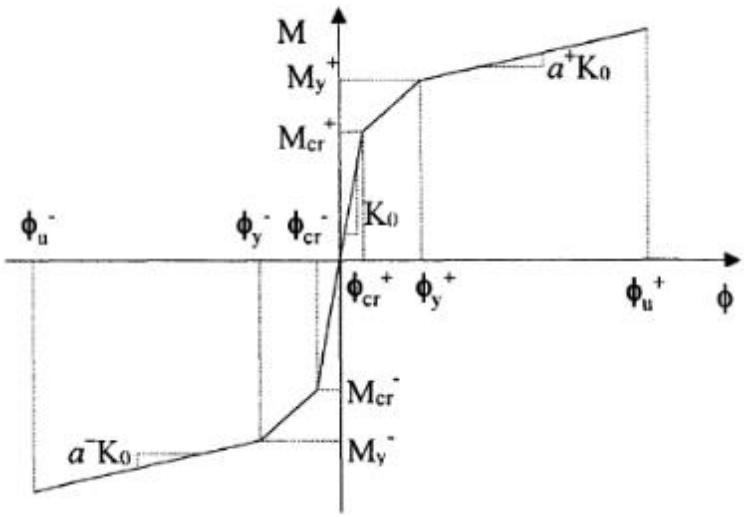

Figure 4.5. Trilinear backbone curve (Sivaselvan and Reinhorn 1999)

Where Φ_{cr}: cracking curvature, Φ_y: yielding curvature, Φ_u: Ultimate curvature, and similarly M_{cr}: Cracking moment, M_y: Yielding moment, K_0: initial stiffness and α: post yield stiffness ratio.

4.2.1 Calibration of Lumped Plasticity

The same displacement time history from the experimental study was assigned to the analytical model on Seismostruct zero length hinge properties and adjustment was done on hysteresis properties (Loading unloading stiffness slopes etc.). An iterative process by adjusting the slopes were considered until the best match was observed. Once the slope ratios were obtained then considered for the case study models. The given Figure 4.6 shows the analytical and experimental models' hysteresis comparison with the same loading data.

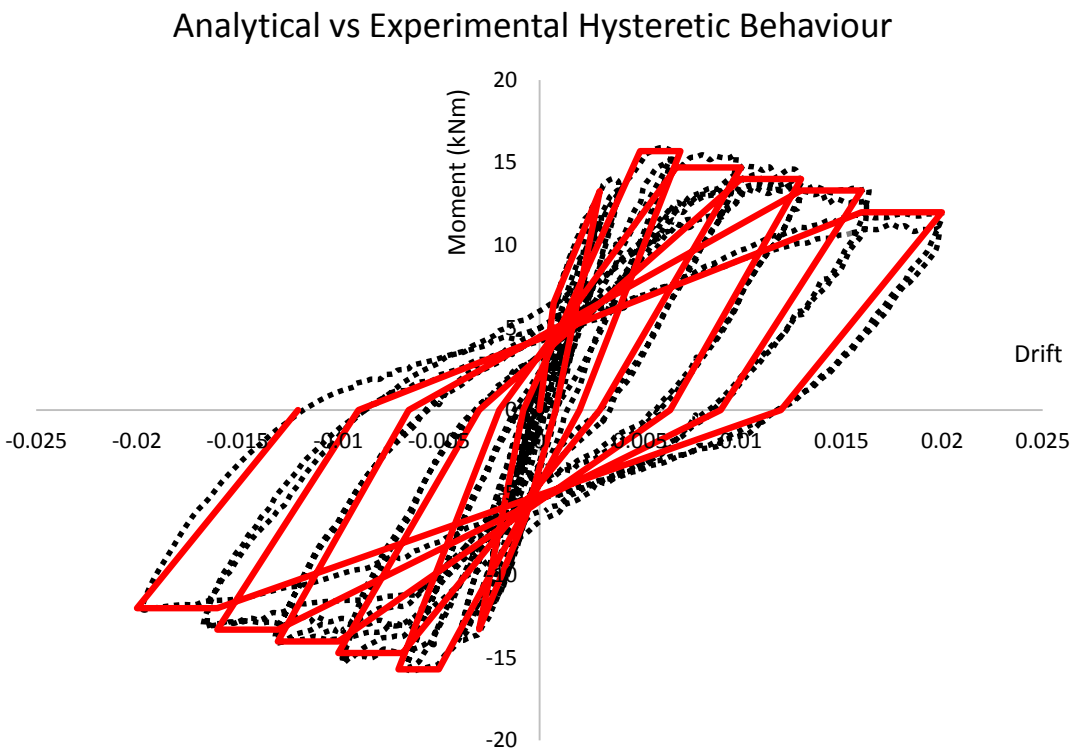

Figure 4.6. Calibration of analytical model with the experimental data (Column #1)

4.3 Viscous Damping Model

According to the recent studies on modelling of elastic viscous damping for nonlinear time history analysis, the use of tangent stiffness proportional Rayleigh Damping Model results an increase in response (Priestly and Grant, 2005). Experimental studies also indicate that, when ductility demand of a structural member increases, the viscous damping energy reduces proportional to the post yield stiffness of the member (Petrini et al., 2008). Due to that reason it is often recommended to use tangent stiffness proportional damping models for the structures that are expected to face large deformations. The tangent stiffness proportional Rayleigh damping model is given in Equation 4.7 (Chopra, 2001).

$$C = (a_0 \,.\, M) + (a_1 \,.\, K_T) \qquad 4.7$$

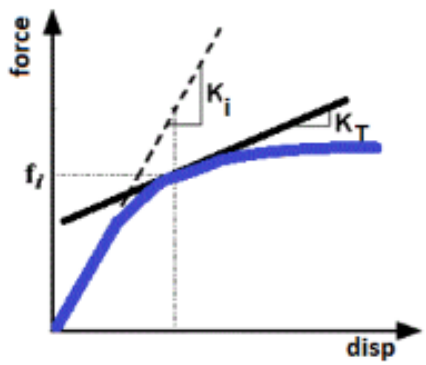

Figure 4.7. Difference Between Initial and Tangent Stiffness

Where C: Damping matrix, a_0: mass coefficient, M: Mass, a_1: Mass coefficient, K_T: Tangent Stiffness. Due to yielding, reduction in stiffness (Figure 4.7) reduces the overall damping forces.

4.4 Damage Index

Seismic assessment codes usually define the 4% drift ratio as a safe "Collapse Prevention" drift limit for assessing the reinforced concrete buildings (Turkish Earthquake Code, 2007). However, the code specified limits may be an un-conservative choice in case of evaluating a non-ductile / deteriorated frame structure. Individual damage thresholds were generated within this study by employing the static adaptive pushover analyses to the sample frames. In order to facilitate brittle and ductile failure modes, the functions of both displacement and base shear results were utilized based on first occurrence (Table 4.4). The displacement based assessment utilises the ultimate deformation capacity (θ_u), which is reached by occurrence of ultimate deformation capacity (shear and/or flexure) of 20% of the columns at same storey. All damage criteria were grouped under CEN Eurocode 8 Annex A (2004) classification. Similar methodology was also suggested by Milutinovic and Trendafiloski (2003), Ulrich et al., (2014) and Silva et al., (2015).

Table 4.4. Damage Classification for Assessment. (Safkan et al., 2017)

	Damage Limitation (DL)	Significant Damage (SD)	Near Collapse (NC)
Base Shear	50% Maximum Base Shear	Maximum Base Shear	20% reduction Maximum Base Shear
Displacement	$\theta_E \leq \theta_Y$	$0.75\ \theta_u \leq \theta_u$	$0.90\ \theta_u \leq \theta_u$

Where θ_e: Elastic Deformation limit, θ_u: Ultimate Deformation and θ_y: Yielding Deformation obtained from the pushover analyses.

Damage Limitation (DL) performance level represents the damage mainly on non-structural elements where the repair could be achieved within the economical measures. The Significant Damage (SD) level recommends important level of damage to the structural elements but expected to resist the after-shock events. Near Collapse (NC) damage level suffers severe structural damage in which an aftershock event may cause the total collapse (EC8, 2004).

4.5 Seismicity of Cyprus

Cyprus experienced many destructive earthquakes through its history. However the development of strong motion networks on the island is rather recent. Earliest recordings started in late 1990's and the database still lacks events with long return periods. The strong motion data of 23 different events (Safkan, 2014) with moment magnitudes in the range 4-6 were listed in Table 4.5. The soft soil amplification was also investigated in the study where the great increase in relative acceleration was observed at longer periods (Figure 4.8).

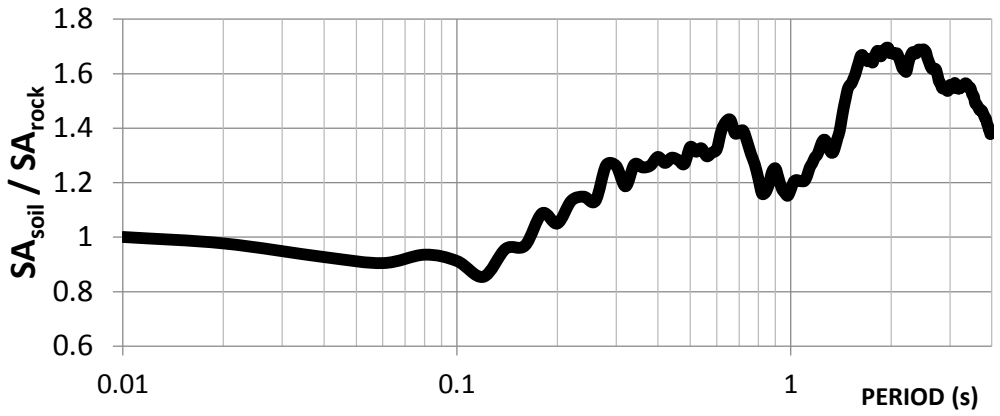

Figure 4.8. Soft soil amplification based on observed data

Table 4.5. Strong motion database of Cyprus

Date	Latitude	Longitude	Ml	Depth (kM)	Nearest Record Distance (kM)	No of Records
13.01.1997	34.294	32.307	5.3	19	79	1
21.04.1998	34.883	33.007	4.2	5	23.9	1
25.05.1999	34.490	32.300	4.8	30	56.3	4
11.08.1999	34.750	33.030	5.2	12	5	3
13.08.1999	34.808	32.981	4.6	5	16.3	1
17.08.1999	34.826	32.998	4.4	5	17.8	1
26.08.1999	34.851	33.026	4.2	5	20.2	1
16.12.2000	33.574	33.358	4.3	30	125.3	1
25.10.2002	34.982	32.743	4.3	38	34.1	2
03.11.2003	34.700	33.060	4	10	3.8	4
18.05.2004	34.620	33.310	4	10	26	1
16.10.2004	34.431	33.286	4.5	30	10.2	5
15.10.2006	34.940	33.960	4.4	32	20.1	1
28.08.2007	34.900	33.500	4.2	11	16.9	3
25.08.2009	34.740	33.090	4.6	31	13.1	4
16.09.2009	34.860	33.060	4.6	10	24.4	5
22.12.2009	35.910	31.430	5.4	25	154.2	4
11.05.2012	34.960	32.380	5.4	17	100.7	2
23.10.2013	36.351	34.332	4.5	21	92.9	2
28.12.2013	35.987	31.342	6	42	167.6	3
03.02.2014	34.813	32.549	4.1	10.3	58.2	9
14.02.2014	36.750	36.040	4.5	15.7	215.8	4
06.03.2014	35.980	31.370	4.3	39.5	157.1	2

Current seismic design practice in North Cyprus is the Turkish Earthquake Code 2007. The code provided acceleration design spectra considers the elongation of period of peak amplitude but do not consider the soil amplification. The new seismic design code which will be in effective by the end of 2018 will consider soil amplification.

4.6 Ground Motion Selection

The use of peak ground acceleration as the only intensity measure may increase the variation of response when choosing ground motions for analysing buildings with time history analysis (Chopra, 2001). In order to reduce this response variance, the spectral acceleration is considered as the intensity measure in this study. The properly selected accelerograms would realistically describe the record-to-record variability that in turn results in coherent structural response estimations. (Ay and Akkar, 2012)

According to Jayaram et al., (2001), the variation of the spectral acceleration intensities at target period range of the chosen ground motion also results inconsistent input acceleration which creates divergence in the overall response of the buildings. The matching target spectrum to the uniform hazard spectrum generates a conservative modification as there will be a single scale factor for the whole period range. The analyses by using the uniform hazard spectrum where the scaling is done uniformly on entire period range, the estimate may result higher responses at longer period range due to nonlinear elongation of fundamental period and excitation of higher modes at shorter period range (Jayaram et al., 2001). The conditional mean spectrum however considers period specific ground motion selection where the divergence due to input acceleration is kept minimum.

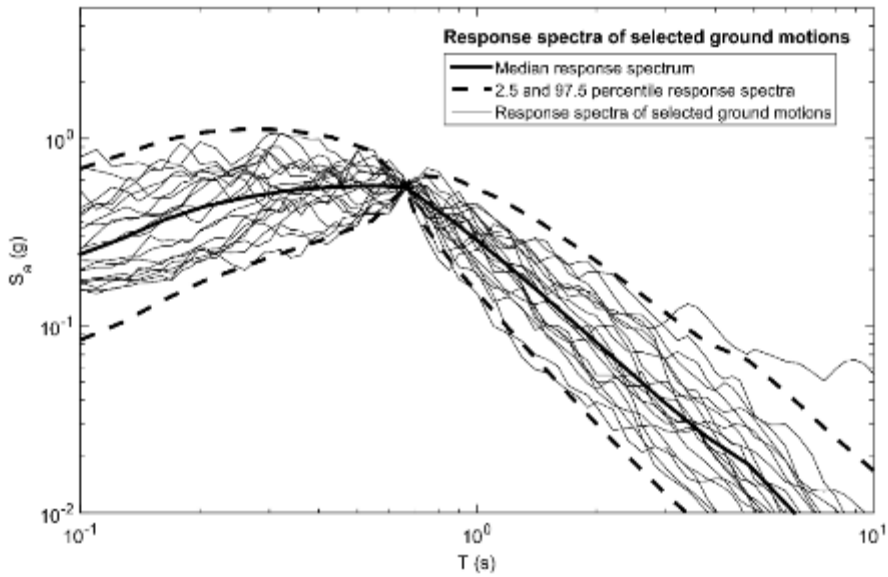

Figure 4.9. Selected ground motion set by using Conditional Mean Spectra (After Jayaram et al., 2001)

The conditional mean spectra (Jayaram et al., 2001) was adopted in this study for ground motion selection and response spectra of the chosen motions are presented in Figure 4.9. A total of 20 ground motions were selected by considering hazard deaggregation study results based on parameters such as magnitude, distance and the target intensity measure (Table 4.6). These deaggregation parameters are obtained based on the recent seismic hazard assessment study of Cagnan and Tanircan (2010). Both return periods of 475 and 2475 years were considered in this study.

Table 4.6. Ground Motion Dataset used for the Incremental Dynamic Analysis

	Name	Year	Location	Mag. (Mw)	RJB (km)	VS (m/s)	FAULT TYPE
1	PEER531	1986	Puerta La Cruz	6.1	67.5	442	Reverse
2	PEER686	1987	Whitter Narrows	5.9	40.9	390	Reverse
3	PEER750	1989	Loma Prieta	6.9	79	623	Reverse
4	PEER2089	2002	Alaska	6.7	106	341	Strike Slip
5	PEER0036	1966	Cholame Shandon	6.2	9.6	290	Strike Slip
6	PEER0163	1975	Oroville	5.7	9.8	590	Normal
7	PEER4500	2009	L`Aquila Italy	6.3	60.8	535	Normal
8	PEER1122	1995	Kozani, Greece	6.4	72.8	650	Normal
9	PEER0266	1980	Sahop Casa Flores	6.3	19.0	242	Strike Slip
10	PEER0268	1980	Sahop Casa Flores	6.3	39.1	260	Strike Slip
11	PEER0313	1981	Corinth, Greece	6.6	10.3	361	Normal
12	PEER0463	1981	Taiwan	5.9	26.4	309	Reverse
13	PEER0534	1986	San Jacinto Valley	6.1	23.0	447	Reverse
14	PEER0535	1986	San Jacinto Valley	6.1	30.7	331	Reverse
15	PEER0548	1986	Chalfant Valley	6.2	21.6	371	Strike Slip
16	PEER0718	1987	Imperial Valley Wildlife	6.2	17.6	179	Strike Slip
17	PEER0729	1987	Imperial Valley Wildlife	6.5	23.9	207	Strike Slip
18	PEER3300	1999	Chi Chi	6.3	27.6	553	Reverse
19	PEER2727	1999	Chi Chi	6.2	76.3	247	Strike Slip
20	PEER441	1983	Borah Peak	6.9	80	324	Normal

Chapter 5

RESULTS AND DISCUSSIONS

Case study models were analysed first by pushover analyses then followed by the incremental dynamic analysis. The pushover analyses were considered for the drift estimation and the IDA assessment led to investigation of seismic capacity reduction due to corrosion. The ductility reduction due to corrosion and concrete strength difference is investigated for pre-seismic and seismic groups individually. In general relatively more brittle behaviour was observed for both groups when lower bound of corresponding concrete class was considered.

5.1 Pushover Analysis

In general the collapse behaviour of the pre-seismic models showed brittle trend where the strength capacity dropped suddenly. In that case the displacement based damage judgment dominated the estimation of SD level as the NC damage level was reached suddenly.

Consideration of detailed corrosion models resulted in a brittle behaviour where the dependence on concrete strength has been magnified. Unlike the study by Berto et al., (2009), when the corroded models' upper and lower bound concrete strengths are compared against ultimate drift ratios, a 34 % difference is observed for the pre seismic models whereas the difference is 12% for the seismically designed models.

Comparison of cover strength degradation for different sections highlights the effect of reinforcement ratio on corrosion vulnerability. The study revealed that the old type sections of the mid-rise buildings having greater diameter bars, resulted in a much greater corrosion product where the concrete cover strength is widely affected. This additional reduction in strength as well as other corrosion related degradation characteristics resulted in great damage to the pre-seismic models. The ultimate drift capacity has dropped by 40% and 30% for the lower (PC1) and upper (PC3) boundary of concrete classes respectively due to corrosion. When the mean groups of the pre-seismic period (PN2 vs. PC2) are compared, the effect of corrosion to global drift ratio is noted as 37%.

Unlike the pre-seismic period, the recently built columns consist high yield strength deformed reinforcement bars, and usual practice observations show that the popular bars for the columns are 14 mm or 16 mm in diameter. When compared with the old type plain 18mm diameter bars, less corrosion product is expected to affect the concrete cover. Also the initial strength of the concrete is also at a higher strength level for seismic period models. Additionally well confined sections are assumed to have non-slender longitudinal bars and the buckling effects were omitted in modelling the compression reinforcement. The corrosion related ultimate drift reduction of the seismic period models are observed to be much less when compared with the pre-seismic models. However, the ultimate drift ratio for the model SC1 shows that the drift levels for the building built according to the seismic design rules may also suffer an important damage at early drift levels. The Turkish Earthquake Code 2007 limits the Significant Damage Level to 4% interstorey drift, where the analysis yielded to 3.7% and 3.9% drift levels for SC1 and SC2 respectively.

The pushover analyses followed by the incremental dynamic analysis allow the assessment of seismic capacity reduction due to corrosion. The ductility of the models are widely affected by concrete strength, seismic design parameters and corrosion deterioration. In general relatively more brittle behaviour was observed for both pre-seismic and seismic models when lower bound of corresponding concrete class was considered. On the other hand, the influence of concrete strength on pre-seismic deteriorated models was rather more significant.

By considering detailed corrosion models resulted in a brittle behaviour where the dependence on concrete strength has been magnified. When the corroded models' upper and lower bound concrete strength are compared against ultimate drift ratios, a 34% difference obtained for the pre seismic models and 12% percent difference obtained for the seismically designed models. Comparing different cover strength degradation for different sections, highlight the effect of reinforcement ratio on corrosion vulnerability. This study also shows that the old type sections of the mid-rise buildings having greater diameter bars due to mild steel properties, resulted in a much greater corrosion product generation where the concrete cover strength is widely effected. This additional reduction in strength as well as other corrosion related degradation characteristics resulted in great damage to the pre-seismic models. The ultimate drift capacity has dropped by 40% and 30% for the lower (PC1) and upper (PC3) boundary of concrete classes respectively due to corrosion. When the mean groups of the pre-seismic period (PN2 vs. PC2) were compared, then the effect of the corrosion to the global drift ratio is noted as 37%.

Unlike to the pre-seismic period, the columns of seismic period buildings, consist high yield strength deformed reinforcement bars usually 14mm or 16mm in diameter.

When compared with the old type plain 18mm diameter bars, less corrosion product is expected to affect the concrete strength. Additionally well confined sections are assumed to have non-slender longitudinal bars and the buckling effects were omitted in modelling the compression reinforcement. The corrosion related ultimate drift reduction of the seismic period models observed to be much less when compared with the pre-seismic models. However, the ultimate drift ratio for the deteriorated model SC1 shows that the drift levels for the buildings constructed according to the seismic design rules may also suffer an important damage at early drift levels. The Turkish Earthquake Code 2007 limits the Significant Damage Level to 4% interstorey drift, where the analysis yielded to 3.7% and 3.9% drift levels for SC1 and SC2 respectively. The fragility parameters of the Damage Limitation (DL), Significant Damage (SD) and Near Collapse (NC) damage levels are presented in Table 5.1 and Table 5.2.

Table 5.1 Interstory Drift Limits (%) for the NC Damage Thresholds (2 Storey Frame Case Study)

	PN1	PN2	PN3	PC1	PC2	PC3	SN1	SN2	SN3	SC1	SC2	SC3
NC	2.7	3.1	3.4	2.1	2.5	2.7	5.2	5.2	5.2	4.1	4.6	4.8

Table 5.2 Interstory Drift Limits (%) for the NC Damage Thresholds (5 Storey Frame Case Study)

	PN1	PN2	PN3	PC1	PC2	PC3	SN1	SN2	SN3	SC1	SC2	SC3
NC	2.0	2.4	2.6	1.2	1.5	1.8	4.6	4.8	4.8	3.7	3.9	4.2

5.2 Fragility Curves

Incremental dynamic analyses were conducted on case models (12 models per frame) by using 20 ground motions and considering frequent scale factors. The increments were kept at minimum level and total of 20 increments per ground motion was

considered. In total 9600 time history analyses were utilised for deriving the following fragility functions. First, the initially derived pushover based damage estimation was applied on IDA curves and probabilistic fragility functions were generated.

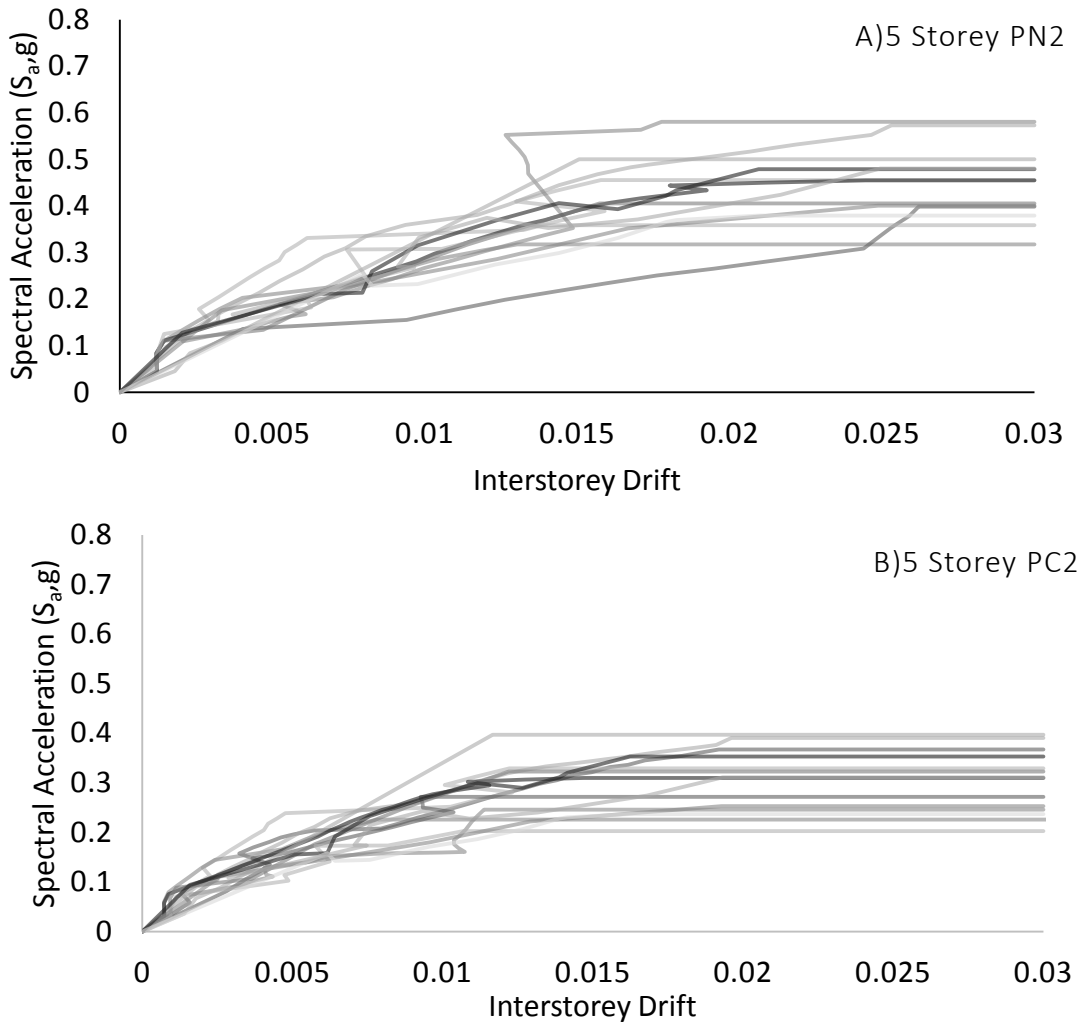

Figure 5.1. Incremental Dynamic Analysis Results of 5 Storey Frame: Comparison of pre-seismic (A) design period behaviour respect to corrosion deterioration (B)

Relatively less dispersed response to the ground motions were observed for the corroded "Pre-Seismic" models due to the increased brittle trend of frame model. Both the acceleration and drift values are reduced due to the corrosion (Figure 5.1). Another predominant difference was the more brittle behaviour of the corroded models yielded to a more flattened results. Uncorroded models on the other hand showed "weaving

behaviour" due to post yield response as discussed by Vamvatsikos and Cornell (2002). The 16th, 50th and 84th percentile IDA curves for the analysed models are utilised and the model specific fragility curves are given as follows. Figures from 5.2 to 5.13 present the short rise fragility curves and from 5.14 to 5.25 present the mid-rise fragility curves. All three Damage Limitation (DL), Significant Damage (SD) and Near Collapse (NC) fragility plots are presented.

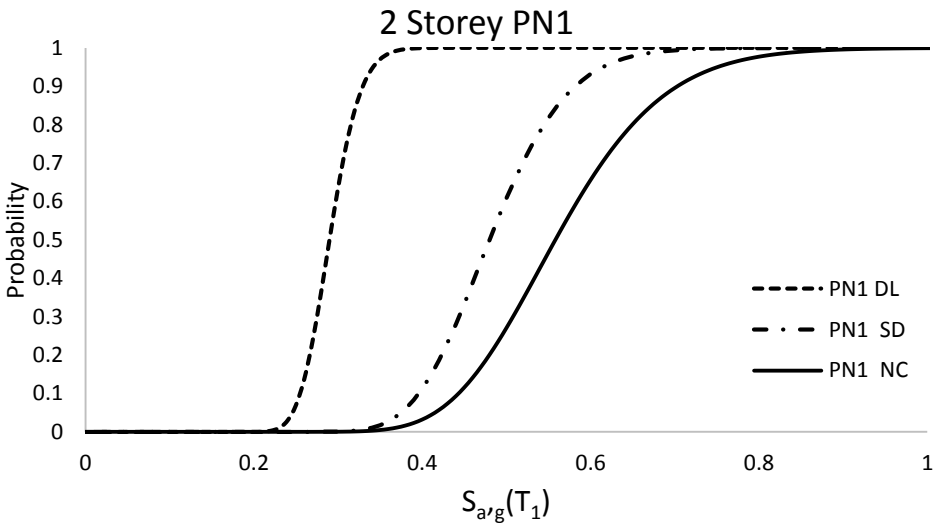

Figure 5.2. Seismic Fragility Curves for 2 Storey PN1 model

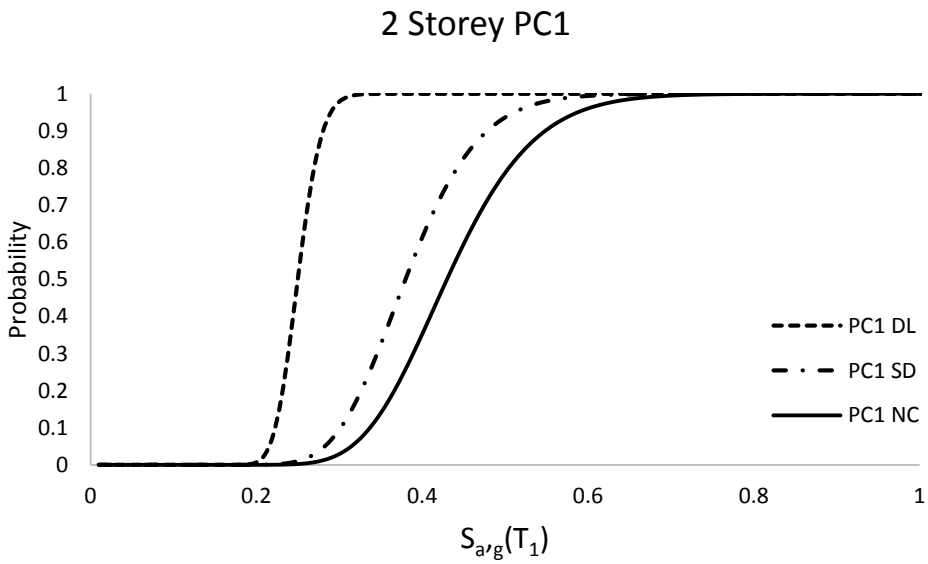

Figure 5.3. Seismic Fragility Curves for 2 Storey PC1 model

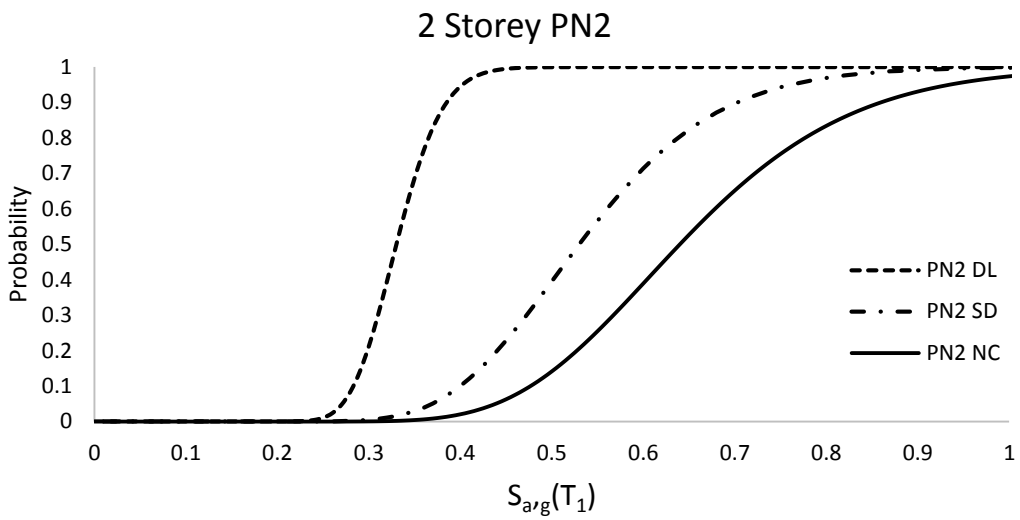

Figure 5.4. Seismic Fragility Curves for 2 Storey PN2 model

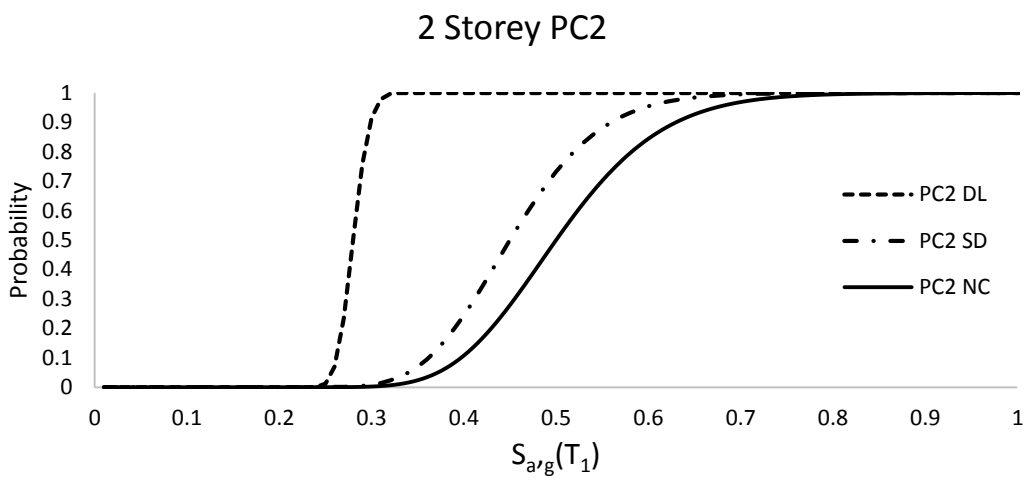

Figure 5.5. Seismic Fragility Curves for 2 Storey PC2 model

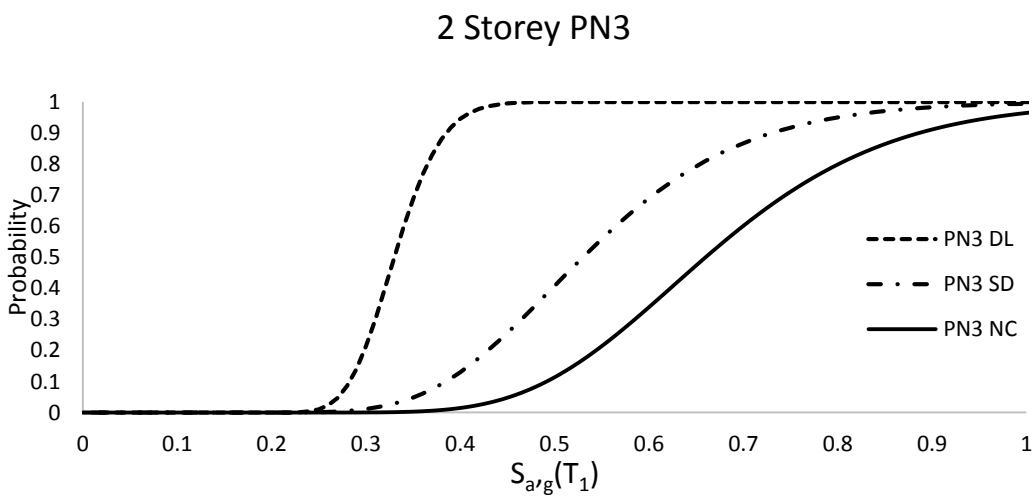

Figure 5.6. Seismic Fragility Curves for 2 Storey PN3 model

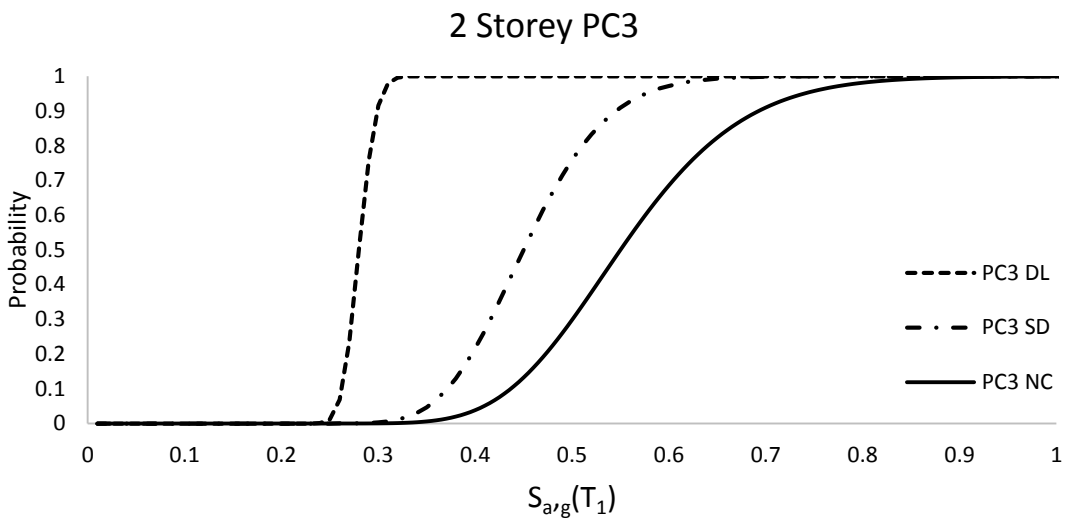

Figure 5.7. Seismic Fragility Curves for 2 Storey PC3 model

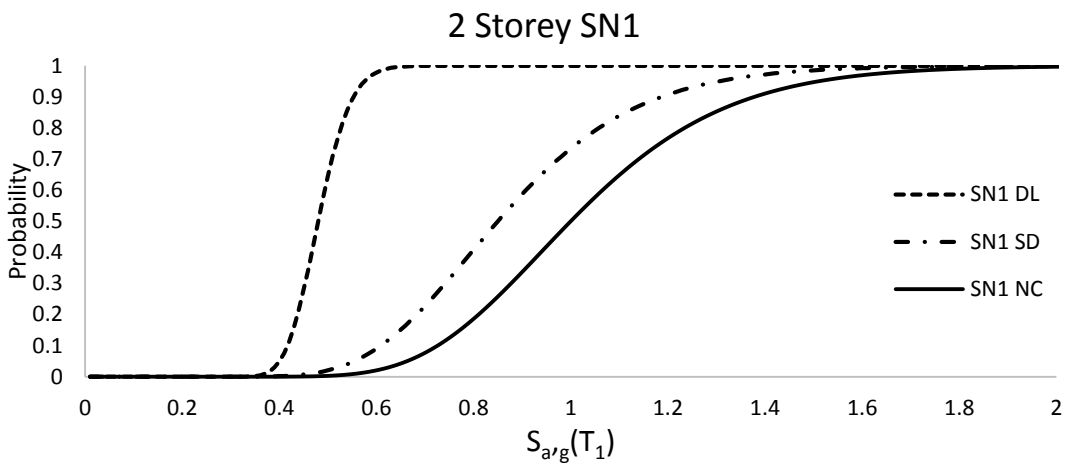

Figure 5.8. Seismic Fragility Curves for 2 Storey SN1 model

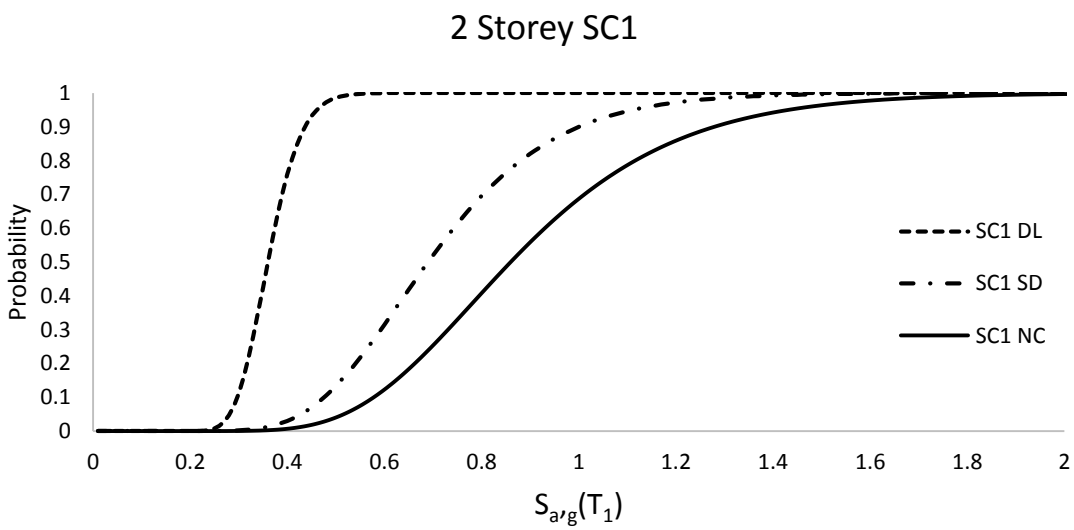

Figure 5.9. Seismic Fragility Curves for 2 Storey SC1 model

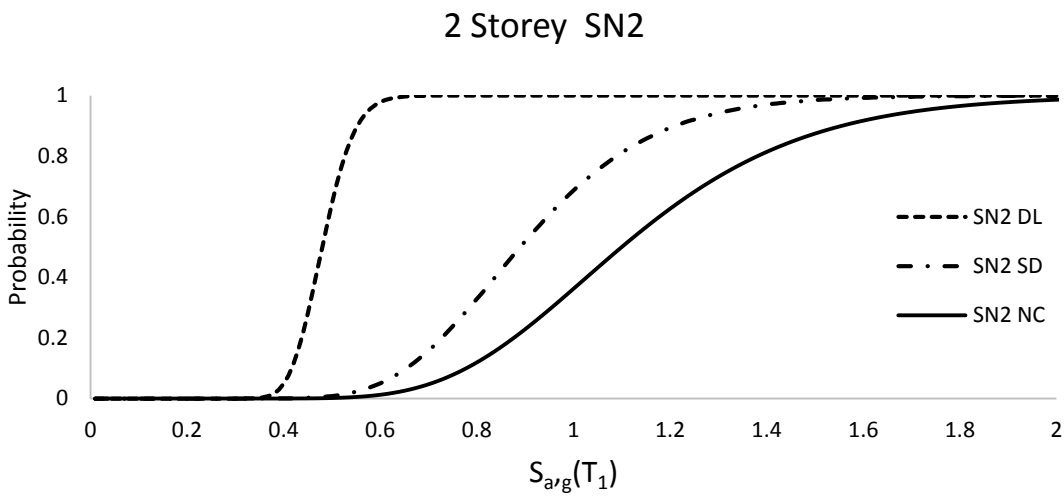

Figure 5.10. Seismic Fragility Curves for 2 Storey SN2 model

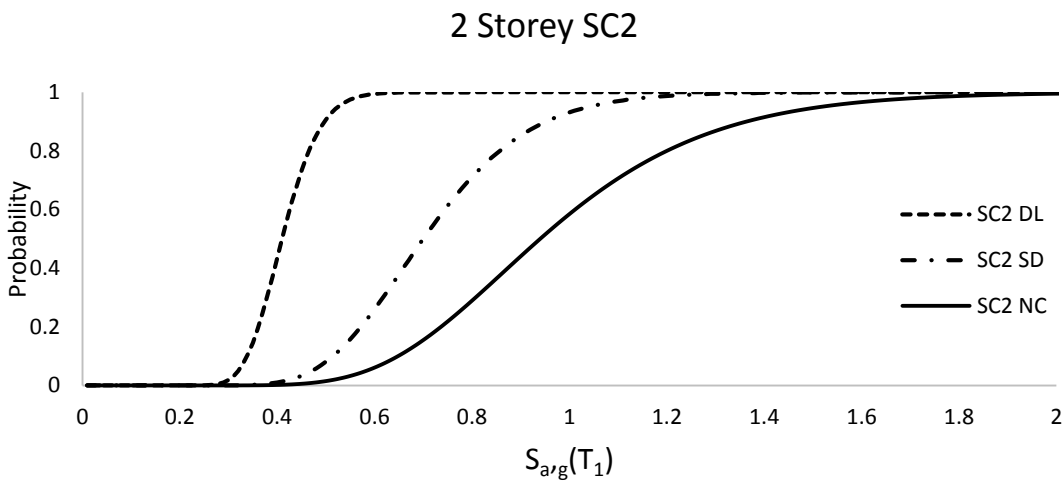

Figure 5.11. Seismic Fragility Curves for 2 Storey SC2 model

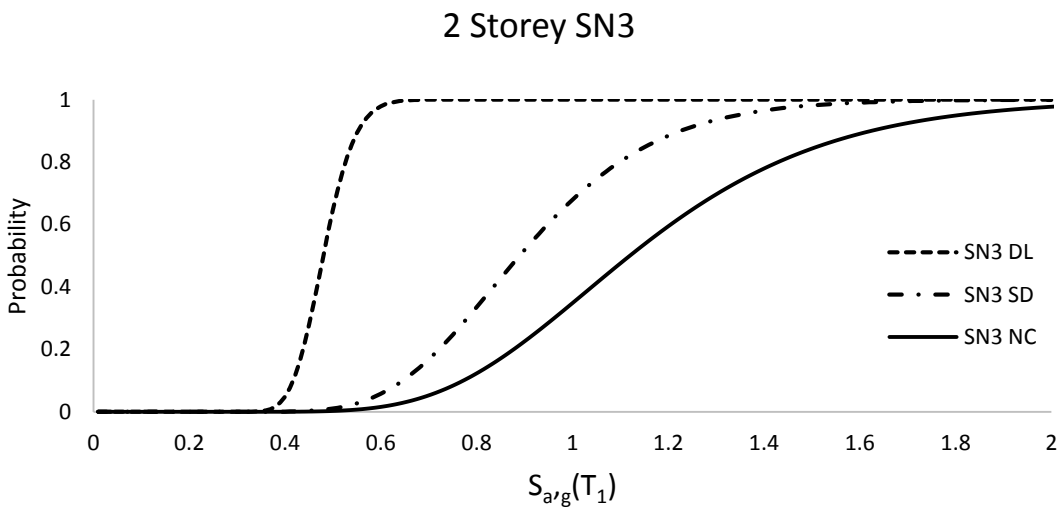

Figure 5.12. Seismic Fragility Curves for 2 Storey SN3 model

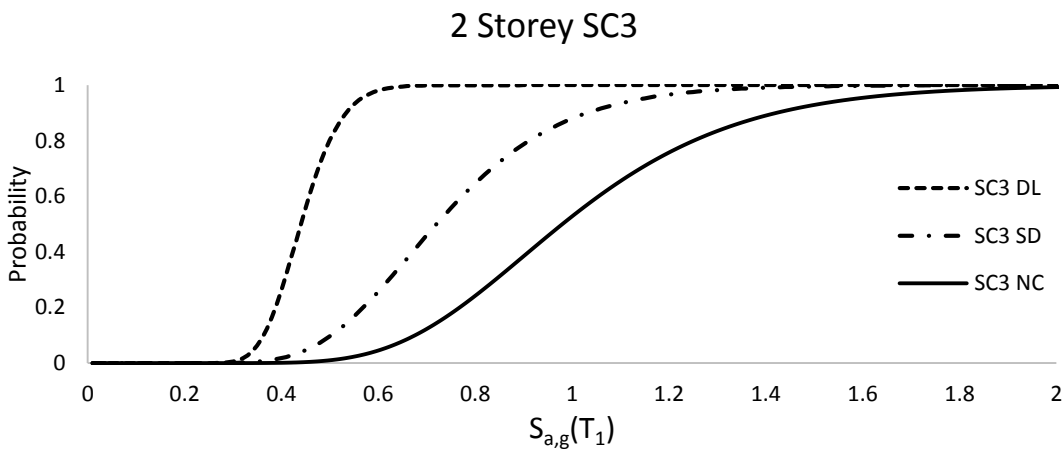

Figure 5.13. Seismic Fragility Curves for 2 Storey SC3 model

Table 5.3 Probabilistic Fragility Function Parameters for 2-storey frame

		PN1	PN2	PN3	PC1	PC2	PC3	SN1	SN2	SN3	SC1	SC2	SC3
DL	Θ	0.29	0.33	0.33	0.25	0.28	0.28	0.48	0.48	0.48	0.36	0.41	0.44
	β	0.1	0.12	0.12	0.09	0.05	0.05	0.11	0.11	0.11	0.15	0.15	0.15
SD	Θ	0.48	0.53	0.53	0.38	0.45	0.45	0.85	0.89	0.89	0.69	0.70	0.72
	β	0.15	0.22	0.25	0.18	0.17	0.15	0.26	0.24	0.25	0.29	0.24	0.28
NC	Θ	0.56	0.64	0.66	0.43	0.5	0.55	1	1.1	1.12	0.86	0.94	0.98
	β	0.18	0.23	0.23	0.19	0.18	0.18	0.25	0.27	0.29	0.31	0.29	0.29

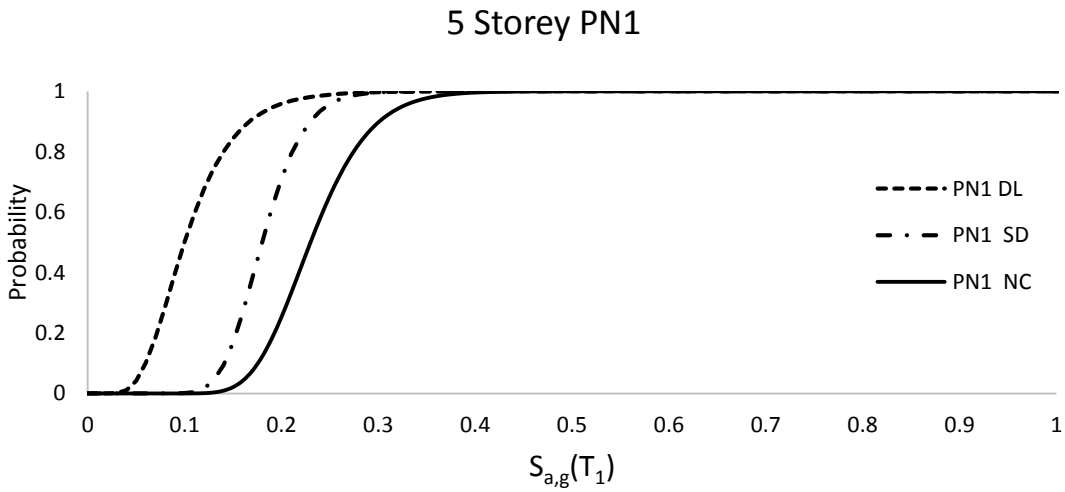

Figure 5.14. Seismic Fragility Curves for 5 Storey PN1 model

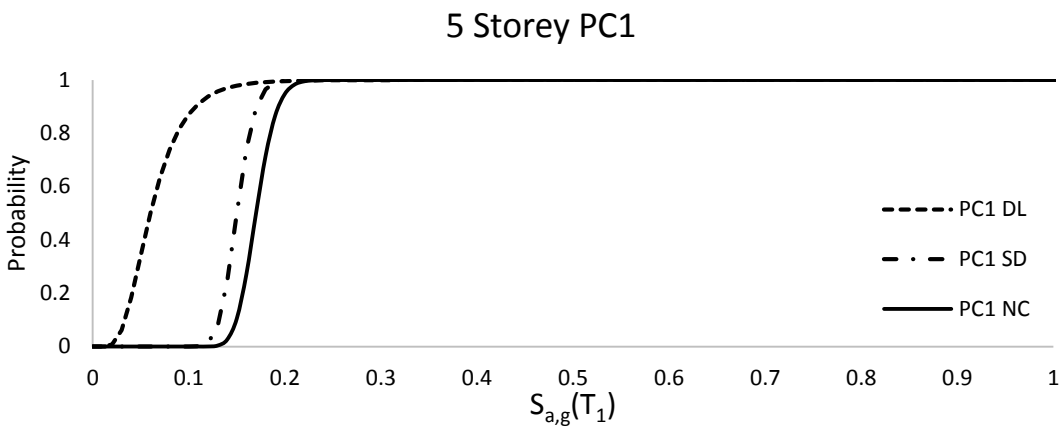

Figure 5.15. Seismic Fragility Curves for 5 Storey PC1 model

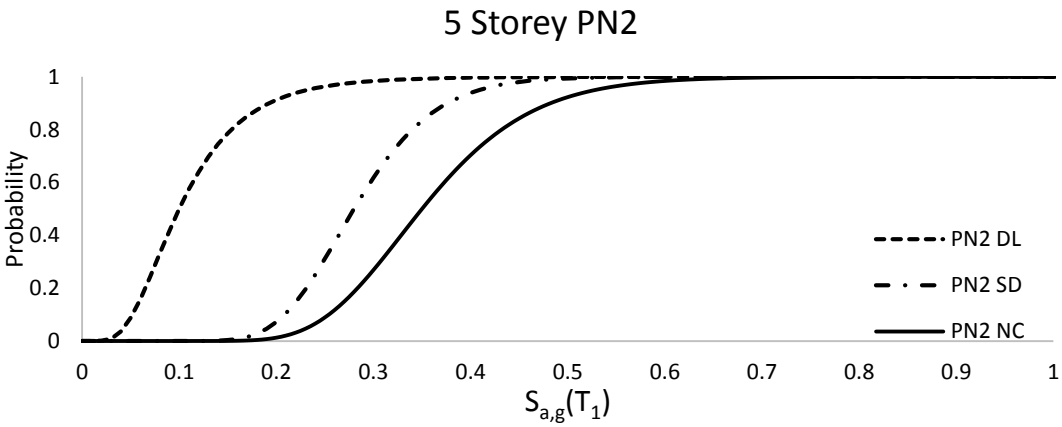

Figure 5.16. Seismic Fragility Curves for 5 Storey PN2 model

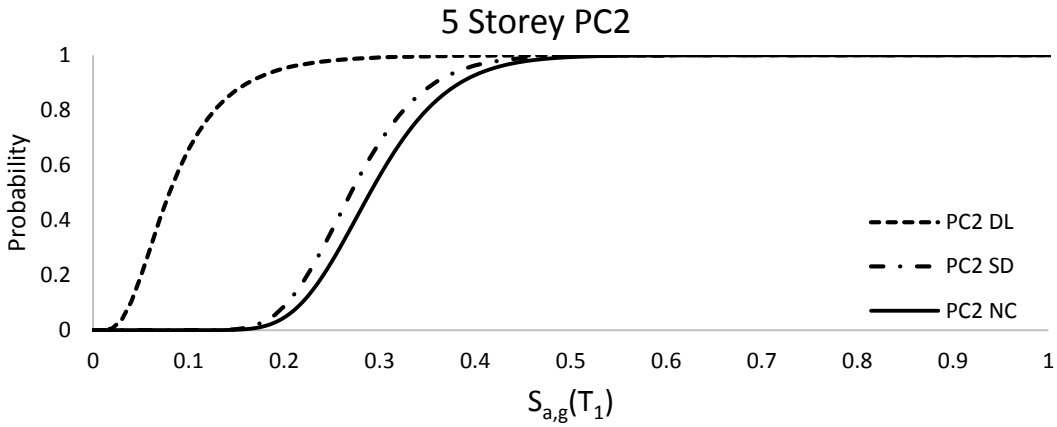

Figure 5.17. Seismic Fragility Curves for 5 Storey PC2 model

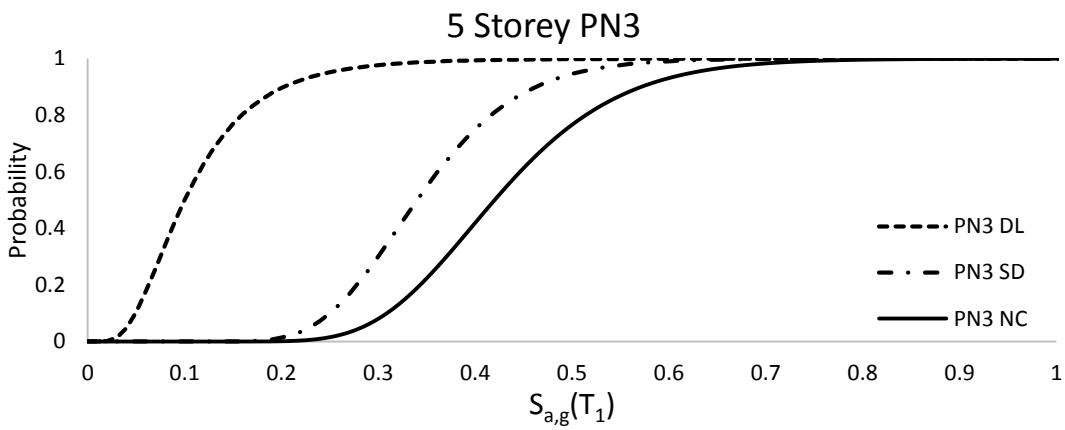

Figure 5.18. Seismic Fragility Curves for 5 Storey PN3 model

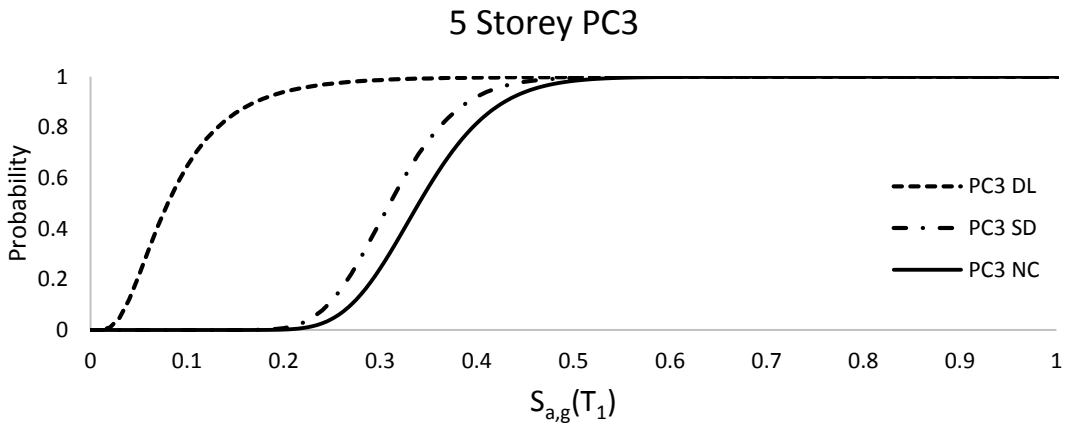

Figure 5.19. Seismic Fragility Curves for 5 Storey PC3 model

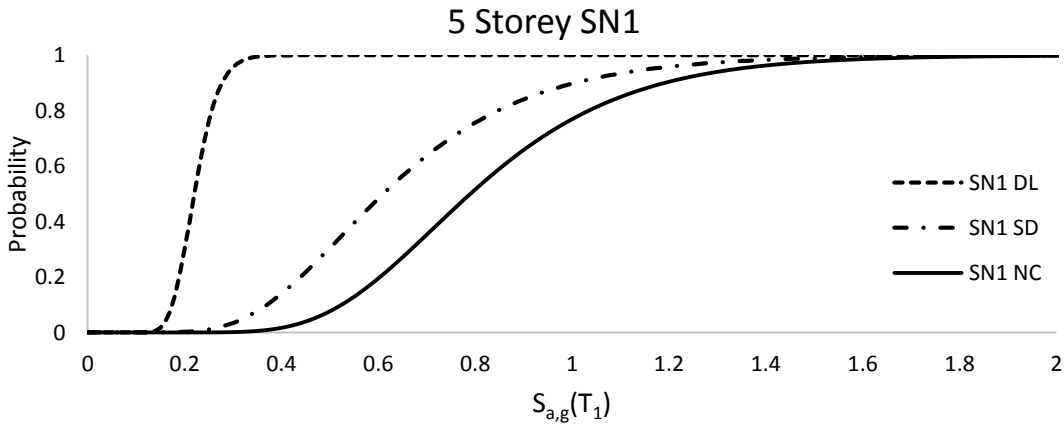

Figure 5.20. Seismic Fragility Curves for 5 Storey SN1 model

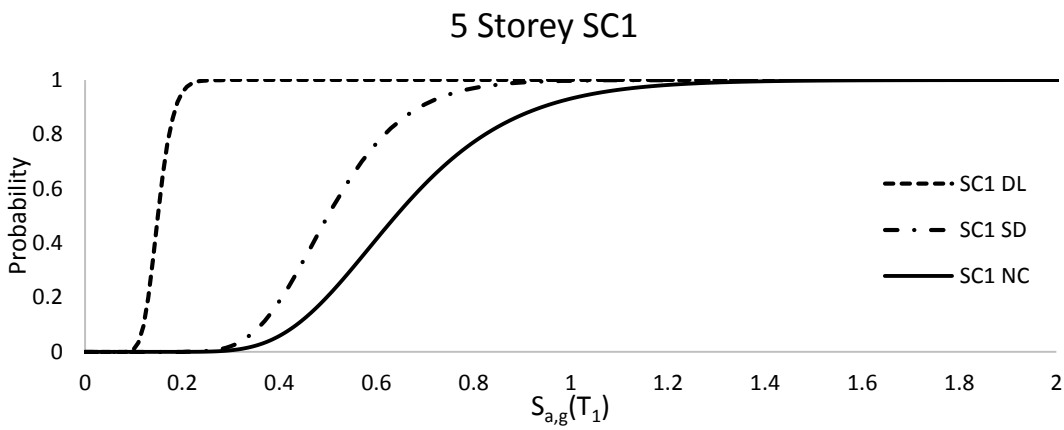

Figure 5.21. Seismic Fragility Curves for 5 Storey SC1 model

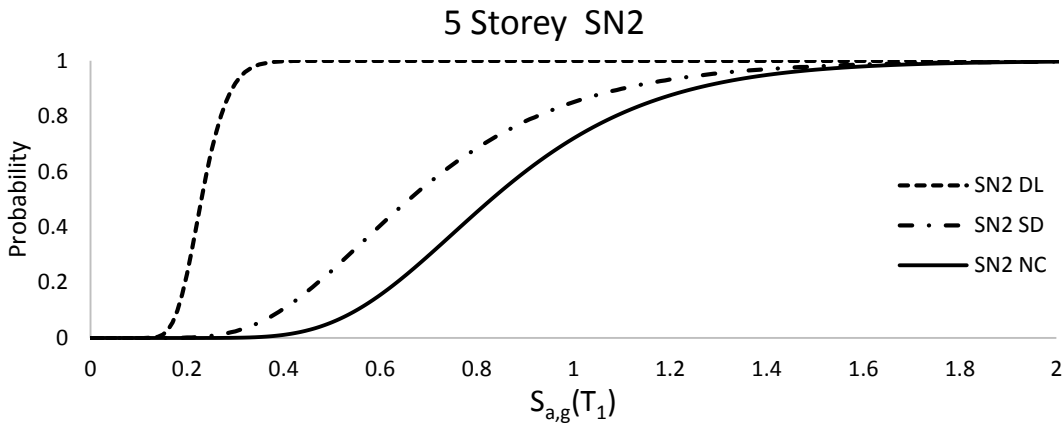

Figure 5.22. Seismic Fragility Curves for 5 Storey SN2 model

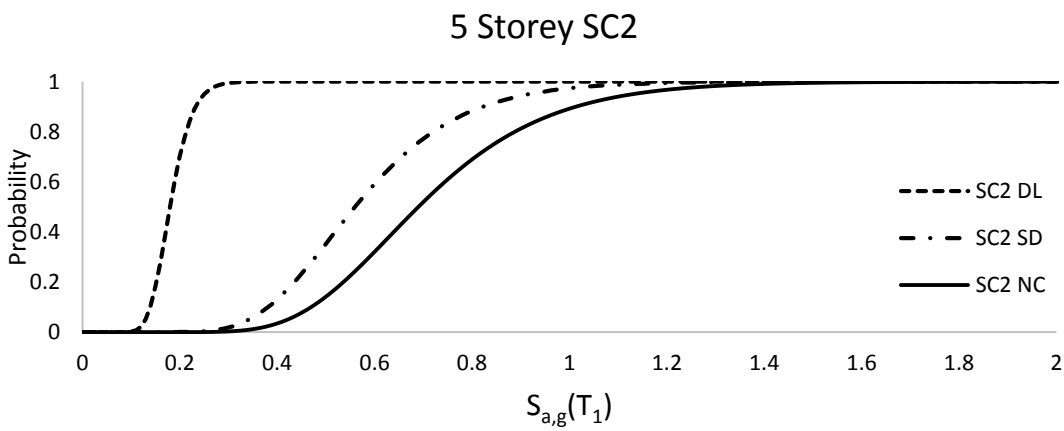

Figure 5.23. Seismic Fragility Curves for 5 Storey SC2 model

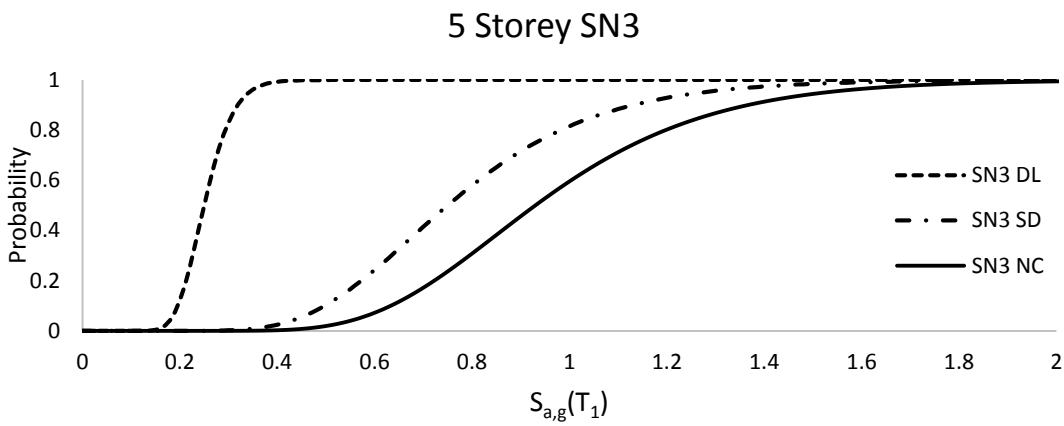

Figure 5.24 Seismic Fragility Curves for 5 Storey SN3 model

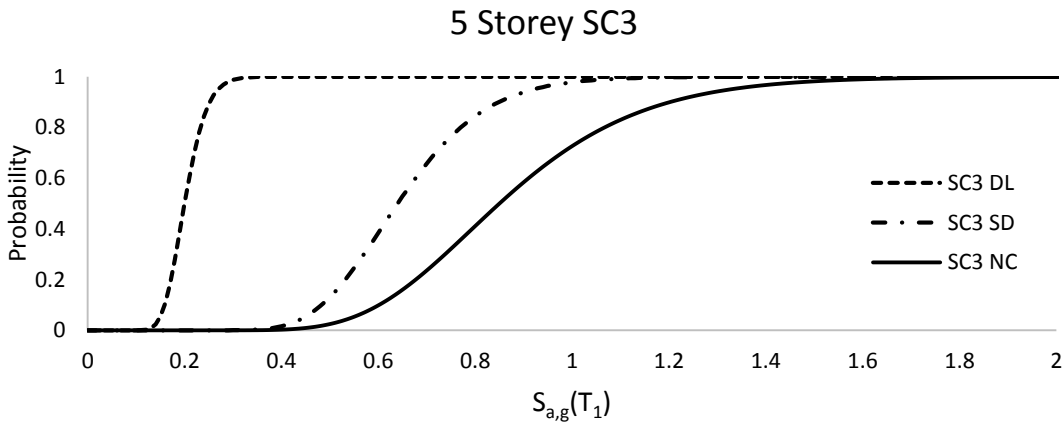

Figure 5.25. Seismic Fragility Curves for 5 Storey SC3 model

Table 5.4 Probabilistic Fragility Function Parameters for 5-storey frame

		PN1	PN2	PN3	PC1	PC2	PC3	SN1	SN2	SN3	SC1	SC2	SC3
DL	Θ	0.10	0.10	0.10	0.06	0.08	0.08	0.22	0.23	0.25	0.15	0.18	0.2
	β	0.40	0.51	0.55	0.45	0.55	0.59	0.18	0.19	0.19	0.17	0.2	0.18
SD	Θ	0.18	0.28	0.34	0.15	0.27	0.31	0.61	0.66	0.75	0.5	0.56	0.64
	β	0.19	0.23	0.24	0.1	0.22	0.18	0.39	0.4	0.32	0.25	0.29	0.22
NC	Θ	0.23	0.35	0.42	0.17	0.29	0.34	0.79	0.83	0.93	0.64	0.69	0.85
	β	0.21	0.25	0.24	0.1	0.22	0.18	0.32	0.32	0.3	0.3	0.3	0.27

As depicted in Table 5.4, insignificant reduction was observed for the median DL values when different concrete strength was assessed. But when more critical damage states were analysed, relatively more performance reduction was observed for the low concrete strength pre-seismic combination due to the consideration of brittle failure modes. When upper and lower boundaries of concrete strength were assessed for the pre-seismic models, 45% reduction in median NC values was observed in mid-rise PN models. In contrast to mid-rise models, the reduction in median NC values is only 15% for the low rise PN models.

Significant loss in median SD values for the brittle PN models are also achieved. Due to the displacement dominated damage criteria on brittle models, the distance in between the DL and SD damage states are observed to reduce with respect to decrease in concrete strength. The median SD value is 1.8 times greater than the DL value for PN1 while this ratio becomes 3.4 for the PN3 for mid-rise buildings. On the other hand this ratio is approximately 1.6 for all short rise PN models.

Corrosion deterioration resulted in significant loss in seismic capacity for all case study models. In general, low dispersion was observed on IDA results for the pre-seismic models. Within the scope of this study, brittle behaviour of the low concrete strength – corrosion combination, observed to cause early collapse mechanism due to shortened plastic range. The strength and ductility are both reduced for corroded low strength models. The influence on NC damage state is relatively more compared to the other damage states. When the corroded midrise pre-seismic models are compared, the NC performance difference between upper and lower concrete strength is 50%. On the other hand as can be seen from the Table 5.4, similarly the difference for the seismic

period is 24%. This difference confirms the fact that the ductile failure mechanism of the seismic period buildings are partially maintained even at lower concrete strength.

The ultimate strain capacity of the naturally corroded reinforcement bars investigated in this study showed a decent performance when 10% mass loss of the corrosion level was considered. The study by Lu et al., (2015), observed the fracture of similar strength but different class bars as result of corrosion attack. However in this study due to the initial strain capacity of the S220 and S420 steel classes, the bars did not suffer from fracture when 10% corrosion level considered. Furthermore as a result of corrosion attack, a global reduction in yield strength and reduction of sectional stiffness is noted.

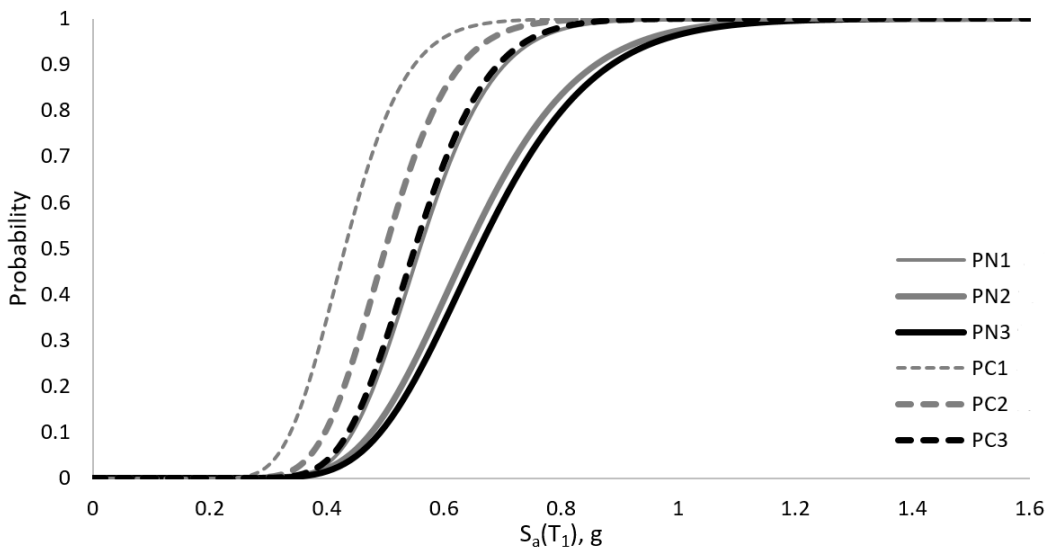

Figure 5.26. Short Rise Pre-seismic frames Near Collapse fragility plots 10% mass loss vs. uncorroded sound condition.

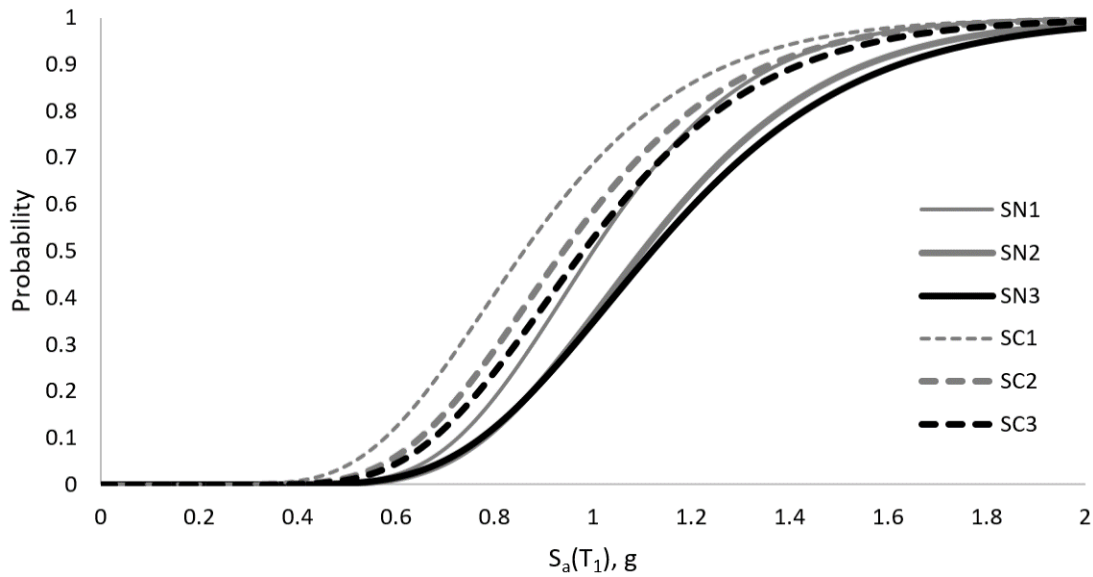

Figure 5.27. Short Rise Seismic frames Near Collapse fragility plots 10% mass loss vs. uncorroded sound condition.

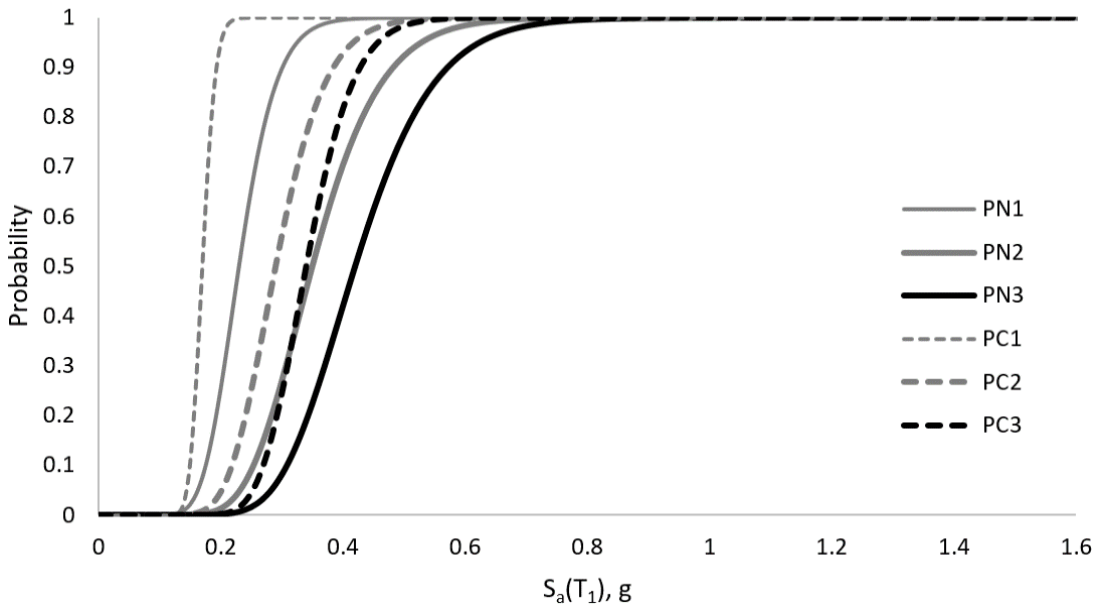

Figure 5.28. Mid Rise Pre Seismic frames Near Collapse fragility plots 10% mass loss vs. uncorroded sound condition.

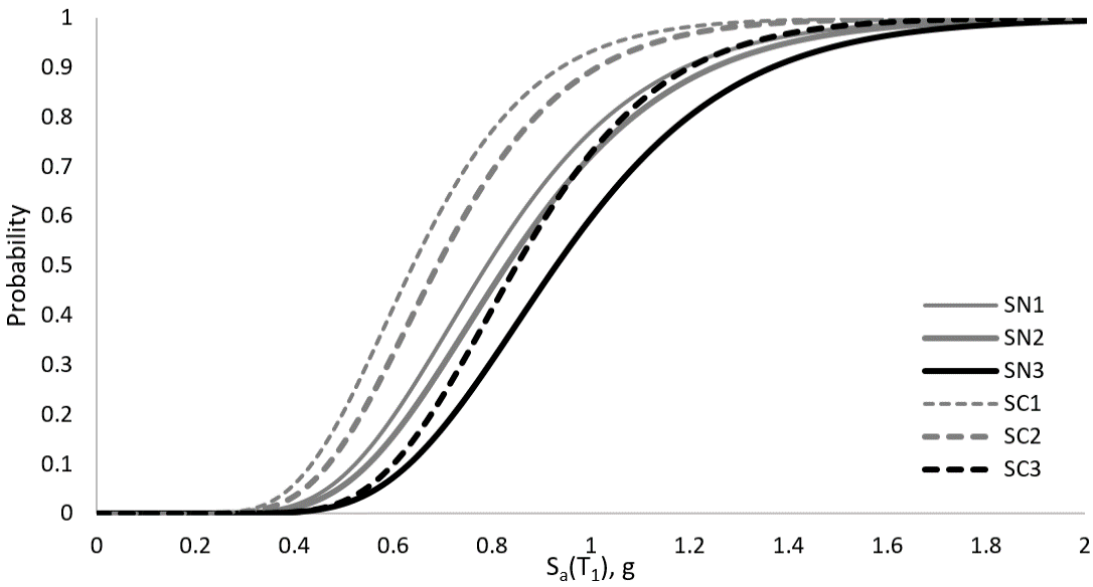

Figure 5.29. Mid Rise Seismic frames Near Collapse fragility plots 10% mass loss vs. uncorroded sound condition.

Corrosion deterioration also lead to an increase in performance variation wih respect to the concrete strength. The NC damage state difference in between the PN3 and PN1 increased in general, indicating that the concrete strength became a more governing parameter.

Similar outcomes are also suggested by Pitilakis et al., (2011) where the European buildings stock was assessed. In general more dispersed results are drawn by the study in which the sudden brittle failure was suggested to be less likely. On the other hand, similarly a great reduction was also suggested by the study due to the corrosion deterioration.

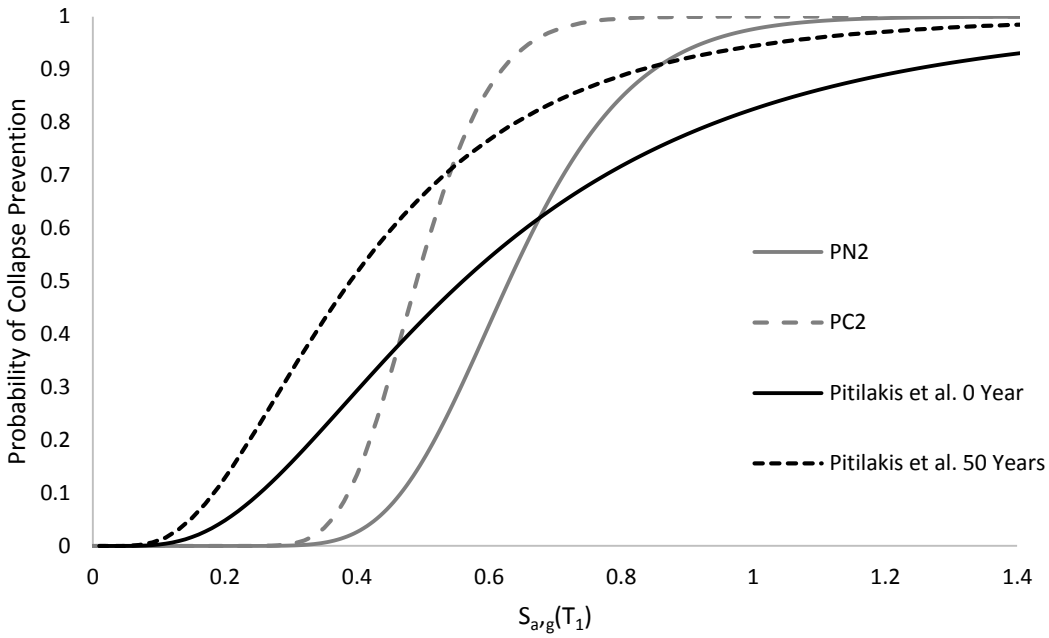

Figure 5.30. Short Rise Pre-seismic models comparison with European Building Stock

5.3 Vulnerability Curves

The influence on seismic loss in terms of mean damage ratio was targeted and vulnerability curves are generated. Due to the consistent design standard between North Cyprus and Turkey, the mean damage ratios are calculated based on CDRs provided by Durukal et al., (2006). Initially developed fragility functions on case study models were utilised to develop the Mean Damage Ratios for each model. When figures from 5.31-5.34 were analysed, in general the performance difference starts at early $S_{a,g}(T_1)$. The variation of vulnerability index with respect to corrosion deterioration and material strength starts at $S_{a,g}(T_1)$:0.38g for pre-seismic short rise group and $S_{a,g}(T_1)$:0.56g for seismic short rise group. On the other hand this is limited to the intensity measure of $S_{a,g}(T_1)$:0.14g for pre-seismic mid-rise models and $S_{a,g}(T_1)$:0.40g. In other words, initially deficient mid-rise models suffer increase in damage earlier stage when compared with low-rise models. When upper and lower concrete strength results were studied, relatively more dispersed results were

observed from MDR: 0.2 onwards. This is due to the post yield stage response difference of the models.

Both seismic and pre-seismic short rise models show insignificant difference in vulnerability MDR values. However when the corroded models were compared, rapid increase in MDR was observed. The increase in MDR due to the corrosion deterioration was observed to be more for the pre-seismic models (Fig. 5.31) in contrast to seismic models (Fig. 5.32).

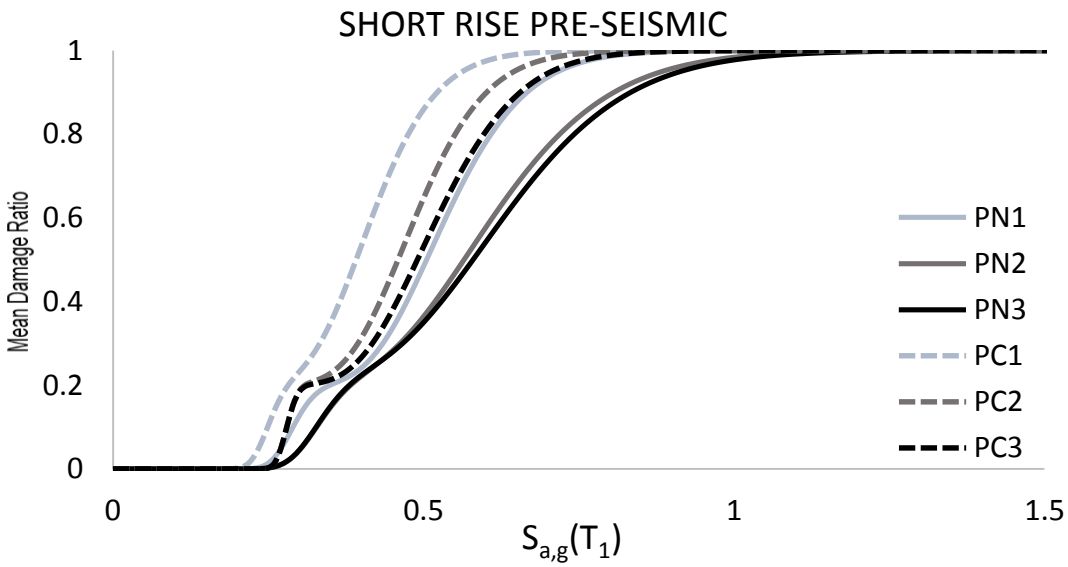

Figure 5.31. Vulnerability Curves for Short Rise Pre-seismic models

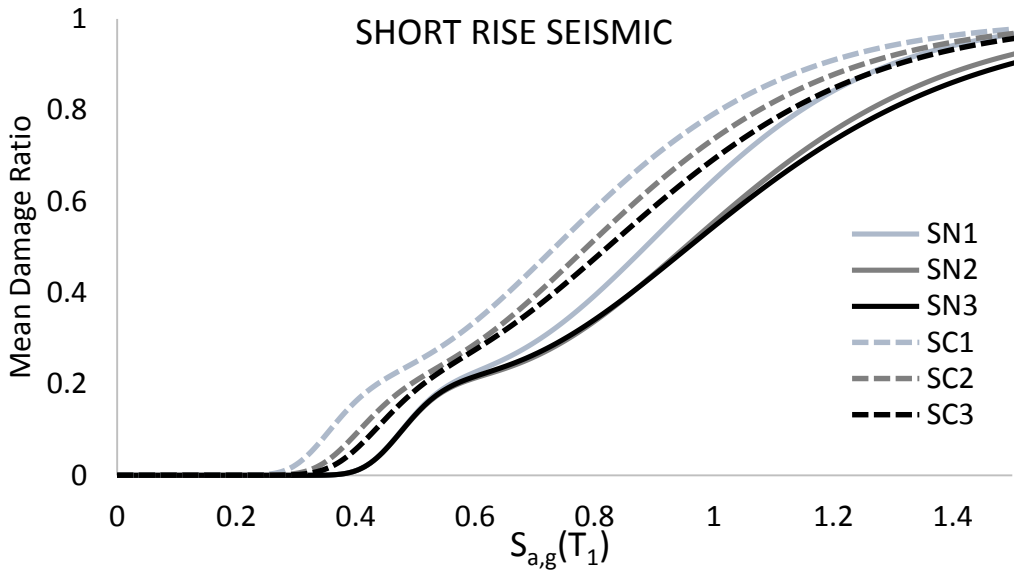

Figure 5.32. Vulnerability Curves for Short Rise seismic models

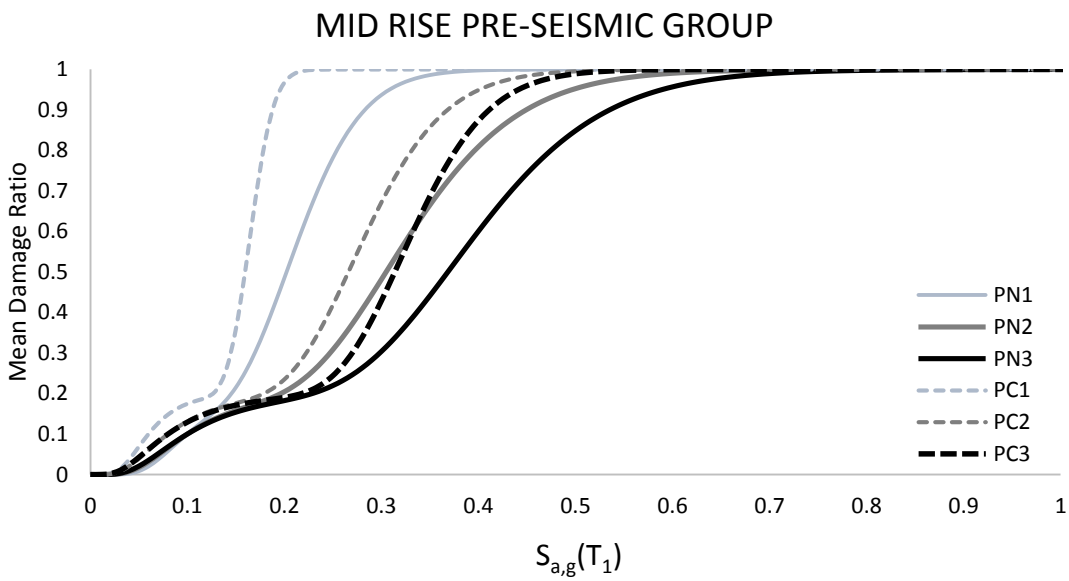

Figure 5.33. Vulnerability Curves for Mid Rise Pre-seismic models

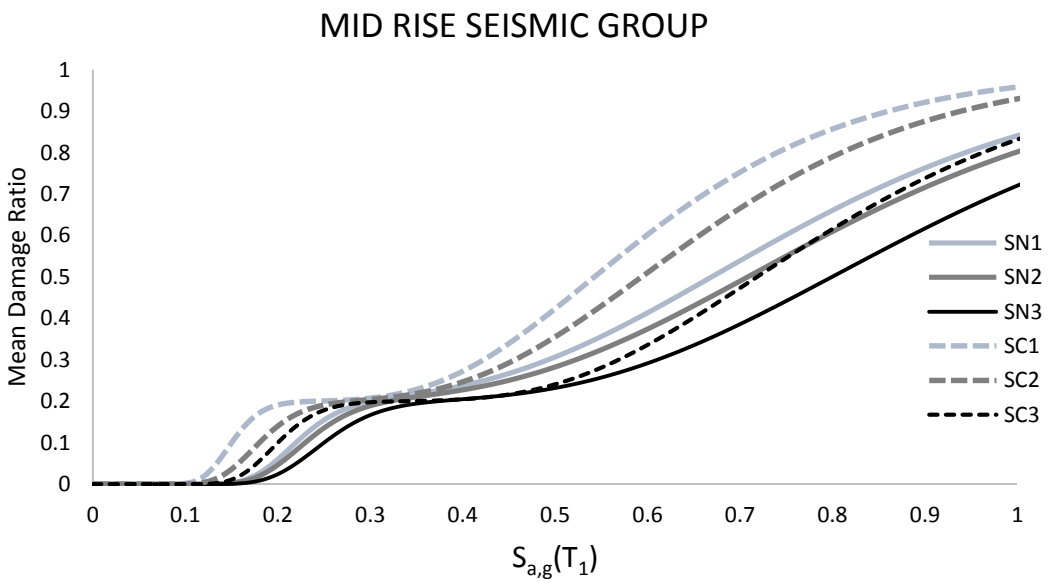

Figure 5.34. Vulnerability Curves for Mid Rise Pre-seismic models

Vulnerability characteristics of the models were derived from the fragility functions for the purpose of assessing corrosion related increase in seismic vulnerability of buildings. Significant increase in vulnerability was observed when upper and lower concrete strength levels are assessed against corrosion deterioration. Unlike to the fragility curves, MDR considers all damage levels at the same time hence 100% MDR is reached earlier than the 100% probability of NC damage level. The effect of upper level concrete strength is more evident in mid-rise behaviour.

Intensity values at complete MDR were compared for the corroded and sound frames. The ratio of intensity values are shown in Figures 5.35 and 5.36. The seismic and pre-seismic period short rise frames did not show significant variation in reduction ratio with respect to concrete strength. However in contrast the mid-rise frames were highly influenced by the concrete strength at corroded condition.

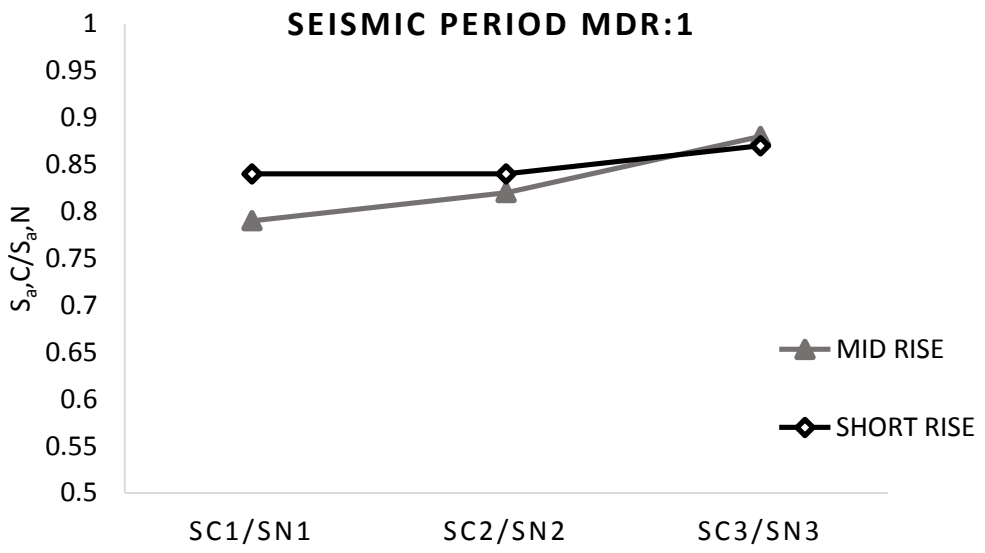

Figure 5.35. Effect of corrosion deterioration on seismic period frames at complete damage ratio and relative reduction of corresponding intensity level

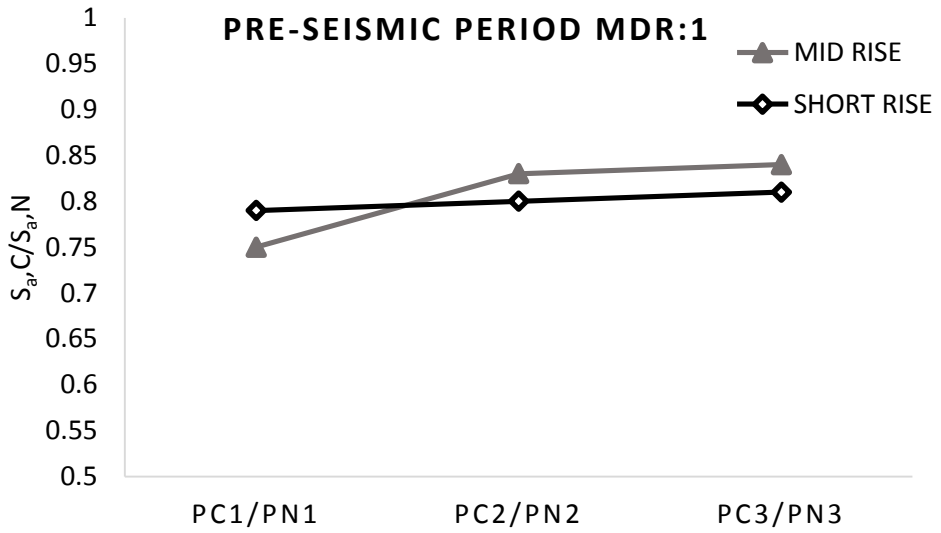

Figure 5.36. Effect of corrosion deterioration on pre-seismic period frames at complete damage ratio and relative reduction of corresponding intensity level

Assessing the vulnerability functions with the use of local seismic hazard information may result in risk based judgement of frames and the corrosion impact on MDR values. The hazard information was adopted from the recent study by Cagnan and Tanircan (2010). Table 5.5 gives information on seismic hazard data for the 475 and

2475 years return period events in Cyprus. Due to the low dispersion in $S_{a,g}(T_1)$, a single value was assumed for the entire North Cyprus (Table 5.5).

Table 5.5. Seismic Hazard Parameters (Cagnan and Tanircan, 2010)

		Mean Magnitude (M_w)	Mean Distance (kM)	Mean Epsilon (Ɛ)	$S_{a,g}(T_1)$
475 Years Return Period	0.25 sec	6.3	29	0.66	0.33g
	0.7 sec	6.5	42	0.8	0.15g
2475 Years Return Period	0.25 sec	6.5	18	0.72	0.67g
	0.7 sec	6.7	23	0.83	0.31g

The seismic hazard values were used to estimate the MDR for the assessed frames in Figures 5.37 and 5.38. The hazard values differ from short rise to mid-rise as the $S_{a,g}(T_1)$ was utilised. The impact of corrosion on MDR for the 475 years return period events is evident especially for the low concrete strength levels. Both short and mid-rise PC1 MDR levels are more than 30% when compared with the PN1 MDR levels. This shows the significance of initial concrete strength to the damage value respect to aging.

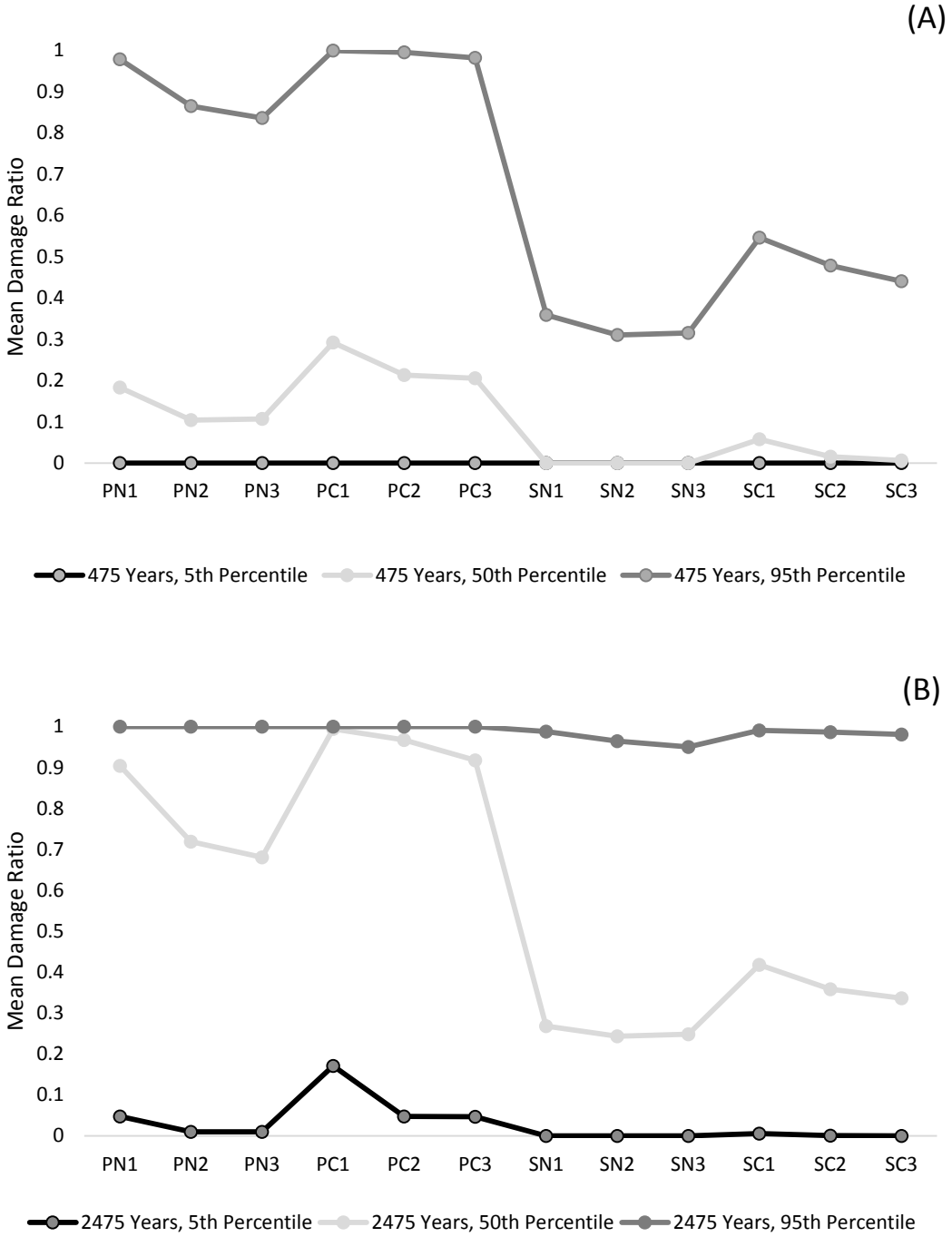

Figure 5.37. Expected damage loss in terms of mean damage ratio for the low rise buildings, A) 475 Years return period B) 2475 years return period hazard estimates

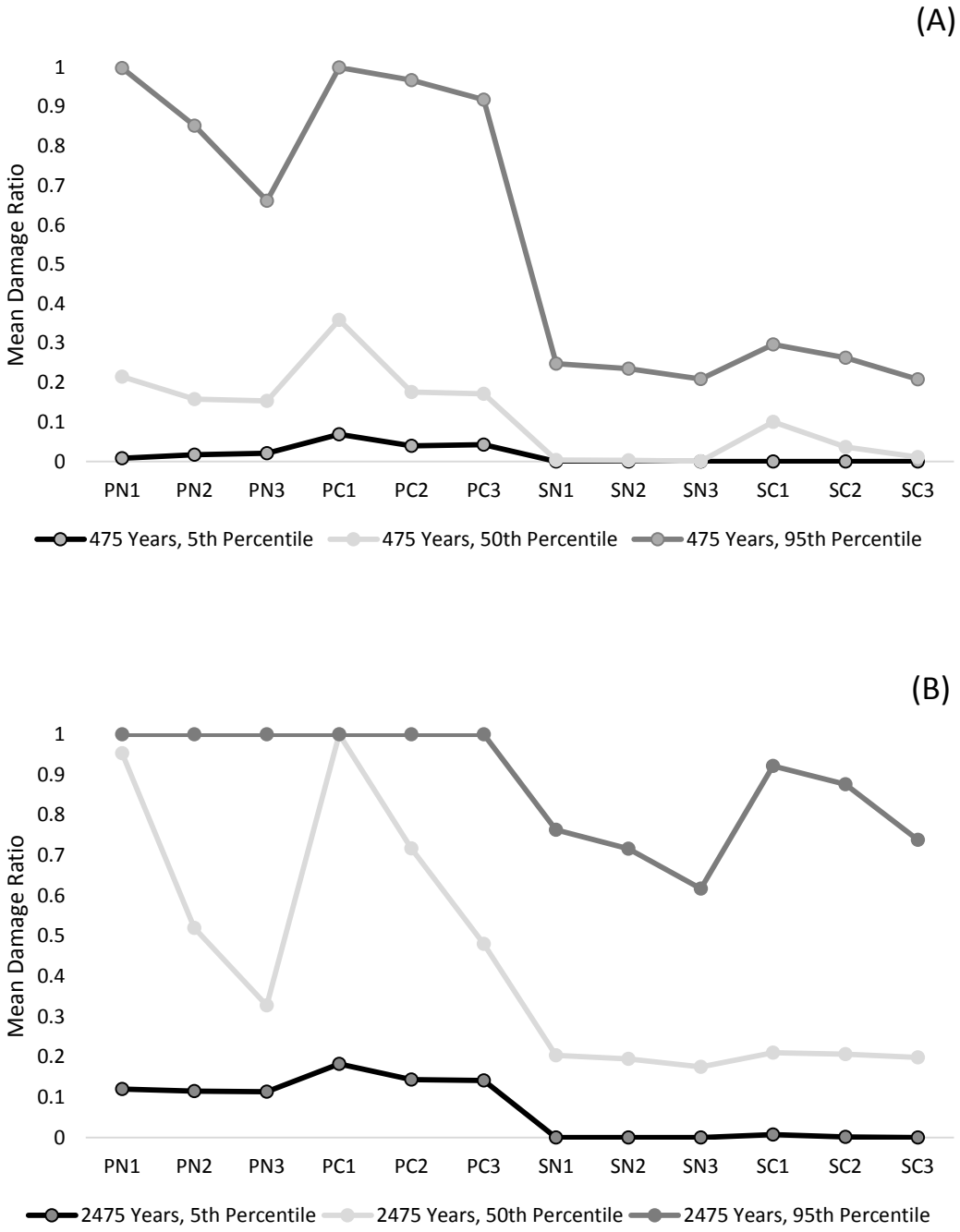

Figure 5.38. Expected damage loss in terms of mean damage ratio for the mid-rise buildings, A) 475 Years return period B) 2475 years return period hazard estimates

Chapter 6

CONCLUSION

Parametrically assessed material strength and seismic design provisions allow the investigation of corresponding seismic performance reduction of corroded reinforced concrete frames. The main objective of this study is to assess the collapse risk of seismic and pre-seismic type moment resisting reinforced concrete frames by using the concrete strength and corrosion deterioration variables. Both material and deterioration variables found to be highly influential on seismic capacity of old-type case study MRF where the effect on seismically designed frame was found to be relatively less. As a result of the advanced corrosion models adopted, the pushover analyses yielded to reduced interstorey drift limits. The code provided inter-storey drift ratios become non-conservative once the deterioration models are considered. As a result the following conclusions can be drawn:

- Significant variation in concrete strength was observed when two time periods seismic and pre-seismic time frames were analysed. Chloride contamination of sea side supplied concrete aggregates resulted in both reduction in concrete strength and corrosion in reinforcement. Mechanical characteristics of two different steel classes also showed variation in ultimate strain capacity when subjected to corrosion. The test data show that the plain mild reinforcement steel is found to be more vulnerable against corrosion when compared with DIN 488 deformed S420 steel. However both bar types satisfy the ultimate strain limit of 0.06 (TEC 2007) even at high corrosion levels. It may be

beneficial to use the initially high ductile reinforcement types for the corrosion prone regions. S420 (DIN488) or S500C (EC8) reinforcing steel types may be a good fit for this purpose.

- Literature highly suggests the consideration of inappropriate use of stirrup hooks on shear critical columns. This study tested the non-shear critical columns with stirrups having 90° hooks. Especially, the confinement effect at post yielding stage was affected where the significant reduction was observed for the post yield strength and stiffness of the members with 90 degrees stirrup hooks.

- The negligible variation of the interstorey drift ratios were observed for the seismically designed uncorroded models, when different concrete strength was assessed. However, when uncorroded old-type models were considered, a huge variation was observed due to the brittle failure modes and great variation in concrete strength. On the other hand when the lower and upper bound concrete strength of each corroded model is analysed, the pre-seismic models are observed to face relatively more reduction in seismic performance. Drift capacity of lower bound pre-seismic and seismic midrise models are reduced by 40% and 20% respectively when subjected to 10% mass loss due to corrosion. Similarly the reduction in drift capacity of low rise models are 22% and 20% for pre-seismic and seismic models respectively.

- As result of dynamic analyses, the aggressive effect of corrosion was compared with different concrete strength models where the fragility functions were developed. Near Collapse damage state was widely altered for

all groups. The 10% mass loss corrosion level on pre-seismic mid-rise models, the reduction in Median NC is 26% for lower bound concrete strength and 20% for the upper bound concrete strength models. On the other hand, when the seismic models are investigated, 19% reduction in Median NC was observed for lower bound concrete strength and only 11% increase was observed for the upper bound concrete strength. For the low rise case study models, the performance drop of median NC damage level due to corrosion deterioration was observed to be 22% for pre-seismic models and 15% for seismic models.

- Better concrete strength is, the more distance is between SD and NC damage levels. In general relatively better NC performance was obtained for the models with upper level concrete strength.

- Significant increase in MDR was observed for the deteriorated pre-seismic models when the local hazard data considered. The deterioration influence on seismic period models are more evident when upper level hazard value was utilised.

- Diameter of the longitudinal steel has a significant impact on corrosion deterioration of the concrete cover. Avoiding dense reinforcement ratio as well as great diameter bars may have a positive impact on extending the lifetime of the initial seismic capacity. Additionally cover concrete thickness has significant influence on corrosion deterioration. Utilising thick cover concrete may delay the deterioration of section at short period of time.

Modelling the corrosion effect only by reducing geometric size of the reinforcement may give inconsistent results and demonstrate a ductile failure mode. It is strongly suggested to consider the additional corrosion related strength/stiffness/ductility modifications especially when assessing the older type reinforced concrete buildings against seismic performance. The interstorey drift ratio is also found to differ with corrosion level variation. It is suggested to evaluate the displacement capacity of the buildings subjected to corrosion prior to assessment. The categorized results allow decision makers to judge the corrosion related deterioration on old and new type RC buildings with different concrete strength classes.

6.1 Recommendations

- In this study, plain and deformed bars were assessed against ultimate strain respect to corrosion. Additionally it is suggested to investigate these two different type of the reinforcements under cyclic experiments where the comparative low cycle fatigue behaviour would be detected.

- Low and mid-rise reinforced concrete buildings were covered in the proposed methodology and application. However it may be beneficial to assess the higher rise buildings with shear wall type structural system.

- The experimental work on stirrups in this thesis only assessed the squared columns with limited axial force. The seismic behaviour of the old type shear wall structures with 90 degrees stirrup hooks should be studied in a future work.

- The distribution of corrosion through the building frame elements is out of scope of this thesis. However it may be beneficial to consider random

distribution of corrosion along the members of frame and assess against earthquake performance.

- Rate of corrosion with respect to time is expected to be different for each concrete strength level. Due to the permeability characteristics of concrete material, the corrosion level is not expected to be reached at the same time for lower and upper levels of concrete strength. It will be valuable to assess the corrosion level for different levels of concrete strength with respect to age.

REFERENCES

Ahmad, S., Kyriakides, N., Pilakoutas, K., Neocleous, K., & uz Zaman, Q. (2015). Seismic fragility assessment of existing sub-standard low strength reinforced concrete structures. *Earthquake Engineering and Engineering Vibration*, 14(3), 439-452.

Akkar, S., Sucuoğlu, H., & Yakut, A. (2005). Displacement-based fragility functions for low-and mid-rise ordinary concrete buildings. *Earthquake Spectra*, 21(4), 901-927.

Alonso, C., Andrade, C., Rodrigues, J., & Diez, J. M. (1998). Factors controlling cracking of concrete affected by reinforcement corrosion. *Materials and Structures*, 31, 435-441.

Alsiwat, J. M., & Saatcioglu M. (1992). Reinforcement anchorage slip under monotonic loading. *Journal of Structural Engineering, ASCE*, 118(9), 2421-2438.

Ambraseys N.N., & Adams R.D. (1992) *Seismicity of the Cyprus region*. Imperial College, ESEE Research Report 92-9,(pp 47–67), London: Imperial College.

Apostolopoulos, C. A., & Papadakis, V. G. (2008). Consequences of steel corrosion on the ductility properties of reinforcement bar. *Construction and Building Materials*, 22(12), 2316-2324.

Applied Technology Council. (1996). *Seismic Evaluation and Retrofit of Concrete Buildings*, ATC-40. California: California Seismic Safety Commission.

Arslan, M. H. (2010). An evaluation of effective design parameters on earthquake performance of RC buildings using neural networks. *Engineering Structures*, 32(7), 1888-1898.

ASTM G1-03. (2003). Standard practice for preparing, cleaning, and evaluating corrosion.

Ay, B. Ö., & Akkar, S. (2012). A procedure on ground motion selection and scaling for nonlinear response of simple structural systems. *Earthquake Engineering & Structural Dynamics*, 41(12), 1693-1707.

Baker, J. W. (2015). Efficient analytical fragility function fitting using dynamic structural analysis. *Earthquake Spectra*, 31(1), 579-599.

Bayhan, B., Moehle, J. P., Yavari, S., Elwood, K. J., Lin, S. H., Wu, C. L., & Hwang, S. J. (2015). Seismic Response of a Concrete Frame with Weak Beam-Column Joints. *Earthquake Spectra*, 31(1), 293-315.

Berto, L., Vitaliani, R., Saetta, A., & Simioni, P. (2009). Seismic assessment of existing RC structures affected by degradation phenomena. *Structural Safety*, *31*(4), 284–297.

Bilham, R., Doyle, P., Evans, R., Greening, P., May, R., Stewart, A., & Vince, D. (2003). In D D'Ayala Matthew Free (eds): The Kocaeli, Turkey Earthquake of 17 august 1999: a field report by eefit. Earthquake engineering field investigation team, Institution of Structural Engineers,

Building Seismic Safety Council (BSSC), (1997). *NEHRP Guidelines for the Seismic Rehabilitation of Buildings*. FEMA 274. Washington, D.C.: Federal Emergency Management Agency.

Building Seismic Safety Council (BSSC), (2000). *Pre standard and Commentary for the Seismic Rehabilitation of Buildings*, FEMA-356, Washington, D.C.: Federal Emergency Management Agency.

Cagnan, Z., & Tanircan, G. B.. (2010). Seismic hazard assessment for Cyprus. *Journal of Seismology*, 14(2), 225-246.

Calvi G.M. (1999). A Displacement-based Approach for Vulnerability Evaluation of Classes of Buildings, *Journal of Earthquake Engineering*, 3, 411–438.

Calvi, G. M., Magenes, G., & Pampanin, S., (2002). Relevance of beam-column joint damage and collapse in RC frame assessment, *Journal of Earthquake Engineering*, 6, 75–100.

Can, O. (1997). *Assessment of seismic hazard for Cyprus*. MS thesis submitted to Eastern Mediterranean University.

Castel, A., François, R., & Arliguie, G. (2000). Mechanical behaviour of corroded reinforced concrete beams—Part 2: Bond and notch effects. *Materials and Structures*, 33(9), 545-551.

Celik, O. C. (2007). *Probabilistic assessment of non-ductile reinforced concrete frames susceptible to Mid-America ground motions.* PhD Thesis, Georgia Institute of Technology.

CEN (2004). *Eurcode 8, design of sturctures for earthquake resistance-part 1: general rules, seismic actions and rules for buildings*, EN 1998-1:2004. Brussels: Comite Europeen de Normalisation.

Chamber of Turkish Cypriot Civil Engineers (CTCCE). (1992). *Seismic Detailing Rules*. Nicosia: Chamber of Turkish Cypriot Civil Engineers.

Chopra, A. K. (2001). *Dynamics of structures: Theory and applications to Earthquake Engineering.* New Jersey: Pearson.

Code, T. E. (1975). *Specification for structures to be built in disaster areas*. Ankara: Ministry of Public Works and Settlement Government of Republic of Turkey.

Code, T. E. (1998). *Specification for structures to be built in disaster areas*. Ankara: Ministry of Public Works and Settlement Government of Republic of Turkey.

Code, T. E. (2007). *Specification for structures to be built in disaster areas 2007*. Ankara: Ministry of Public Works and Settlement Government of Republic of Turkey.

Colangelo, F. (2008). On the computation of seismic fragility curves. *The 14th World Conference on Earthquake Engineering*, Oct.12-17, Beijing, China.

Coronelli, D. & Gambarova, P. (2004). Structural Assessment of Corroded Reinforced Concrete Beams: Modeling Guidelines. *Journal of Structural Engineering*, 130 (8), 1214-1224.

Crowley, H., Pinho, R. & Bommer, J. (2004), A Probabilistic Displacement-based Vulnerability Assessment Procedure for Earthquake Loss Estimation," *Bulletin of Earthquake Engineering*, 2(2): 173–219.

CTSPO: Cyprus Turkish State Planning Organisation (2017). *Building Construction Statistics in North Cyprus*. Nicosia: Cyprus Turkish State Planning Organisation.

Cyprus Civil Engineers and Architects Association (CCEAA) (1994). *Seismic Code of Cyprus*. Nicosia, Cyprus: Cyprus Civil Engineers and Architects Association, Earthquake Engineering Committee,

Cyprus Geological Survey Department (2013) Cyprus Strong Motion Database.

De Stefano, M., Tanganelli, M., & Viti, S. (2013). Effect of the variability in plan of concrete mechanical properties on the seismic response of existing RC framed structures. *Bulletin of Earthquake Engineering*, 11(4), 1049-1060.

Dhakal, R. P., & Maekawa, K. (2002). Modeling for post yield buckling of reinforcement. *Journal of Structural Engineering*, 128(9), 1139-1147.

DIN 488-1, (1986). Reinforcing steel grades, properties, marking. German Institute for Standardization

Du, Y.G., L. A. Clark, L. A., & A. H. C. Chan, A.H.C. (2005). Effect of corrosion on ductility of reinforcing bars. *Magazine of Concrete Research*, 57(7), 407-419.

Du Béton, F. I. (2013). Fib model code for concrete structures 2010. Berlin, Germany: International Federation for Structural Concrete

Durukal, E, Erdik, M & Sesetyan, K. (2006). Expected earthquake losses to buildings in Istanbul and implications for the performance of the Turkish catastrophe insurance pool. In *Proceedings of geohazards, international engineering conferences*. Lillehammer, Norway.

Elenas, A., & Meskouris, K. (2001). Correlation study between seismic acceleration parameters and damage indices of structures. *Engineering Structures*, *23*(6), 698-704.

Elwood, K. J., & Moehle, J. P. (2005). Drift capacity of reinforced concrete columns with light transverse reinforcement. *Earthquake Spectra*, 21(1), 71-89.

Erdik M, Birgoren G, Apaydin N, & Onur T (1997) A probabilistic assessment of seismic hazard in Cyprus in terms of spectral amplitudes. In *The 29th General Assembly of the International Association of Seismology and Physics of the Earth's Interior* (IASPEI 1997), paper no. 1801, Thessaloniki, Greece.

Ersoy, U., Özcebe, G. , & Tankurt, T. (2008). *Reinforced concrete*. Ankara: Middle East Technical University.

Fabbrocino, G., Verderame, G. M., Manfredi, G., & Cosenza, E. (2004). Structural models of critical regions in old-type RC frames with smooth rebars. *Engineering Structures*, 26(14), 2137-2148.

Federal Emergency Management Agency. (1997) NEHRP Guidelines for seismic rehabilitation of buildings. Federal Emergency Management Agency Report: FEMA 273. Washington D.C.

Federal Emergency Management Agency (FEMA). (2005). 440, Improvement of nonlinear static seismic analysis procedures. *FEMA-440, Redwood City*.

Federal Emergency Management Agency (FEMA). (2007). FEMA 461. *Interim Protocols For Determining Seismic Performance Characteristics of Structural and Nonstructural Components Through Laboratory Testing*. Washington, D.C.

Federal Management Agency (1997). *Rehabilitation of Buildings*, FEMA-273, Washington, D.C.: Federal Management Agency.

Galanis, P. H., & Moehle, J. P. (2015). Development of collapse indicators for risk assessment of older-type reinforced concrete buildings. *Earthquake Spectra*, 31(4), 1991-2006.

Galanopoulos, A. G., & Delibasis, N. (1965). The seismic activity in the Cyprus area. *Prakt. Akad. Athenon*, 40, 387

Ghobarah, A., & Biddah, A. (1999). Dynamic analysis of reinforced concrete frames including joint shear deformation. *Engineering Structures*, *21*(11), 971-987.

Ghobarah, A., Abou-Elfath, H., & Biddah, A. (1999). Response-based damage assessment of structures. *Earthquake engineering & structural dynamics*, *28*(1), 79-104.

Harajli, M. H., & Dagher, F. (2008). Seismic strengthening of bond-critical regions in rectangular reinforced concrete columns using fiber-reinforced polymer wraps. *ACI Structural Journal*, 105(1), 68.

Harrison, R.W., Newll, W.L., Batıhanlı, H., Panayides, I., McGeehin, J.P., Mahan, S.A., Özhür, A., Tsiolakis, E., Necdet, M. (2004). Tectonic framework and Late Cenozoic tectonic history of the Northern part of Cyprus: implications for earthquake hazards and regional tectonics. *Journal of Asian Earth Sciences*, 23, 191-210.

Haselton, C. B., Baker, J. W., Liel, A. B., & Deierlein, G. G. (2009). Accounting for ground-motion spectral shape characteristics in structural collapse assessment through an adjustment for epsilon. Journal of Structural Engineering, 137(3), 332-344.

Hwang, H., Liu, J. B., & Chiu, Y. H. (2001). Seismic fragility analysis of highway bridges. Mid-America Earthquake Center CD Release 01-06.

Hwang, HM, Xu, M., & Huo, J-R. (1994). Estimation of seismic damage and repair cost of the University of Memphis buildings, Memphis, Tennessee.

Jaehong Kim J., & James M. LaFave, (2007) Key influence parameters for the joint shear behaviour of reinforced concrete (RC) beam–column connections. *Engineering Structures*, 29 (10), 2523-2539,

Jayaram, N., Lin, T., & Baker, J.W. (2011). A Computationally Efficient Ground-Motion Selection Algorithm for Matching a Target Response Spectrum Mean and Variance. *Earthquake Spectra*, 27, 797–815.

Kalogeras I, Stavrakakis G, Solomi K (1999). The October 9, 1996 earthquake in Cyprus: seismological, macroseismic and strong motion data. *Ann. Geofi.s* 42, 85–97-405.

Kashani, M. M., Lowes, L. N., Crewe, A. J., & Alexander, N. A.. (2015). Phenomenological hysteretic model for corroded reinforcing bars including

inelastic buckling and low-cycle fatigue degradation. *Computers & Structures,* 156, 58-71.

Kaushik, H., Bevington, J., Jaiswal, K., Lizundia, B., & Shrestha, S. (2016). Buildings (EERI Earthquake Reconnaissance Team Report: M7. 8 Gorkha, Nepal Earthquake on April 25, 2015 and its Aftershocks) (pp. 5-1). Earthquake Engineering Research Institute.

Khan, I., François, R., Castel, A. (2014). Prediction of reinforcement corrosion using corrosion induced cracks width in corroded reinforced concrete beams. *Cement and Concrete Research*, 56, 84–96.

Kwak, H. G., & Kim, J. K. (2006). Implementation of bond-slip effect in analyses of RC frames under cyclic loads using layered section method. *Engineering structures*, 28(12), 1715-1727.

Lam, S. S. E., Wu, B., Wong, Y. L., Wang, Z. Y., Liu, Z. Q., & Li, C. S. (2003). Drift capacity of rectangular reinforced concrete columns with low lateral confinement and high-axial load. Journal of Structural Engineering, 129(6), 733-742.

Lee, H. S., & Cho, Y. S. (2009). Evaluation of the mechanical properties of steel reinforcement embedded in concrete specimen as a function of the degree of reinforcement corrosion. *International Journal of Fracture*, 157(1-2), 81-88.

Lee, H. S., Noguchi, T., & Tomosawa, F. (2002). Evaluation of the bond properties between concrete and reinforcement as a function of the degree of reinforcement corrosion. *Cement and Concrete Research*, 32(8), 1313-1318.

Lehman, D. E., & Moehle, J. P. (2000). Seismic performance of well-confined concrete bridge columns. Pacific Earthquake Engineering Research Center. Report No. PEER-1998/01, (p. 316). University of California, Berkeley.

Lynn, A. C. (2001). *Seismic Evaluation of Existing Reinforced Concrete Building Columns*. PhD Thesis. University of California at Berkeley.

Mander, J. B., Priestley, M. J., & Park, R. (1988). Theoretical stress-strain model for confined concrete. *Journal of structural engineering*, *114*(8), 1804-1826.

MathWorks, Inc. (2002). *Curve fitting toolbox: for use with MATLAB®: user's guide*. MathWorks.

Milutinovic Z., & Trendafiloski, G.(2003) WP4 Vulnerability of current buildings, chapter 4.2. AUTH WP4WG Approach, Technical report, Risk-UE: *An advanced approach to earthquake risk scenarios with applications to different European towns*, European Commission.

Molina, F. J., Alonso, C., & Andrade, C. (1993). Cover cracking as a function of rebar corrosion. II: Numerical model. *Mater. Struct.*, 26, 532–548.

Mouroux P., (2004), “An advanced approach to earthquake risk scenarios with application to different European towns”, RISK-UE Project, France.

MSD (2017). Importance of Concrete Cover in Bond Behaviour of Concrete structures. Retrieved from http://www.msd-eng.com/en/msd-reports/concrete-cover/

Musson, R. M., Grünthal, G., & Stucchi, M. (2010). The comparison of macroseismic intensity scales. *Journal of Seismology*, 14(2), 413-428.

Nataj, A. B., Şensoy, S., & Razaqpur, G. (2018). Seismic Behavior and Strength of RC Columns with Embedded Drain Pipe. *Magazine of Concrete Research*, 1-10.

Nepal, J., & Chen, H. P.. (2015). Assessment of concrete damage and strength degradation caused by reinforcement corrosion. *Journal of Physics: Conference Series*, 628 (1), 012050).

Otani, S., & Sozen, M.A. (1972). Behaviour of multi-story reinforced concrete frames during earthquakes. *Structural Research Series*. University of Illinois, Urbana. No. 392, p. 551.

Ozmen H. B. & Inel M. (2012). Effect of Material Strength and Reinforcement Detailing on Displacement Capacity of Existing RC Buildings. *15WCEE*, Lisboa.

Park, S., & Mosalam, K. M. (2013). Simulation of reinforced concrete frames with nonductile beam-column joints. *Earthquake Spectra*, 29(1), 233-257.

Park, Y. J., & Ang, A. H. S. (1985). Mechanistic seismic damage model for reinforced concrete. *Journal of Structural Engineering*, 111(4), 722-739.

Pasquale G.D., Orsini G., Romeo R.W., (2005), New development in seismic Risk Assessment in Italy. *Bulletin of Earthquake Engineering*, 3 (1), 101-128.

Pedrosa, F. & Andrade, C. (2017). Corrosion induced cracking: Effect of different corrosion rates on crack width evolution. *Construction and Building Materials*, 133, 525–533.

Petrini, L., Maggi, C., Priestley, M. N., & Calvi, G. M. (2008). Experimental verification of viscous damping modeling for inelastic time history analyzes. *Journal of Earthquake Engineering*, 12(S1), 125-145.

Pilidou, S., Priestley, K., Jackson, J., Maggi, A. (2004). The 1996 Cyprus earthquake: a large deep event in the Cyprean arc. *Geophysical Journal International*, 158, 85-97.

Pinho, R., Bommer, J.J. & Glaister, S. (2002), A Simplified Approach to Displacement-based Earthquake Loss Estimation Analysis. In *Proceedings of the 12th European Conference on Earthquake Engineering*, London, U.K., Paper No. 738.

Pitilakis, K. D., Karapetrou, S. T., & Fotopoulou, S. D.. (2014). Consideration of aging and SSI effects on seismic vulnerability assessment of RC buildings. *Bulletin of Earthquake Engineering,* 12(4), 1755-1776.

Priestley, M. J. N., & Grant, D. N. (2005). Viscous damping in seismic design and analysis. *Journal of Earthquake Engineering*, 9(2), 229-255.

Prota, A., De Cicco, F., & Cosenza, E. (2009). Cyclic behaviour of smooth steel reinforcing bars: experimental analysis and modeling issues. *Journal of Earthquake Engineering*, 2009: 13(4), 500-519.

Rossetto, T., & Elnashai, A. (2003). Derivation of vulnerability functions for European-type RC structures based on observational data. *Engineering Structures*, *25(*10), 1241-1263.

Safkan, I. (2012). Comparison of Eurocode 8 and Turkish Earthquake Code 2007 for Residential RC Buildings in Cyprus. In *15th World Conference on Earthquake Engineering* (Vol. 24). Lisbon.

Safkan, I. (2014). Cyprus Strong Motion Database: Response Spectra for Short Return Period Events in Cyprus. In *2nd European Conference on Earthquake Engineering and Seismology.* Istanbul.

Safkan, I., Sensoy, S., & Cagnan, Z. (2017). Seismic behaviour of the old-type gravity load designed deteriorated RC buildings in Cyprus. *Engineering Failure Analysis*, 82, 198-207.

SeismoStruct (2016). A computer program for static and dynamic nonlinear analysis of framed structures. Retrived from http://www.seismosoft.com.

Sezen, H., & Chowdhury, T. (2009). Hysteretic model for reinforced concrete columns including the effect of shear and axial load failure. *Journal of Structural Engineering*, 135(2), 139-146.

Sezen, H., & Moehle, J. P. (2004). Shear strength model for lightly reinforced concrete columns. *Journal of Structural Engineering*. 130(11), 1692-1703.

Sezen, H., & Setzler, E.J. (2008). Reinforcement slip in reinforced concrete columns. *ACI Structural Journal*. 105(3), 280-289.

Sezen, H., Whittaker, A. S., Elwood, K. J., & Mosalam, K. M.. (2003). Performance of reinforced concrete buildings during the August 17, 1999 Kocaeli, Turkey earthquake, and seismic design and construction practice in Turkey. *Engineering Structures*, 25(1), 103-114.

Silva, V., Crowley, H., Varum, H., Pinho, R., & Sousa, L. (2015). Investigation of the characteristics of Portuguese regular moment-frame RC buildings and development of a vulnerability model. *Bulletin of Earthquake Engineering*,13(5), 1455-1490.

Sivaselvan M., & Reinhorn A.M. (1999). Hysteretic models for cyclic behaviour of deteriorating inelastic structures. Report MCEER-99-0018, MCEER/SUNY/Buffalo.

Tiedemann, H. (1992). *Earthquakes and Volcanic Eruptions. A Handbook on Risk Assessment*. Zurich: Swiss Reinsurance Company

Turkish Standards Institute (1984). TS500, *Requirements for design and construction of reinforced concrete structures*, Ankara, Turkey.

Tüzün, C. (2008). *A Seismic Vulnerability Analysis procedure for Urban Loss Assessment*. PhD Thesis, Boğaziçi University, Istanbul, Turkey.

U.S. National Department of Commerce (1975). *Natural Hazards Evaluation of Existing Buildings.* Building Science Series 61. Washington: National Bureau of Standards

Ulrich, T., Negulescu, C., & Douglas, J. (2014). Fragility curves for risk-targeted seismic design maps. Bulletin of earthquake engineering, 12(4), 1479-1491.

Vamvatsikos, D., & Cornell, C. A. (2002). Incremental dynamic analysis. *Earthquake Engineering and Structural Dynamics*, 31(3), 491-514.

Verderame, G.M., Fabbrocino, G., & Manfredi, G., 2008. Seismic response of RC columns with smooth reinforcement. Part I: Monotonic tests. *Engineering Structures* 30, 2277–2288.

Vidal, T., Calstel, A., & François, R. (2004). Analyzing crack width to predict corrosion in reinforced concrete. *Cement and Concrete Research*, 34, 165 – 174.

Whitman, R. V., Reed, J. W., & Hong, S. T. (1973). Earthquake damage probability matrices. In *Proceedings of the Fifth World conference on earthquake engineering* (Vol. 2, pp. 2531-2540). Rome, Italy.

Wood, H. O., & Neumann, F. (1931). Modified Mercalli Intensity Scale of 1931: *Seismological Society of America Bulletin*, 21(4), 277-283.

Yalciner, H., Eren, O., & Sensoy, S. (2012). An experimental study on the bond strength between reinforcement bars and concrete as a function of concrete cover, strength and corrosion level. *Cement and Concrete Research*, 42(5), 643-655.

Yalciner, H., Sensoy, S., & Eren, O. (2015). Seismic Performance Assessment of a Corroded 50-Year-Old Reinforced Concrete Building. Journal of Structural Engineering, 141(12), 05015001.

Yu, L., François, R., Dang, V. H., L'Hostis, V., & Gagné, R.. (2015). Structural performance of RC beams damaged by natural corrosion under sustained loading in a chloride environment. *Engineering Structures*, 96, 30-40.

Zhou, H., Lu, J., Xv, X., Dong, B., & Xing, F. (2015). Effects of stirrup corrosion on bond–slip performance of reinforcing steel in concrete: An experimental study. *Construction and Building Materials*, 93, 257–266.